Natural Environment Research Council
Institute of Geological Sciences

Mineral Reconnaissance Programme Report

A report prepared for the Department of Industry

D. Ostle
Programme Manager
Institute of Geological Sciences
Nicker Hill, Keyworth,
Nottingham NG12 5GG

No. 59

Stratabound arsenic and vein antimony mineralisation in Silurian greywackes at Glendinning, south Scotland

INSTITUTE OF GEOLOGICAL SCIENCES

Natural Environment Research Council

Mineral Reconnaissance Programme

Report No. 59

Stratabound arsenic and vein antimony mineralisation in Silurian greywackes at Glendinning, south Scotland

Geology
M. J. Gallagher, PhD, MIMM
P. Stone, PhD
A. E. S. Kemp, MA
M. G. Hills, BSc

Geochemistry
R. C. Jones, BSc
R. T. Smith, MSc, Dip Geochem
D. Peachey, BSc,
B. P. Vickers

Geophysics
M. E. Parker, BA
K. E. Rollin, BSc

Mineralogy
B. R. H. Skilton, BSc

London 1983

A report prepared for the Department of Industry

Mineral Reconnaissance Programme Reports

The Institute of Geological Sciences was formed by the incorporation of the Geological Survey of Great Britain and the Geological Museum with Overseas Geological Surveys and is a constituent body of the Natural Environment Research Council

Bibliographic reference
Gallagher, M. J. and others. 1983. Stratabound arsenic and vein antimony mineralisation in Silurian greywackes at Glendinning, south Scotland. *Mineral Reconnaissance Programme Rep. Inst. Geol. Sci.*, No. 59

Printed in England for the Institute of Geological Sciences by Four Point Printing

CONTENTS

FIGURES

TABLES

SUMMARY

Stratiform and disseminated pyrite-arsenopyrite concentrations are overprinted by fracture-controlled polymetallic mineralisation including stibnite through at least tens of metres of Silurian sediments at Glendinning, near Langholm. Three shallow boreholes were drilled on an anomaly defined by VLF–EM and IP surveys and by antimony values >20 ppm in thin B–C horizon soils. A parallel conductive zone with an accompanying soil anomaly but lacking an IP response was investigated by a fourth hole. The stratabound sulphides form disseminations and bands parallel to the bedding and are particularly concentrated in intraformational breccia units regarded as debris flows, which, together with the presence of small scale slump folds in the greywackes, testify to the existence of an unstable slope during sedimentation. The thickest such unit has a true thickness of 4 m and together with 8 m of adjoining greywackes grades 0.7% As.

Phases of fracture-controlled Fe–As–Sb–Pb–Zn–Cu–(?)Hg mineralisation associated with widespread dolomite and quartz veinlets and narrow breccia veins are superimposed on the stratabound mineralisation. Their spatial association with the stratabound mineralisation, the presence of up to 0.33% Sb in the stratiform arsenopyrite and as much as 5% As in the stratiform pyrite, favour a common source for the arsenic and antimony. This source was probably a synsedimentary metal accumulation in a mid or lower fan environment where euxinic conditions periodically developed.

INTRODUCTION

LOCATION

The old Louisa Mine at Glendinning lies 13 km north-north-west of Langholm (Figure 1) and 26 km south-west of Hawick in southern Scotland. It can be reached from Langholm via the B709 Eskdalemuir road thence by a minor road from Georgefield to the hamlet of Glendinning. A rough track leads eastwards for 1.5 km from Glendinning hamlet to the old mine.

MINING RECORDS

The documentary evidence on this mine is scant and at times at variance with the field evidence. Dewey (1920) stated that the mineralisation was first discovered about 1760 but does not say which vein. A section of the mine is recorded in the margin of a Leadhills mine plan dating from the mid-nineteenth century, but this only shows a single worked structure (*op cit* p. 55). A total production of nearly 200 tonnes of antimony is recorded from Glendinning Mine, the main periods of production being 1793–1798 and 1888–1891 (*op cit*).

Field observation suggests that there are three structures which have been worked, as well as several small trials and lines of costean pits. It seems likely that the first discovery of ore minerals took place in Glenshanna Burn as outcrop is scarce elsewhere. The earliest workings lie about 100 m below the main mine dumps [3112 9662] where there is a collapsed adit in the stream bank driven towards the main shaft at a small angle to the stream. About 30 m along this there is possibly a shaft from the surface close to the remains of a dam and wheel pit. On the south side of the stream (Figure 6) there are small dumps and crushing floors on which samples of stibnite abound. A further 50 m downstream from these there is a powder hut of a later phase of working south of which a trench is aligned with the col into Trough Hope (Figure 3). The remains of a shaft with a dump which is now well covered with vegetation occur nearby. It is possible that there were occasions other than those mentioned above on which ores were extracted from the workings. The early phases of operation apparently lacked any mechanisation, or even a track along which a wheeled vehicle might have gained access to the workings.

The main workings, which are probably of mid to late 19th century age, lie on the north side of Glenshanna Burn, and are of a much larger scale than those described above. The vein is described by Wilson (in Dewey, 1920) as trending to the north-east, and dipping at 80° to the SE, or vertical. According to Wilson, quoting unspecified sources, the walls are horizontally slickensided and about 1.3 m apart, within which a zone of small stringers of ore occurred in brecciated country rock. The distribution of ore is said to be very patchy and the volume of gangue minerals small. The mine workings were inaccessible when visited by Wilson more than sixty years ago. He describes the ore as being a highly complex mixture of stibnite, galena, jamesonite and sphalerite, with a little chalcopyrite.

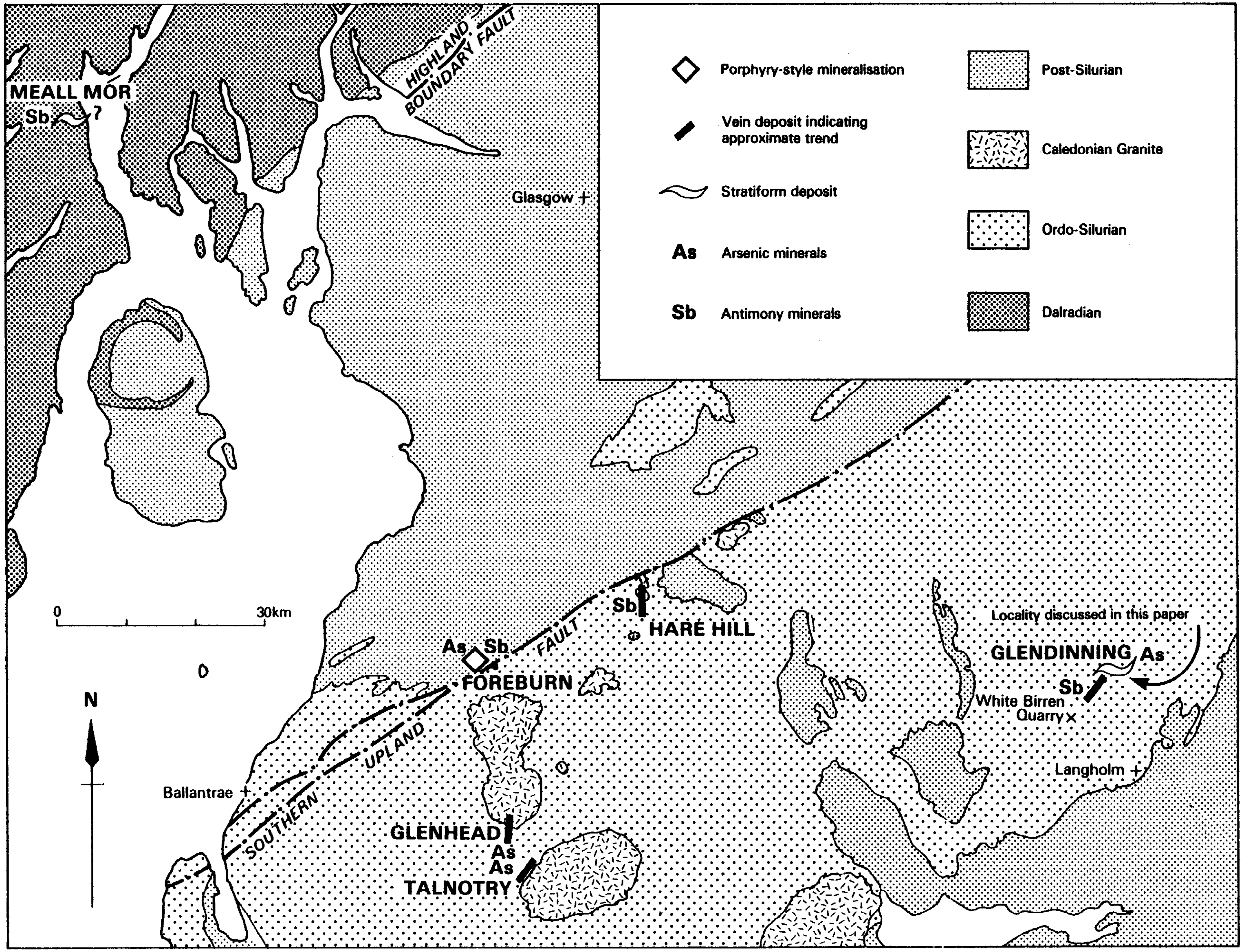

Fig 1 Sketch geological map of the south of Scotland showing the principal known occurrences of antimony and arsenic

The gangue comprises quartz, calcite and baryte. The major part of the workings, to which it is presumed that Wilson's description applies, comprises three levels, the top one of which is an adit on the flank of Grey Hill (Figure 6). The levels are interconnected by two or possibly three shafts and a number of winzes. Drainage seems to have been a problem on the lower two levels, and it is unlikely that much production took place from them. The last phase of operation took place c.1920 when reinforced concrete footings were built for winding gear and the shafts were cleaned out. However, it seems that most of the capital was spent on elaborate facilities, and production was small before the venture collapsed. Costean pits were sunk on the south side of Glenshanna Burn, and small excavations in the hillside suggest that trial adits were driven in search of a southward extension of the mineralised structure, but there is nothing to suggest that anything was found.

Westwards from the mine site towards Meggat Water (Figure 3) two small adits open into the south bank of the stream. The adjoining dumps are barren of mineralised material. Another small trial occurs in the main valley to the east of Megdale Farm [3003 9576], which may have been developed in the early part of this century, and was only abandoned because of a drop in the price of antimony ores. There is evidence of a smelting hearth on the banks of Meggat Water adjacent to Glendinning Farm, and another beside Tod Syke, which appears to be related to one of the later phases of working, at which time a proper track was cut to the mine.

SCOPE OF THE PRESENT INVESTIGATION

Glendinning Mine is geographically remote from other mining districts in southern Scotland and even prior to this investigation its geological characteristics were regarded as unusual – an isolated vein in Lower Palaeozoic sediments unrelated to major faulting and distant from granitic intrusions. Apart from a few baryte veinlets exposed in Glenshanna Burn there is no outcropping metalliferous mineralisation in the area of Glendinning Mine. The lack of mineralisation controls, evidence of antimony anomalies in drainage samples (Figure 2) and the high value of the metal itself formed the main reasons for this investigation.

As exposure is very poor in the mine area, geochemical soil sampling and geophysical surveys formed the main surface investigations, commencing in 1979. Traverses were oriented NW–SE on the assumption that the mining record of a north-east trending vein was correct. However, coincident soil anomalies and VLF–EM anomalies trending at 015° were obtained in ground where little or no evidence of earlier workings existed. On this new evidence, four shallow boreholes were drilled in 1980. Drill cores were logged on site, then in more detail at the field base. Half-core samples were taken for geochemical analysis and mineralogical study and the remainder stored in Edinburgh.

REGIONAL GEOLOGY

In Britain the northern sector of the Caledonides fold belt (the orthotectonic Caledonides) is essentially a high grade metamorphic terrain whereas the southern sector (the paratectonic Caledonides), although containing highly deformed strata, has suffered only very low grade metamorphism. The boundary between the orthotectonic and paratectonic Caledonides probably lies in the vicinity of the Southern Upland Fault and coincides with a continental margin beneath which oceanic crust was consumed at a north-westerly dipping subduction zone during the Lower Palaeozoic (Dewey, 1969; Phillips and others, 1976).

When the present Atlantic Ocean is closed so that the continents are restored to their pre-Mesozoic relationships (e.g. Smith and Briden, 1977) Britain and Ireland are brought into close proximity to Newfoundland and Greenland. The continuity of the Laurentian continental foreland outcrops in east Greenland, north-west Scotland and Newfoundland is then emphasised. In Scotland the Dalradian Supergroup originated in a late Pre-cambrian to Cambrian ensialic basin within this foreland (Harris and others, 1978) and has a probable analogue in the Fleur de Lys Supergroup of Newfoundland (Kennedy, 1975). Ophiolite complexes at Ballantrae and in Newfoundland are generally believed to represent oceanic crust obducted onto the continental margin from a series of back-arc basins (Dewey, 1974).

South-east of the Southern Upland Fault a systematic sequence of stratigraphically distinct, steeply dipping greywacke-shale units trends north-east to south-west separated by major strike faults. Within each individual unit the dominant direction of stratigraphic younging is to the north-west but overall progressively younger units crop out sequentially towards the south-east (Walton, 1965; Leggett and others, 1979). This trend is particularly well defined in the north-western half of the Southern Uplands but becomes more confused southeastward. The fault-bounded units are thought to have originated as an accretionary wedge formed above a subduction zone consuming the Lower Palaeozoic Iapetus oceanic plate (McKerrow and others, 1977; Leggett and others, 1979). The wedge built up as successive thin layers of sediment were sheared from the surface of the downgoing plate and underthrust beneath a stack of similar slices. Some rotation of the sedimentary pile may have been caused by the underthrusting but final rotation to the present sub-vertical

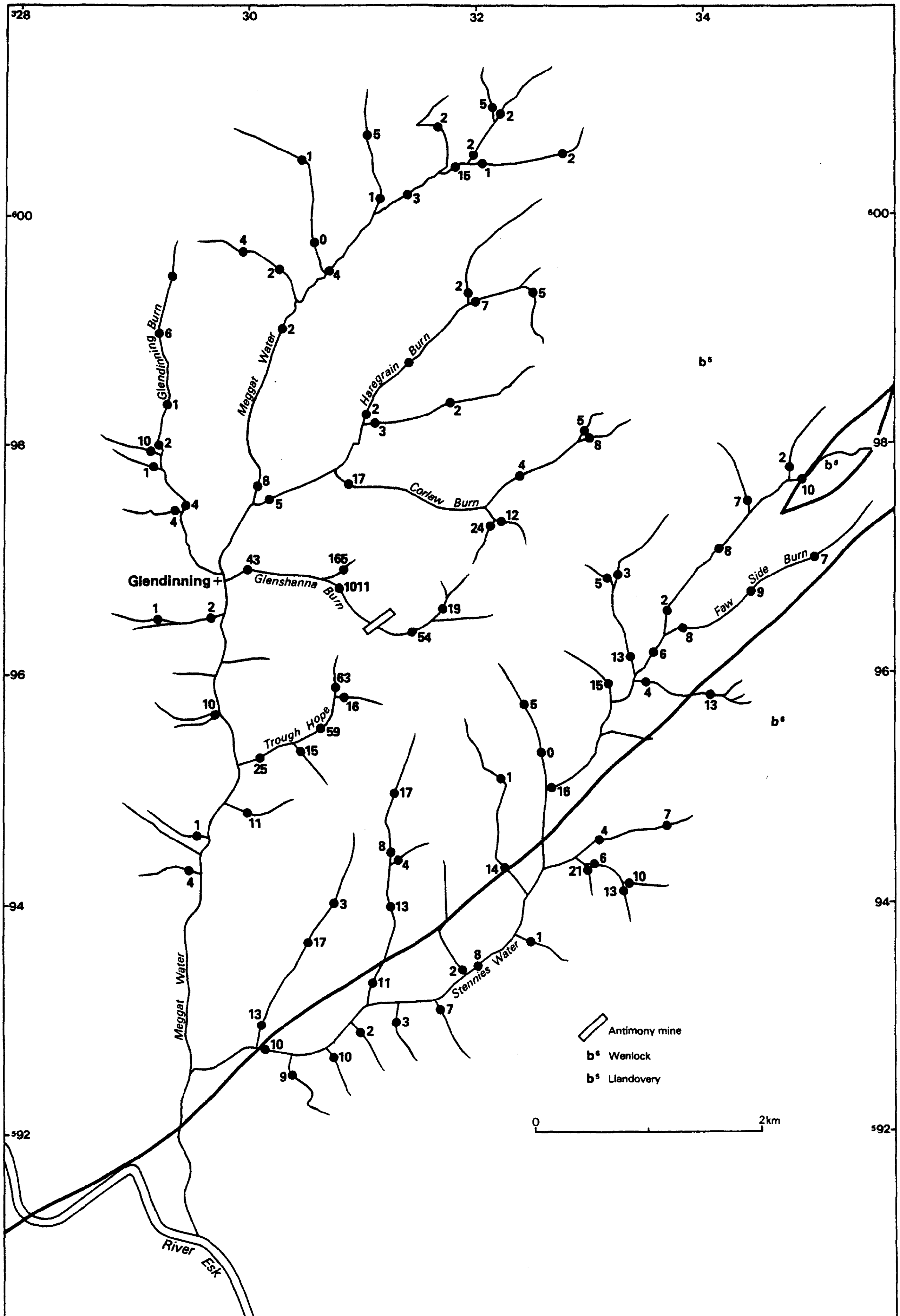

Fig.2 Distribution of antimony (ppm) in heavy mineral concentrates from drainage near Glendinning. Geology from one-inch Geological Sheet 10 (Scotland)

attitude was probably caused by continental collision as the Iapetus Ocean finally closed. The resultant suture is believed now to underlie the Solway Firth.

GEOLOGY OF THE GLENDINNING AREA

STRATIGRAPHY

The Glendinning area lies within the broad belt of Silurian strata which forms the south-eastern part of the Southern Uplands. The succession consists of medium to fine-grained greywackes well-bedded on the scale of a few centimetres to several metres. Well-developed grading is only occasionally seen but interlamination of the fine greywacke with siltstone is common, together with widespread cross-bedding. A number of intraformational breccia horizons were encountered in the boreholes, some with siltstone and fine sandstone clasts set in a muddy matrix and others with mudstone clasts in a coarser-grained matrix. Of the breccias rich in fine-grained matrix some contained clasts cut by fine quartz and carbonate veins. These may have originated as mass-flow deposits derived from a more distant source than the intraformational breccias. The assemblage of sedimentary features observed suggests deposition in a mid or lower fan environment (e.g. Walker, 1979). Grey and red mudstones are in places interbedded with the greywackes and are frequently mutually interlaminated. The mudstone horizons range up to 1 m in thickness and probably represent a pelagic or hemipelagic deposit.

Good palaeocurrent evidence was obtained at several exposures and, after correction only for bedding inclination, showed a consistent current trend towards the west and south-west. However, at White Birren quarry, 6 km along strike to the south-west there is good evidence for palaeocurrent flow towards the east (Figure 4). This along-strike variation in current direction reinforces the suggestion of deposition in a mid or lower fan environment.

No evidence for contemporary vulcanicity was found in the Glendinning district, but tuffaceous horizons have been reported (Lumsden and others, 1967, p. 14) within the neighbouring Silurian sequence of the Langholm area. The closest of these to Glendinning crops out approximately 11 km to the south-south-east.

In the past unfossiliferous sequences of the type exposed in the Glendinning area have been referred to as the 'Hawick Rocks', an ill-defined assemblage traditionally included in the Llandovery stage of the Silurian (Peach and Horne, 1899; Rust, 1965a). However, work by Craig and Walton (1959) in Galloway, and Warren (1964) near Hawick has suggested that the uppermost parts of the 'Hawick Rocks' sequences in those areas may be Wenlock in age. The stratigraphic position of the Silurian greywackes of the Glendinning area is therefore uncertain, and because of the paucity of outcrop, the steeply inclined nature of the beds, and borehole evidence of rapid lithological variation it has not been possible to devise a local lithostratigraphy.

STRUCTURE

The principal structural elements of the Glendinning area are summarised in Figure 3. Regional bedding strike is north-east to south-west although in places a dextral deflection is apparent, for example in the western part of the Corlaw Burn. Strata are generally steeply inclined with a south-eastward dip. The overall sense of younging is to the north-west (thus most beds are slightly inverted) but south-easterly younging horizons were noted in several places. This alternation of younging direction in adjacent horizons with similar attitudes is likely to be the result of tight folding. Several poorly preserved sub-horizontal fold hinges, usually with an associated axial-plane cleavage, were observed within the mine area and are probably of the same general style as the folds well exposed at White Birren quarry 6 km to the south-west (Figure 4). In the quarry section tight folds with sub-horizontal hinges have an associated axial planar slaty cleavage dipping steeply to the south-east. Folding of this style, and its associated irregularly developed axial plane cleavage, probably continues across the Glendinning area. However, the impersistence of the reverse younging belts along strike suggests that the individual folds may themselves be discontinuous.

Superimposed on the sub-horizontally hinged folds are tight folding zones with hinges plunging steeply to the west-south-west. In style these range from simple S or Z folds with amplitude and wavelength of up to 2 m, to complex fold zones several metres broad (Figure 5). It is possible that these are associated with fracture zones trending north-north-east which form a prominent lineament across the Glendinning area (Figure 3). In situ brecciated and mineralised bedrock has been collected from the surface expression of one such lineament close to BH 3. It is probable that the mined galena-sphalerite-stibnite vein was contained within such a north-north-east trending fracture.

No minor intrusions were observed in the vicinity of the old mine workings but 2.5 km and 4.5 km to the south-west Tertiary dolerite dykes crop out with a trend approximately perpendicular to the regional strike. In the White Birren quarry section a highly altered dolerite dyke is of Lower Devonian type. The Glendinning area is remote from the major Caledonian batholiths of the south of Scotland; the Criffel granite 45 km to the south-west and the postulated Tweeddale granite (Lagios and Hipkin, 1979) 40 km to the north are the closest. There is no geophysical evidence for a major intrusive body beneath the mineralised zone.

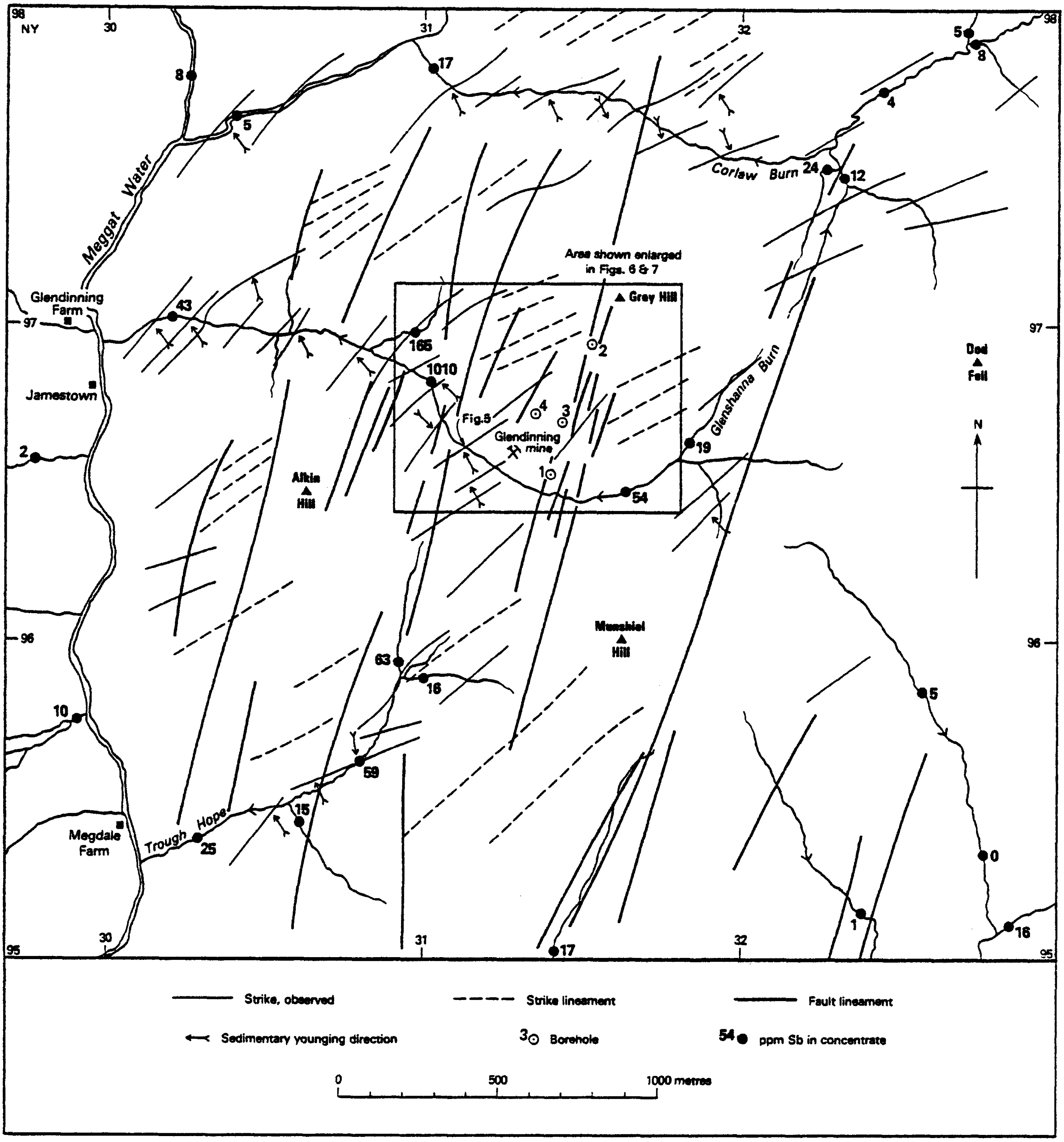

Fig.3 Geology of the area around Glendinning mine, north of Langholm. Fault lineaments inferred from aerial photographs. Antimony distribution in heavy mineral concentrates from tributary alluvium also shown

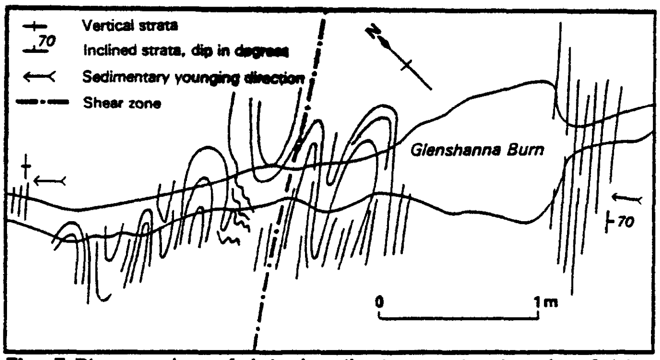

Fig. 5 Plan section of tight-isoclinal, steeply plunging folds. Located on Fig. 3

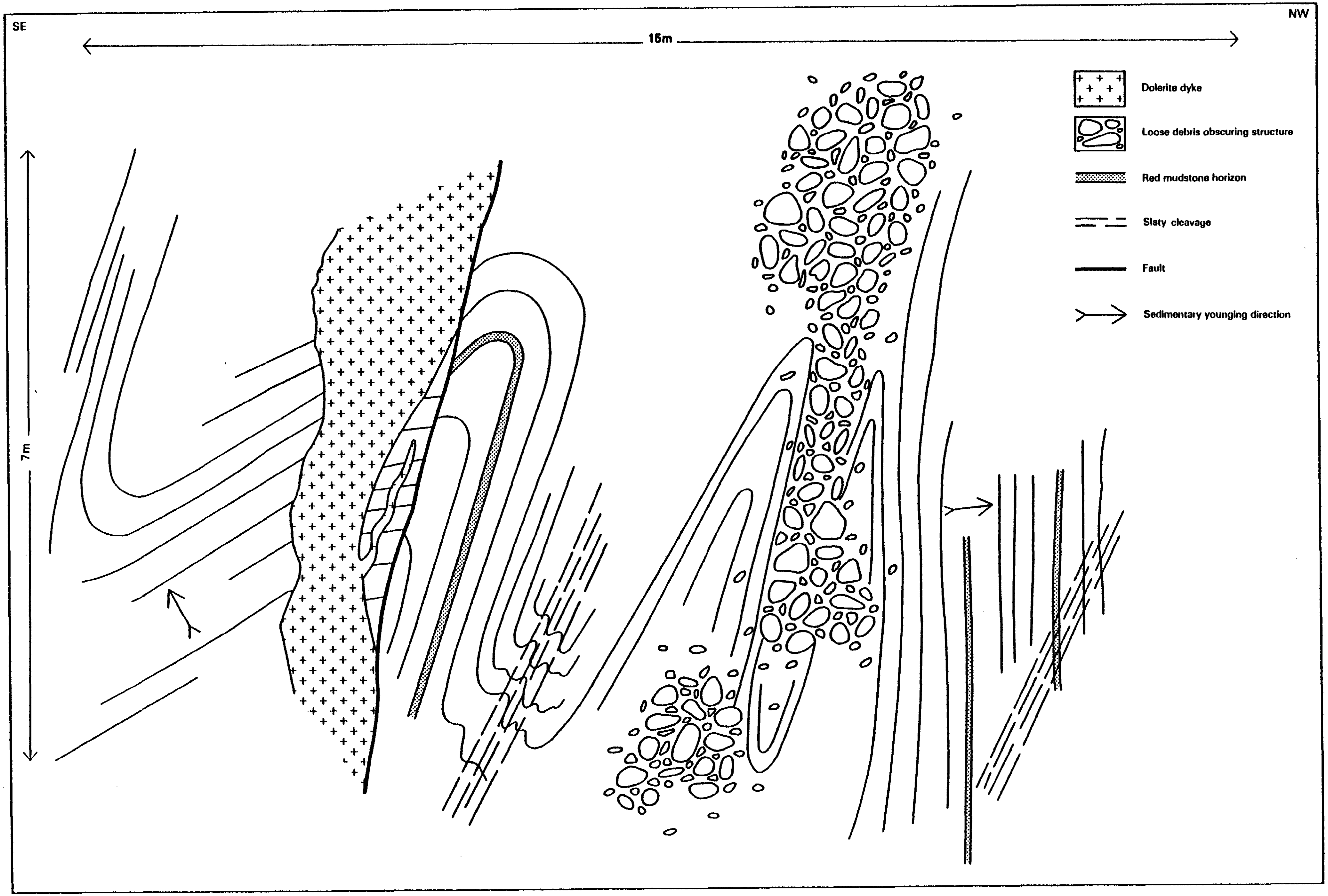

Fig.4 Tight, gently plunging folds exposed in the southwestern face of White Birren Quarry (located on Fig. 1)

GEOCHEMISTRY

DRAINAGE SAMPLING

From the results of geochemical orientation studies carried out over Lower Carboniferous sediments and lavas to the west of Langholm (Gallagher and others, 1977; Smith, Gallagher and Fortey, 1978), heavy mineral concentrates were identified as the optimum sample type in locating sulphide mineralisation occurring in both veins and disseminations. As a consequence of significantly increased base metal abundances and improved geochemical contrast for Pb, Zn, Cu, Ba, Ni, Fe and Sb relative to minus 150 μm stream sediments, heavy mineral concentrates were used in a high density geochemical reconnaissance survey of the Borders extending from Ecclefechan north-eastwards to Berwick (Smith and others, *in preparation*).

Samples of heavy minerals 20–30 g in weight, recovered by panning about 3 kg of minus 2.5 mm stream sediment, were subsampled to 12 g (Leake and Aucott, 1973) and analysed by an automatic XRF technique (Leake and others, 1978). Results for antimony and associated anomalous elements in the Glendinning area are presented in Figures 2–3 and in Appendix V, Figures 1–8. Simple statistical analysis of the total sample population indicates in the case of antimony a significant change of slope on the cumulative frequency curve at 20 ppm Sb. Values above this level are regarded as highly anomalous at the regional scale and are mainly confined to Glenshanna Burn, Trough Hope and Corlaw Burn.

Very high antimony (and lead) values in Glenshanna Burn downstream of the mine are considered to reflect severe heavy metal contamination from previous mining activity. Further evidence of contamination is provided by the extensive dispersion of mine dump material downstream of the old workings, the high concentrations of fresh sulphides recovered by panning and the presence of anomalous concentrations of tin in some samples (Appendix V, Figure 7). However, highly anomalous antimony values occurring in the minor north bank tributary, in the main stream above the old mine, and in adjacent catchments are thought to be related to a wider zone of mineralisation extending along strike for 2–3 km north-east and south-west of Glendinning Mine. The distribution of arsenic (Appendix V, Figure 8) is also indicative of a NE–SW trending zone of mineralisation some 5 km in length. Glacial dispersion of ore minerals from the area of outcropping mineralisation in Glenshanna Burn is unlikely to account for the observed distribution of anomalous antimony and arsenic values.

Anomalous values of 11–20 ppm Sb also occur in the catchment of Stennies Water, particularly downstream of its junction with Faw Side Burn (Figure 2). However, dispersion trains are apparently short, and there are no very high antimony or associated ore metal values indicative of a local bedrock source. Further sampling of soils or basal tills would, therefore, be required to establish whether these anomalies are the result of glacial dispersion of heavy minerals over a wide area or of suboutcropping mineralisation obscured by drift on the valley sides or interfluve areas.

Comparison of the distribution of antimony with other elements suggests an association with iron (Appendix V, Figure 1) which is relected in the Sb against Fe correlation coefficient of 0.45 for all samples (650) derived from Silurian rocks in the regional survey (Smith and others, *in preparation*). The regional mean value of iron based on log data is 5.5% whereas higher values (6.5–17%) characterise areas of known or inferred antimony mineralisation.

Lead and zinc are both highly enriched in heavy mineral concentrates from the mine area in Glenshanna Burn but decrease downstream to almost background concentrations over a distance of 1 km (Appendix V, Figures 2–3). Elsewhere in the Glendinning area, low levels of lead, zinc, copper and barium are comparable to or lower than the regional means of 20, 100, 23 and 515 ppm respectively, and do not correlate with antimony. In contrast, nickel concentrations (av. 55 ppm) exhibit a small but consistent increase compared with the regional mean (40 ppm) and are notably higher in samples from Trough Hope and Glenshanna Burn (Appendix V, Figure 5).

SOIL SAMPLING

In order to test for possible extensions of the known mineralisation soil samples were collected on a grid pattern around the workings. A sample spacing of 10 m by 100 m was chosen along the same traverses as the geophysical surveys (Figure 7), but this was reduced to 20 m by 100 m on the top of Grey Hill. Samples of B or C horizon soil weighing around 100 g were taken from a depth of 1 m, or as deep as possible in the shallower soils of the higher ground.

The soils of the area are mostly well-oxidised yellow-brown silty clays, in which the content of angular lithic fragments gradually increases with depth. The change from bedrock to residual soil is gradational, and the weathering profile is pockety. The borehole sections show that oxidation penetrates bedrock for some distance, particularly along fracture planes. These soils bear a close resemblance to the residual soils of south-west England. In upper Glenshanna Burn there are considerable accumulations of head deposits, and a short distance above the mine these are overlain by boulder clay, which is well exposed in the stream section where it is about 10 m thick. The boulder clay is ill-drained and covered by up to 1.5 m of peat. Peat development seldom exceeds 0.15 m on the residual soils, presumably due to their free drainage.

The samples were oven dried in their bags and

Table 1 Accuracy limits of XRF analysis

	Ba	Sb	Pb	Zn	Cu	Ca	Ni	Fe	Mn	As
Upper limit (%)	1	1	1	1	1	30	1	30	1	1
Lower limit (ppm)	18	7	9	2	4	–	3	–	4	5

sieved to pass 200 μm mesh. From each fine fraction a subsample of 12.0 g was obtained by cone and quartering, to which 4 g of elvacite was added. This mixture was ground to around 80 μm mesh and pressed into a pellet for X-ray fluorescence determination of Ce, Ba, Sb, Sn, Pb, Zn, Cu, Ca, Ni, Fe, Mn, Ti and As (see Table 1 for limits of detection).

The data were analysed on the Rutherford Laboratory dual IBM 360/195 computer using the G–EXEC program package, from which graphical displays were generated on a Calcomp drum-plotter.

Cerium, tin and titanium showed no significant variation over the area, and were not considered further. The other elements showed near lognormal distributions and hence were log-transformed before further analysis. Log concentration against probability plots were used to determine population breaks or inflection points (Table 2). These were used to chose contour intervals for the isopleth maps (Figure 6 and Appendix VI).

ELEMENT DISTRIBUTIONS IN OVERBURDEN

The normal background level of *antimony* in soil is <1 ppm (Wedepohl, 1972). Sixty percent of the samples analysed contain >7 ppm, which is the analytical detection limit and all of these samples must be considered to be anomalous. The top population, >55 ppm Sb, is probably related to the presence of mineralised material in the samples, and values of 7–55 ppm to secondary dispersion of antimony in the soil. The maximum concentrations are found in two near-linear zones, the western one of which can be traced north-north-east from the mine workings for 500 m; the second runs parallel, about 130 m to the east, and is of a similar size (Figure 6). Neither appear to be the surface expression of the worked vein from what can be seen of the orientation of the adit. A small antimony anomaly occurs on the south side of Glenshanna Burn close to the old powder hut [3104 9667]. It yields a maximum value of 16 ppm Sb, and measures 150 m by 20 m. Further anomalies occur in the bottom of Trough Hope (Appendix VI, Figure 2), but are closely related to high iron concentrations and may therefore be of secondary type. A single sample containing 28 ppm Sb found at [3066 9619] on the southern spur of Alkin Hill may be of some significance as it coincides with high values of copper, lead and nickel.

Background *barium* levels are relatively low in the Glendinning area, the mean level for the background population being 165 ppm. There is a higher level population containing in excess of 330 ppm, with a transitional zone down to 210 ppm. Contours at the top and bottom of the transitional population produce a coherent pattern, which coincides with maxima of other elements. In the lower part of the eastern anomaly barium coincides with calcium, and for 200 m on the flank of Grey Hill with copper, zinc, nickel and antimony. In the western anomaly barium occurs with calcium, copper, lead and nickel. Transitional values of barium are found in the vicinity of the

Table 2 Summary statistics, soil samples

Element	Maximum	Minimum	Geometric mean	Median	Points of inflection and percentiles	
Ba	482	101	186	175	205 (79%)	330 (89%)
Sb	198	0	6.6	8.2	7.2 (43%)	55 (99.3%)
Pb	213	6	28	27	38 (77%)	
Zn	232	12	52	53	100 (85%)	126 (99%)
Cu	134	1	13	14	13 (44%)	39 (97.5%)
Ca	4970	290	708	570	660 (68%)	2300 (89%)
Ni	92	6	27	27	71 (95%)	
Fe%	11.6	.86	4.89	6.2	6.6 (54%)	
Mn	1860	30	245	270	550 (74%)	
As	2637	0	34	27	24 (46%)	750 (97%)

All values in ppm except Fe(%): 453 samples

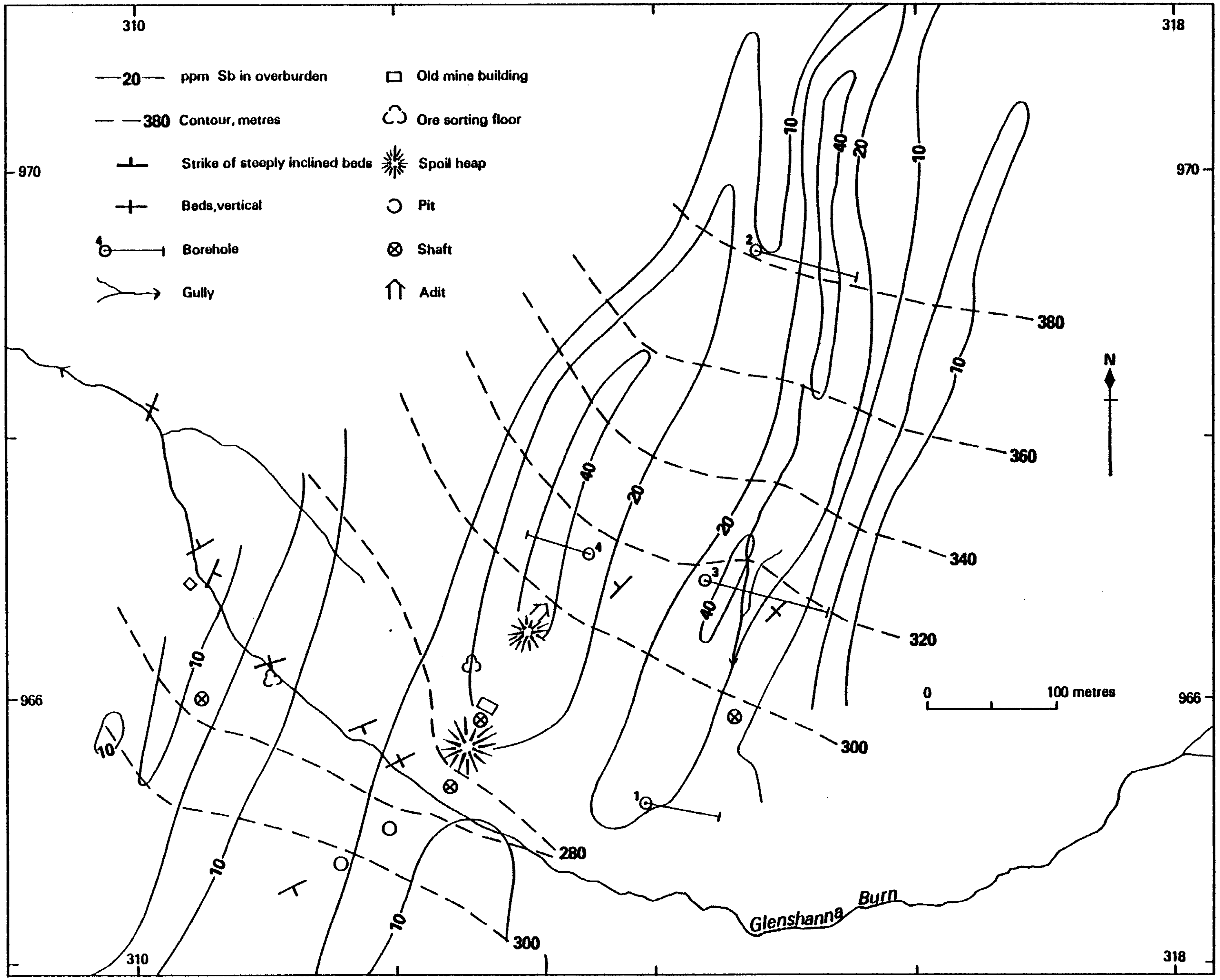

Fig 6 Geology and topography of the area around Glendinning Mine showing distribution of antimony in —150μm shallow overburden samples (see Fig. 3 for location and Fig. 7 for sampling traverse lines)

old workings on the south side of Glenshanna Burn, and the boulder clay in the valley floor contains concentrations in excess of 330 ppm downstream of the workings. There is a sharp increase in the barium concentration in the lower part of Trough Hope, where values lie in the range of 200—400 ppm, which may be due to secondary concentration on humic acids or iron and manganese oxides. All the barium concentrations are low when compared with other mineralised areas, and the median concentration is about half that given as the mean for greywackes (Wedepohl, 1972).

Calcium levels are generally low in the greywackes surrounding the mine, and in the boulder clay in the valley bottom. Over the mineralised structures, however, much higher levels are encountered and these anomalies appear to have given rise to calcium-rich soils in the valley bottom downstream from the mine site. The eastern anomaly displays the highest concentrations, which occupy a zone 40 m wide and more than 400 m long on the side of Grey Hill (Appendix VI, Figure 4). There are two smaller anomalies to the east of this, the more intense of which is associated with high zinc and barium concentrations. In the case of calcium, the western anomaly is limited to 100 m in length, much less than for accompanying anomalous elements. Beneath the gap into Trough Hope there is another area of high calcium concentrations associated with copper, zinc, nickel, barium and antimony, though this rapidly dies out southwards.

The background level of *copper* in this area is around 13 ppm, but 2% of the samples fall into a separate population with concentrations >39 ppm. Most of these anomalous samples lie in the valley bottom in peat-covered boulder clay, though two of them are within the previously described anomalous zones on Grey Hill, and coincide with high lead, zinc, nickel and antimony values in the western anomaly and with calcium, barium and lead in the eastern anomaly. A contour at 20 ppm encloses all the valley bottom, and also both the mineralised structures. The old workings around the powder hut are also marked by copper concentrations of up to 39 ppm. There are isolated higher values in the bottom of Trough Hope, and also on the south side of Alkin Hill and on the west side of Munshiel Hill. The copper distribution is complex, with higher levels over peat-covered boulder clay as well as around the mineralised structures. It is probable that hydromorphic transport is important in governing the abundance of copper in soil.

There are two overlapping populations amongst the *iron* analyses with a point of inflection at 6.6%. The western anomaly is clearly marked by high iron concentrations, but only two small patches of the eastern anomaly are similarly marked. Parallel to the western anomaly but further west there is a broad anomalous zone coincident with high manganese values. To the east of the eastern anomaly there are two anomalous patches which are coincident with high antimony and copper values. Other anomalous concentrations occur on the south bank of Glenshanna Burn around zones of seepage, in the bottom of Trough Hope, and on the east side of Alkin Hill where a thin linear anomaly coincides with a lineament conspicuous in the aerial photographs.

The *lead* analyses form two populations with a point of inflection at around 40 ppm, but an examination of the geographic distribution of these samples suggests that there is considerable overlap between the background and anomalous populations. Contours at 50 ppm and 70 ppm enclose the eastern and western anomalies and the valley of Trough Hope (Appendix VI, Figure 5). Both anomalous zones appear to extend across Glenshanna Burn to the south and to die out after about 150 m near the top of the slope. The anomalous zone enclosed in Trough Hope measures 500 m by 100 m. To the west of this there is another small anomalous zone on the flank of Alkin Hill coincident with high copper, nickel and antimony values, suggesting that there might be another small-scale structure in that area.

Background concentrations of *manganese* appear to extend up to 560 ppm and account for 74% of the samples analysed. A contour drawn at that value delineates the western anomaly and part of the eastern anomaly, but diverges westwards near the base of the slope. Two small patches of manganese concentration to the east of the eastern anomaly lie close to a minor zone of antimony and lead anomalies. To the west of the western anomaly there is a parallel zone of high manganese and iron without any base metal enrichment. There are several narrow anomalous areas running down the south bank of Glenshanna Burn, which are coincident with seepages. High values prevail throughout the lower parts of the Trough Hope valley and over the gap into the valley of Glenshanna Burn valley in damp and ill-drained ground. Conversely on the top of Grey Hill where the drainage is good on the porous soils manganese concentrations are very low.

Nickel concentrations fall into three populations with breaks at 21 ppm and 71 ppm. The highest population marks the eastern, western and 'powder hut' anomalies more sharply than any other element. A contour at 50 ppm follows the 71 ppm contour, but shows that the dispersion is chiefly in a westerly direction, which would be the direction of hydromorphic or ice transport, or both. The 30 ppm contour encloses much of the bottom of the valley of Glenshanna Burn and follows the eastern and western anomalies to the summit of Grey Hill (Appendix VI, Figure 6). Low-order nickel anomalies are also found in the bottom of Trough Hope where these may be related to concentration on humic acids, iron and manganese oxides, and on the southern spur of

Alkin Hill where they are associated with copper, lead and antimony anomalies.

The background concentration for *zinc* ranges between 0 and 100 ppm with a mean value of 48 ppm. Samples containing >130 ppm Zn form the topmost population, and were collected in peaty hollows. Values between 100 ppm and 130 ppm delineate the western and 'powder hut' anomalies, the boulder clay in between them, and also the bottom of Trough Hope. The eastern anomaly is not marked by any increase in zinc concentration but a small anomaly further to the east is coincident with anomalous copper and barium values.

The distribution of *arsenic* clearly marks both the eastern and western anomalies. An analysis of the data reveals three populations with boundaries at 25 ppm and 350 ppm. The highest of these coincides with the highest antimony concentrations over the two major anomalies, the enclosed area being attenuated towards the summit of Grey Hill (Appendix VI, Figure 3). The middle population surrounds this, broadening to enclose the entire area of the boulder clay around Glenshanna Burn, and almost reaching the watershed on the south side of the valley, except at the foot of Alkin Hill above the powder hut. Further values in this population are found on the eastern side of Trough Hope, but in this case they do not coincide with high concentrations of other elements. It is probable that the geographical distribution of this element is partially controlled by overburden conditions resulting in relatively low concentrations in the thin porous soils of the hilltops. The highest concentrations are clearly derived from the weathering of arsenical fracture-controlled mineralisation, but taking into account the relatively high background values and the unfavourable conditions for the accumulation or retention of mobile heavy metals in the soil in the background areas it is likely that the underlying greywackes form a diffuse source of arsenic in addition to that derived from the fracture-controlled mineralisation.

After this investigation was completed, soil sampling was extended north-eastwards along strike from the area of Glendinning mine. Anomalous arsenic values were found, utilising the rapid field method of analysis described in Appendix VII, and will be described in a subsequent report.

GEOPHYSICAL SURVEYS

METHODS

Stibnite is non-conducting and non-magnetic (Telford and others, 1976; Parasnis, 1971) and therefore undetectable by the usual geophysical prospecting methods. In the mineralised structure worked at Glendinning Mine, however, it was reported to occur with galena, arsenopyrite, jamesonite and chalcopyrite (Dewey, 1920), all of which are electrical conductors. Two electrical methods were therefore used – induced polarisation (IP) and very low frequency electromagnetic (VLF–EM). Total magnetic field measurements were also made, but the only anomalies found were due to artificial sources. For the IP survey, the expanding dipole–dipole array was used, with a 30 m dipole length. The VLF–EM survey used the transmissions from Rugby, England (GBR, 18 kHz).

RESULTS OF GROUND SURVEYS

Anomalies were found with both IP and VLF–EM and are summarised on Figure 7 and Appendix VI, Figure 1. The VLF–EM results are shown as contours of the filtered in-phase component (Fraser, 1969) and the IP anomaly is given as the position of suboutcrop of high chargeability material interpreted subjectively from the pseudosections. Full geophysical profiles of the five lines on which IP measurements were made are given in Appendix IV, with pseudosections of apparent resistivity, chargeability and VLF current-density (calculated by the method of Karous and Hjelt, 1977), and profiles of VLF in-phase and out-of-phase components.

Two distinct linear trends can be recognised on the Fraser-filter contour map. The main anomaly follows the stronger trend, oriented 105°. A broad VLF–EM crossover of about 80% maximum amplitude giving Fraser-filter values of up to 60 is accompanied by a zone of high chargeability (up to 35 ms against background variations of 3 to 8 ms). The width of the source, estimated from pseudosections of chargeability and VLF current-density, is 30 to 50 m and it is probably near-vertical. The absence of steep marginal gradients on the pseudosections suggests that the source is diffuse or fails to reach the surface. In the north, the anomaly becomes confused by cultural noise, while to the south it becomes slightly weaker before running out of the area surveyed. Geophysical logs of BHs 3–4, which were drilled to investigate this anomaly, show a correlation of chargeability, conductivity and SP with fine-grained sulphide regarded as mainly stratabound on petrographic evidence (Figure 8). However, the mise-à-la-masse method failed to show electrical continuity between the mineralisation intersected by these two boreholes.

Several other VLF–EM anomalies share the 015° orientation which is the same as that of the fault lineaments in the district (see Figure 3). The strongest anomalies in fact coincide with the individual fractures or swarms of fractures. Only the main anomaly already described has significantly high chargeability but two noteworthy VLF–EM features with this trend are the double-peaked anomaly 350–400 m west of the main anomaly, and the weaker, relatively narrow feature intersected by BH4. The geo-

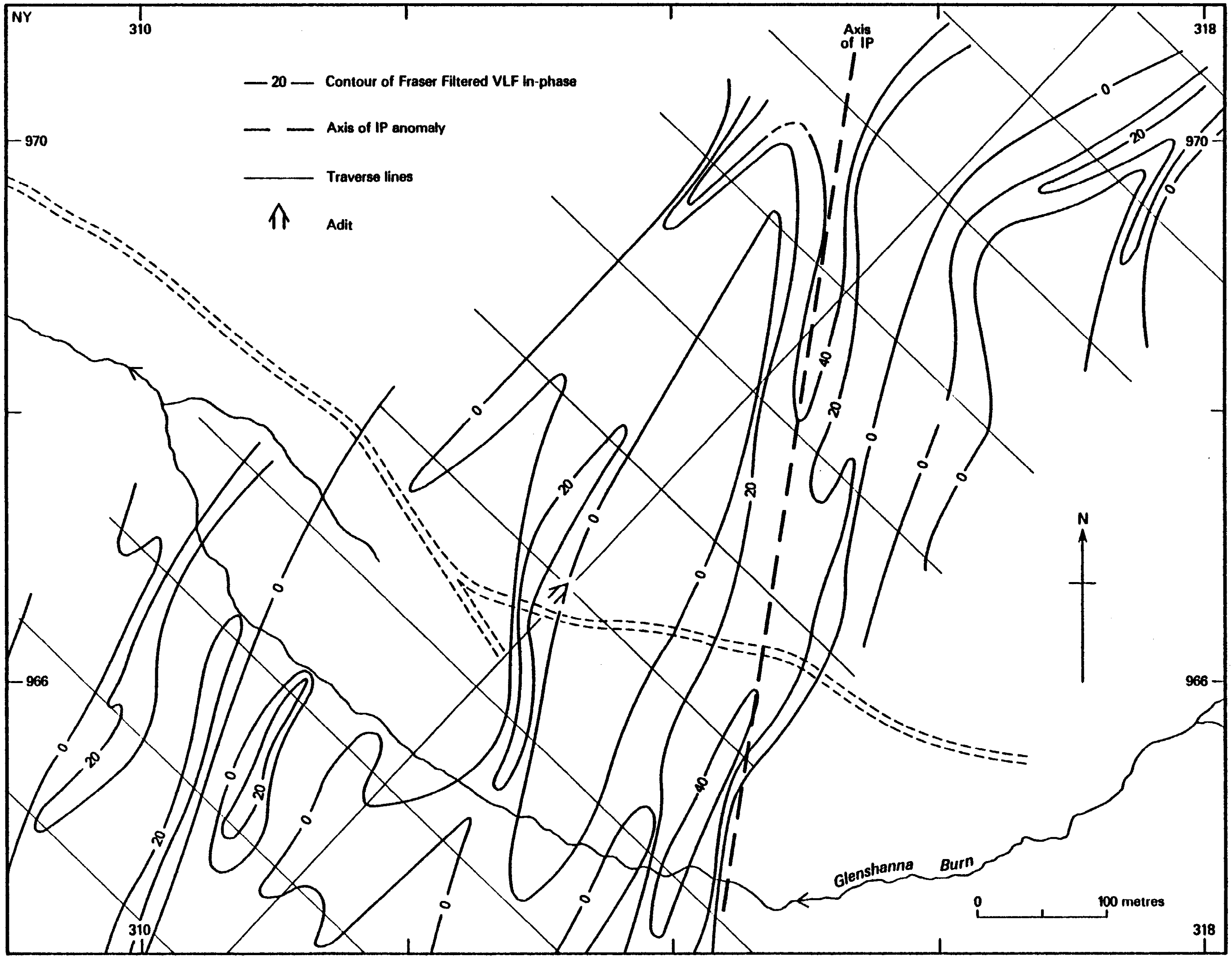

Fig. 7 VLF—EM map of the area shown in Fig. 6; IP maxima also shown

physical logs of this borehole show only a narrow zone of high chargeability, conductivity and SP, corresponding to an intersection of fine-grained stratabound sulphide (Figure 8).

The second linear trend visible on the Fraser-filter map runs roughly parallel to the geological strike and to the old workings described by Wilson (in Dewey, 1920). It is much weaker than the first trend; indeed, by subjective contouring it can be reduced to insignificance. Three main anomalous zones may be recognised, lying 150–200 m north of the baseline, approximately along the baseline, and about 150 m to its south. Two of the old workings occur at intersections of these anomalies with anomalies on the 015° trend.

BOREHOLE GEOPHYSICS

Boreholes 2, 3 and 4 were logged at 1 m intervals with a lateral IP–SP sonde. The electrode configuration was $C_2P_1P_2$ with C_2 up the hole and P_1P_2 0.105 m. Self potentials were measured relative to a stationary electrode at ground level; chargeabilities were measured over the period 150–1020 ms after switch off of a 2 second polarising pulse.

Borehole 2 was logged from 10 m to 110 m (Figure 9). Apparent resistivities ranged from 80 to 4500 ohm metres and chargeabilities range from 4 to 170 m secs. Values above 70 ms occur in three zones, 52–61 m, 70–74 m and 91–96 m. These zones also have reduced apparent resistivities down to 80 ohm metres. Anomalous zones of SP at 55 m and 93 m correlate well with IP anomalies.

Borehole 3 was logged from 6 to 190 m. Apparent resistivities ranged from 33 to 14000 ohm metres and chargeabilities from 0 to 193 ms. Numerous zones with chargeabilities above 70 ms were identified (Figure 8) and coincide closely with arsenic and therefore sulphide distribution. The form of the transient decay curve in non-mineralised sections of the borehole is substantially different from that in sulphide-rich sections and indicates a different 'IP' process in operation. SP anomalies up to 100 mV again correlate well with the anomalous zones of IP.

The IP log for BH4 (13–82 m) shows only two thin zones at 26 and 32 m with chargeabilities above 20 ms. These also show small SP anomalies and coincide very closely with the observed distribution of sulphides in the core (Figure 8).

Continuity of mineralisation between boreholes 2 and 3 was partly explored by 'mise-à-la-masse' techniques. A current electrode was placed in a zone of low resistivity at 57 m depth in borehole 2 and the sonde (with the other current electrode and the potential electrodes) was operated in BH 3. No obvious continuity was found between conductive zones in the two boreholes.

The detailed downhole logs, together with descriptions of the methods used, are available in an internal report (Rollin, 1980) from the Head, Applied Geophysics Unit, Institute of Geological Sciences, Nicker Hill, Keyworth, Nottingham NG12 5GG.

BOREHOLE RESULTS

INTRODUCTION

The shallow drilling carried out near Glendinning mine was designed to investigate the bedrock sources of closely coincident geochemical and geophysical anomalies in ground where exposure is limited to a few small outcrops of unmineralised greywacke. These anomalies are referred to as the eastern and western anomalies in the preceding text and are shown in Figures 6 and 7 together with the sites of the boreholes. Table 3 lists the general characteristics of the boreholes, and a summary of the principal metalliferous intersections obtained is given in Table 4. Details of the lithology of the drill cores and of the mineralisation they display are presented in Appendix I. Geochemical analyses of the cores are given in Appendix II together with summaries of their lithology, mineralisation and the development of features of brecciation, debris flow characteristics and faulting. The petrography and mineralogy of selected core samples are described in Appendix III.

Sections through the four boreholes (Figures 8 and 9) do not differentiate between the main lithologies of the greywacke sequence because of their gradational character and rapid alternation. Approximately 80% of the sequence is composed of grey greywacke ranging from siltstone to sandstone. Mudstone is a minor component, varying

Table 3 Location and general characteristics of boreholes

Borehole No.	Nat. Grid Ref. (NY)	Elevation m	Inclination degrees	Azimuth degrees	Depth m
1	3139 9652	290.0	50	098	85.27
2	3147 9693	380.1	50	103	118.80
3	3143 9669	317.1	60	104	197.82
4	3135 9671	316.6	50	287	84.87

All located on 1:10 560 Grid Sheet NY 39 NW

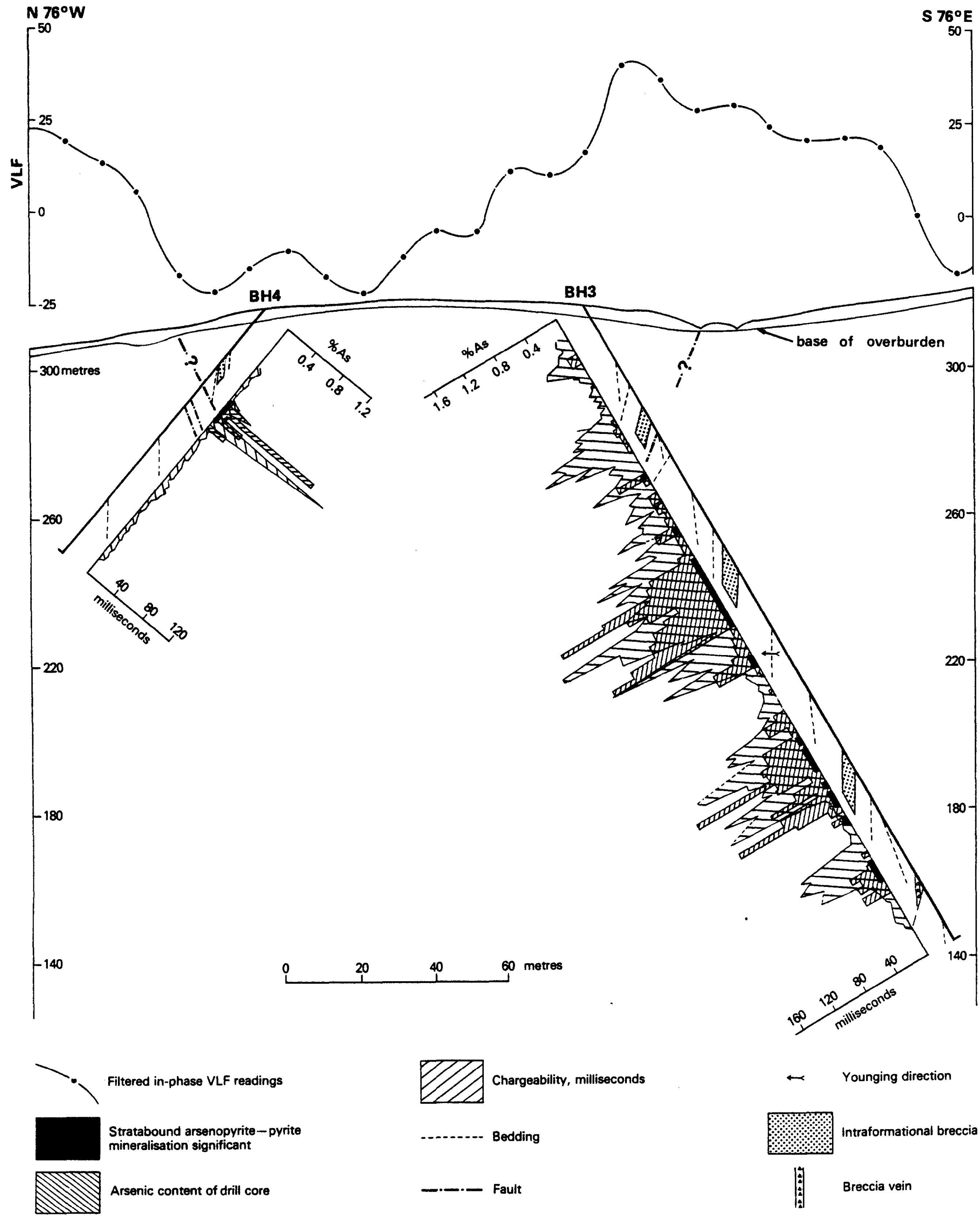

Fig. 8 Geological section through boreholes 3 and 4 at Glendinning (located on Fig. 6) showing distribution of stratabound arsenopyrite—pyrite assemblages, arsenic distribution and IP (chargeability) logs; surface VLF measurements are also given.

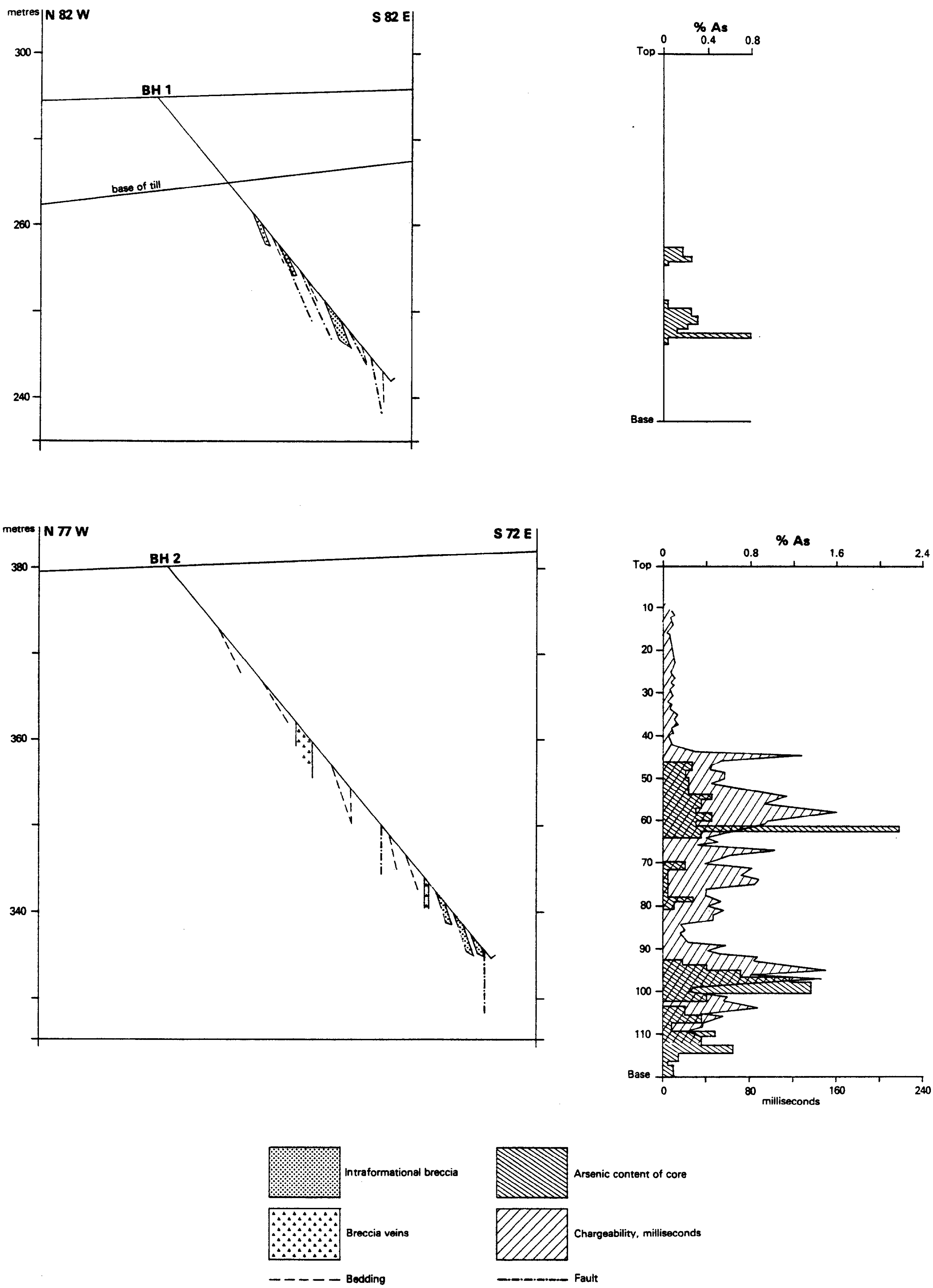

Fig. 9 Geological sections through boreholes 1 and 2 showing arsenic distribution in drillcore and the IP log of borehole 2.

Table 4 Principal metalliferous intersections in the boreholes

Borehole	Depth (m)	Inclined	True	Generalised lithology	% Fe	Cu	Zn	ppm As	Sb	Pb
1	58.99–67.37	8.38	2.2	IFB, siltstone, sandstone	4.28	28	23	2867	55	279
2 (a)	44.38–61.69	17.31	8.6	Siltstone, breccia vein, sandstone, mudstone	4.79	30	22	4226	70	35
(b)	90.77–114.73	23.96	c4	Siltstone, IFB, sandstone, breccia vein	4.34	37	23	4728	48	47
3 (a)*	73.52–107.62	34.10	11.8	IFB, siltstone, sandstone, mudstone	4.51	33	124	6880	145	315
(b)	124.22–153.05	28.83	7.3	IFB, sandstone, siltstone	4.46	35	19	5008	98	115
4	24.39–34.10	9.71	c6	Siltstone, sandstone	5.11	30	153	3098	229	505
General average			(40m)		4.55	32	60	5066	105	187

*On the basis of this intersection, the base metal (Cu:Zn:Pb) ratio of the deposit is 7:26:67

from grey to green in colour and in places stained maroon. The bedding of these lithologies is commonly disrupted and clasts of one or more types can be incorporated in a matrix of a third (note the high incidence of Feature D in Appendix II logs).

Intraformational breccias (IFBs) and breccia veins are distinctive lithologies characteristically enriched in sulphides and are, therefore, depicted in Figures 8 and 9 along with bedding plane and fault directions inferred from core measurements (see note a, Appendix I). The accompanying histograms of arsenic distribution, based on analyses of half-cores, nevertheless illustrate that arsenopyrite and arsenical pyrite (Appendix III, Table VI–VII) are also widespread in the greywackes, both as stratabound and vein minerals (Appendix II). Other sulphide minerals (see Table 6) occur in very minor amounts and are restricted to ubiquitous quartz and carbonate veinlets. The down-hole variations in chargeability for BHs 2–4 correspond closely to the distribution of arsenic which, as can be seen from Figure 9, is essentially controlled by the observed incidence of stratabound arsenopyrite and pyrite.

Core recovery of 99% or better was achieved throughout the drilling, despite the faulted and brecciated nature of much of the rock. Coring in the important intraformational breccias was complete and bedrock was successfully intersected beneath thick boulder clay in BH 1.

BOREHOLE 1

This hole was collared in drift filling the valley of Glenshanna Burn and inclined eastwards to cut the eastern anomaly near its southern end (Appendix VI, Figure 1). Boulder clay persisted to an inclined depth of 26 m and clay-rich bands within it carry higher values of arsenic, antimony and lead than the topmost bedrock (cf. results for CXD 1001–1004 with those for CXD 1005–1007, Appendix II, Table I). Bedding apparently dips at 70°E or steeper and is accompanied by several faults (Figure 9).

Arsenopyrite and pyrite, both stratabound and vein in type, are best developed over some 2 m of IFB and adjoining greywacke at about 50 m below surface. Lead values are somewhat enhanced and traces of stibnite occur in veinlets together with dickite. Gold was detected at the 0.01–0.1 ppm Au level in three of five samples analysed, and traces of mercury are present (Appendix II, Table V).

BOREHOLE 2

This hole was sited in weathered bedrock on the south side of Grey Hill some 400 m NNE of BH 1 to intersect the northern part of the eastern anomaly. Bedding is less steeply inclined in the upper and lower sections of the borehole, suggesting folding, while faulting is less common than in BH 1.

Mineralisation of significance commences some 35 m below surface. A 2 m-thick breccia vein containing disseminated pyrite and arsenopyrite (evidenced by high iron values and low calcium values in samples CXD 1131–1132, Appendix II, Table II), is accompanied by sulphide disseminations in adjacent greywackes, yielding an 8.6 m intersection averaging 0.42% As which extends to 48 m below surface. A second thick zone of stratabound sulphide occurs at 70–90 m below surface in greywackes, IFB units and a breccia vein (Table 4 and Figure 9). Because the dip of the bed appears to be almost the same as that of the borehole (50°) the true thickness of this zone is estimated to be only about 4 m. The contents of antimony and base metals in the sulphide zones intersected by BH 2 are unexceptional.

BOREHOLE 3

A borehole drilled midway between BHs 1 and 2 to intersect the IP maximum associated with the eastern anomaly proved to be the most successful of the four. Pyrite and arsenopyrite, mostly stratabound in character, occur through several tens of metres of rock, although variations in the apparent dip in the upper and lower parts of the section (Figure 8) may signify repetition by folding. A fault at around 40 m inclined depth is a further source of complication. This fault may extend eastwards to surface where a small topographic depression follows the 015° direction of faulting characteristic of the district. A westerly younging direction was inferred from graded bedding observed in the greywackes at 109 m inclined depth.

The highest sulphide concentrations are in two well developed IFBs at around 65 m and 120 m below surface. The upper one is about 4 m thick and together with 8 m of adjoining greywackes grades 0.69% As. Antimony, lead and zinc are somewhat enriched in this zone while calcium is depleted relative to less mineralised rocks higher in the borehole (Appendix II, Table III). The lower IFB is probably 3 m in thickness and when included with 4–5 m of adjacent greywackes yields a grade of 0.5% As (Table 4). Calcium is again depleted but the levels of antimony and base metals are unexceptional. A third zone of lower but nevertheless significant arsenic content is associated with a breccia vein or IFB about 1 m thick 150 m below surface.

The borehole was terminated in greywackes carrying only traces of pyrite and stibnite, but further concentrations of stratabound sulphide may occur at greater depth.

BOREHOLE 4

The final borehole was collared 56 m north-east of the main adit portal and drilled westwards to intersect the western geochemical-geophysical anomaly. In the roof of the portal 0.5 m of brecciated greywacke is exposed trending approximately 030°. This structure is probably represented in the zone of faulting intersected at 25–34 m inclined depth where the only mineralisation of note in BH 4 is developed (Figure 8). Pyrite and arsenopyrite are disseminated through the broken greywackes and also occur in veinlets with semseyite, bournonite and sphalerite, thus accounting for the relatively high values of antimony, lead and zinc in this intersection (Table 4). The estimated thickness of 6 m for this faulted zone of mineralisation is based on measurements of bedding in unfaulted, apparently vertical strata elsewhere in the borehole (Appendix I, Table IV). Analyses of four samples from the mineralised zone show that traces of mercury and in one instance a trace of gold are present (Appendix II, Table V).

PETROGRAPHY

NOMENCLATURE

The predominent lithological type is greywacke. Following Warren's (1963) definition of greywacke as 'a rock comprising poorly sorted angular rock and mineral fragments ranging from sand to conglomerate set in a substantial matrix of finer material', the term has been further augmented and greywacke-sandstone is used to denote those rocks which are of sand grade. The terms greywacke-siltstone and greywacke-mudstone are used to denote those rocks which are below sand grade but which are otherwise comparable with greywackes. These rocks frequently form part of the same sedimentary unit in that the greywacke-siltstone and greywacke-mudstone form the top part of a graded greywacke bed. For brevity, the prefix 'greywacke' has been omitted in the following account.

SANDSTONES

These rocks are mainly grey in colour but when weathered they become greenish-grey or brownish (e.g. CXD 1537, Appendix III, Table I). Quartz is the dominant mineral. It is generally angular to sub-angular and ill-sorted and frequently displays undulose strain extinction.

Albite-oligoclase is a minor constituent, forming grains which are always smaller and more rounded than those of quartz. Traces of potassic feldspar are also present, and many of the grains are cloudy due to sericitic alteration. Almost total replacement of feldspar by carbonate is not uncommon.

Chlorite occurs probably as a replacement of earlier ferromagnesian mineral fragments and is also assumed to be present in the turbid, undifferentiated matrix, together with small sericite flakes. Large shreds of muscovite showing strained optical characters are of frequent occurrence. Many specimens contain abundant detrital biotite which is invariably altered to hematite. Some of the flakes were isolated and identification as hematite confirmed by X-ray diffraction (CXD 1531, Appendix III, Table III).

Ferroan dolomite is the most abundant carbonate mineral present. It is a major constituent of the matrix of most of the sandstones although in some instances (e.g. CXD 1537, Appendix III, Table I) it is conspicuous by its absence. As a matrix component it is generally very fine grained and as such its distribution throughout the matrix is only apparent after staining. The mineral is also observed replacing some of the sandstone components such as the feldspars and rock fragments and in some instances replacement has been almost total, thus masking much of the fabric and mineralogy. A second carbonate component again consisting of ferroan dolomite, is associated with epigenetic veins where it occurs as large inter-

Table 5 Modal analyses of greywackes

CXD No.	1518	1505	1506	1537	1517	1541	1526
PTS No.	5865	5852	5853	5859	5864	5874	5871
Quartz	37.20	40.40	51.86	41.86	51.86	35.26	57.73
Feldspar	0.06	1.06	1.46	1.53	0.13	0.13	0.20
Sulphide	0.86	1.33	0.26	0.66	0.53	6.20	1.73
Iron oxide	0.06	0.06	0.73	0.86	0.33	–	–
Tourmaline	0.06	0.13	0.13	0.13	0.06	–	–
Zircon	0.13	0.73	0.26	0.20	0.06	0.33	0.06
Matrix including dolomite	59.0	51.53	44.73	54.20	46.40	56.80	38.86
Rock fragments:							
Acid igneous	–	–	–	–	0.06	–	0.13
Basic igneous	–	–	0.06	0.06	–	–	–
Sedimentary	2.26	2.53	0.26	0.33	0.33	0.33	0.20
Metamorphic	0.33	1.66	0.20	0.20	0.20	0.93	1.06
TOTAL %	99.96	99.97	99.96	99.96	99.96	99.98	99.97

Based on counts of 1500 points on each specimen

locking rhomb-shaped crystals. Wall rock alteration is associated with these carbonate veins and can be quite intense, extending as a front of waning intensity, usually over distances of 0.5 to 1.5 cm.

Carbonate replacement, the most extensive of the chemical changes affecting the wall rock at Glendinning, is a regional phenomenon. Rust (1965b) and Weir (1974) describe intense carbonate replacement in Silurian greywackes from south-west Scotland, and consiser that the often patchy carbonate distribution and subsequent replacement may be due to the redistribution of primary material in the sediments. On this basis the matrix dolomite in the sediments at Glendinning may be considered to be of synsedimentary and/or diagenetic origin.

Iron oxide (hematite) occurs throughout the rocks, predominantly as a replacement of biotite and pyrite. It also probably accounts for the red iron staining on most of the rock surfaces and the russet colour of the sub-microscopic matrix. Minor amounts of detrital zircon and tourmaline were noted in most sections.

Small numbers of rock fragments, mainly of sedimentary type, are present in most of the sections examined. However, as already stated, diagenetic carbonate replacement has often been intense so that the composition of many fragments is conjectural. The fragments considered to be of metamorphic origin are usually coarse quartz aggregates which exhibit variegate extinction. Some extremely fine-grained siliceous fragments, tentatively classed as acid igneous in type, could alternatively represent a fine-grained metamorphic rock or even chert fragments. Two fragments of black glass with feldspar phenocrysts representing basic igneous rocks, were also recognised.

Modal compositions of seven sandstones (Table 5) do not correspond to normal greywacke because of carbonate replacement. The matrix contains quartz, chlorite, mica, clay mineral (illite) and hydrated iron oxides as well as dolomite. The nature of the sulphides present is discussed later in the report.

SILTSTONES

These are normally greenish-grey, laminated rocks which are essentially a fine-grained equivalent of the sandstones; the grain size is between that of fine sand and silt. Identification of contained rock fragments is very difficult because of their small particle size.

MUDSTONES

The mudstones in the drill cores are greenish-grey to dark grey or reddish in colour. Cleavage is not well developed but they are frequently laminated with bands measuring 0.5 to 2 mm in width. Some of the mudstones (e.g. CXD 1507, Appendix I, Table I) contain lenses of a more silty character which imparts a distinctive, discontinuous streakiness to the rock. The colour of these pelagic sediments reflects slight differences in mineralogy. Those of greenish aspect are more rich in chlorite while reddish varieties contain abundant hydrated iron oxide. Compositionally the mudstones may be considered as being similar to the matrix of the sandstones. Bulk XRD analysis (CXD 1565, Appendix III, Table III) indicates a composition of quartz, dolomite, illite and a trace of hydrated iron oxide.

INTRAFORMATIONAL BRECCIAS

The breccias are dark grey in colour and consist of large angular fragments of mudstone, siltstone and sandstone. The finer-grained members are frequently strongly sericitised and appear greenish in colour. These fragments frequently contain abundant thinly banded and disseminated pyrite and arsenopyrite (e.g. CXD 1558, Appendix I, Table II). The matrix usually consists of coarsely crystalline quartz with traces of carbonate and abundant disseminated pyrite and arsenopyrite. In one instance (CXD 1566, Appendix I, Table II) have a reddish appearance which can be arsenopyrite with a trace of carbonate. These brecciated rocks are invariably dissected by many discontinuous carbonate veinlets which also contain small amounts of pyrite and arsenopyrite. Some breccias (CXD 1562, Appendix III, Table II) have a reddish appearance which can be attributed to the presence of hematite possibly formed by circulating groundwater. The form and distribution of the sulphide minerals in these rocks is described later in the report.

Where unaffected by tectonic shearing, veining and fracturing, certain intraformational breccias display the characteristics of debris flows as described by Middleton and Hampton (1973), namely

a. a matrix supported framework,
b. a texture which is internally structureless, and
c. an unsorted and wide range of clast size.

Typical examples are found in BH 3 (75–83 m and 134.7–140.6 m) and BH 4 (15.06–16.19 m).

Some of the clasts of siltstone and fine-grained sandstone in the debris flows contain veins which apparently do not persist into the more mud-rich matrix, suggesting incorporation of clasts from a lithified and veined sequence removed from the area of debris flow deposition. However, many of the clasts in the debris flows seem very similar to material in the bedded greywacke sequence, suggesting a local provenance.

CLASSIFICATION OF THE TURBIDITE SEQUENCE

Although there has been no recent sedimentological study of the Silurian rocks of southern Scotland, a broad interpretation of the sequence observed in the borehole cores can be made based on existing models of turbidite fan sedimentation (e.g. Walker and Mutti, 1973). Most of the sediment comprises classical proximal turbidites (typically Ta, e) and classical distal turbidites (typically, Tc, d, e), facies C and D respectively (see Figure 10). Debris flows and slumped horizons (facies F) occur at various positions evidencing downslope mass movement (see below). Local mudstone dominant sections, especially in BH 4 may represent basin–plain or mainly pelagic sedimentation.

The high proportion of facies C and D together with the predominance of fine to very fine sandstone and coarse siltstone suggest a depositional environment ranging from mid fan (depositional lobes) to outer fan for most of the sequence. The presence of crude thickening and coarsening upward sequences (as in Figure 10a) supports this interpretation. Although major slumping and thick debris flows are generally confined to the inner fan environment, minor occurrences are not uncharacteristic of mid-outer fan areas (e.g. Ricci–Luchi, 1975).

The sediment in the boreholes displays a comprehensive range of features indicating downslope movement, from disrupted bedding involving extensional deformation (e.g. boudinage) through slump folds to debris flows. This represents a consistent progression and might further suggest that the debris flows represent truly *intraformational* deposits (i.e. they are derived from the same formation) as opposed to being derived from older sources. The observed thickness range (⩽4 m) also suggests that they may be local deposits.

ORE MINERALOGY

INTRODUCTION

The composition of the worked antimony mineralisation at Glendinning can now only be gauged from dump material and especially from ore fragments remaining on two small sorting floors (Figure 6). The mineral composition of a small number of sorting floor specimens is summarised in Appendix III (Table V). Early records of the lead-antimony sulphide semseyite (Smith, 1919) and of the antimony oxide valentinite (Dewey, 1920) have been confirmed (MacPherson and Livingstone, 1982) but not those of jamesonite, kermesite and cervantite (Dewey, 1920). Material named jamesonite and cervantite in the Royal Scottish Museum collections are respectively zinkenite and stibiconite (MacPherson and Livingstone, 1982). Traces of valentinite and kermesite may be present in the borehole cores but their identification has not been validated by X-ray studies.

The mineral assemblage recorded in this investigation, based on examination of borehole cores, is listed in Table 6 and in the following sections the main characteristics of the sulphide minerals are described. Figure 11 summarises the paragenetic sequence proposed for the strata-bound and vein mineralisation at Glendinning.

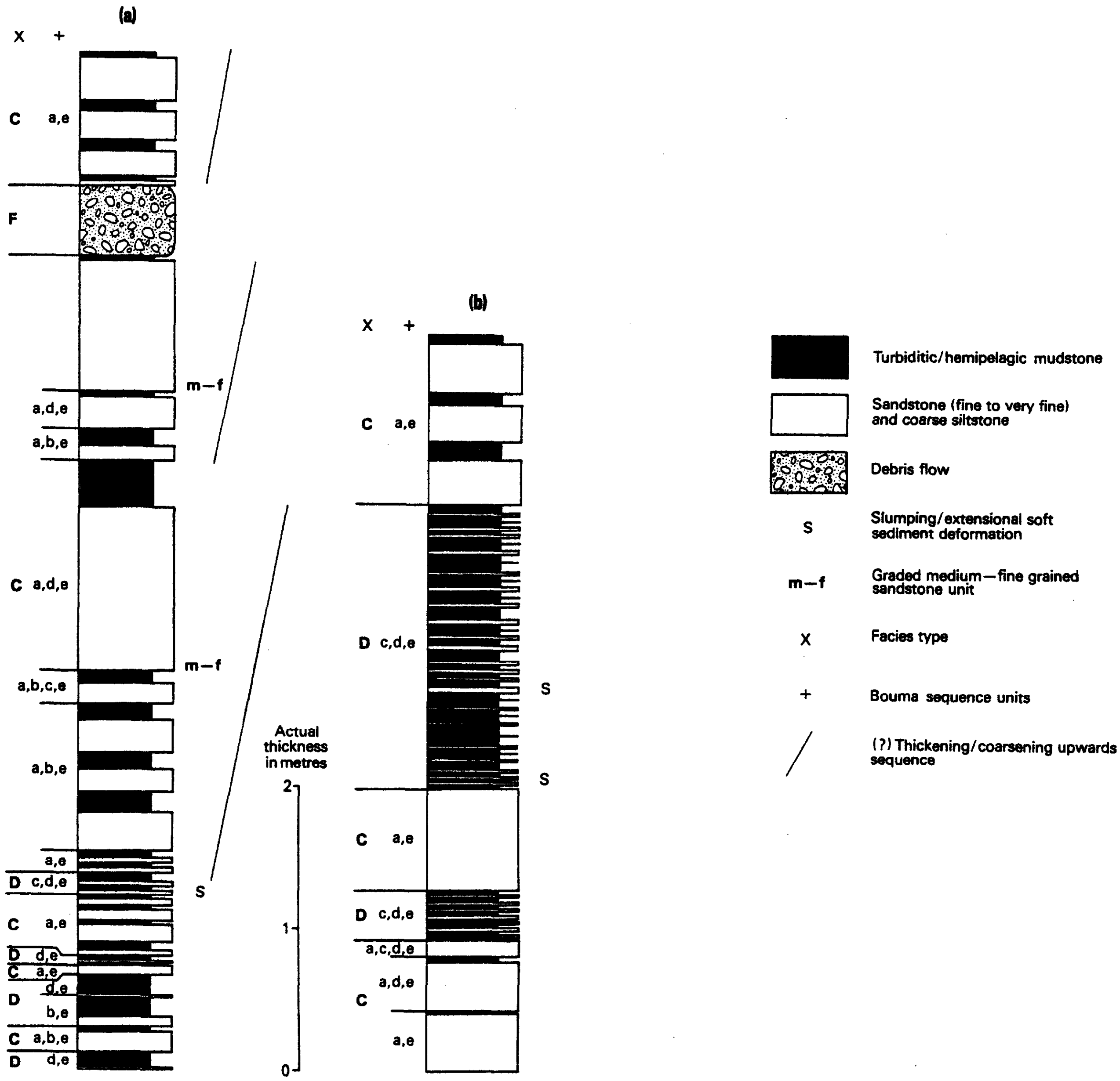

Fig 10 Classified greywacke sequences from the Silurian at Glendinning: (a) BH4, 7.7–17·4 m inclined depth, (b) BH3, 191.3 (stratigraphic base) – 181.0m inclined depth. Facies type after Walker and Mutti (1973)

Table 6 Minerals recognised from drill core, boreholes 1–4

Silicates	*Sulphate*
Quartz	Baryte
Plagioclase	
Potassic feldspar	*Sulphides*
Biotite	Pyrite*
Sericite	Arsenopyrite*
Muscovite	Galena
Chlorite (not differentiated)	Sphalerite
Illite	Semseyite
Dickite	Bournonite
Tourmaline	Chalcopyrite
Zircon	Stibnite
	Tetrahedrite
Oxides	Tennantite
Hematite	
Goethite	*Others*
?Valentinite	Apatite
?Kermesite	Undifferentiated hydrated iron oxides
Carbonates	
Dolomite	
Calcite	
Aragonite	

*Sulphides found in both stratiform and vein assemblages

SULPHIDES

Pyrite

Recognised by its colour – pale brass yellow – splendent lustre and crystal habit, the cube [100] and the pyritohedron [210] being dominant. As stratabound mineralisation pyrite can form massive bands of euhedral to subhedral crystal aggregates (0.1–1.5 mm grain size), but it is more commonly disseminated throughout the rocks in grains up to 0.5 mm across. Pyrite was also noted as disseminated globular crystals (up to 0.5 mm diameter), and more rarely as euhedral crystals in later epigenetic quartz and carbonate veins.

Following the method of Ramdohr (1969, p. 781) several thin sections were etched in a solution of H_2SO_4+$KMnO_4$ which enabled structural and textural features to be observed. The interlocking pyrite grains of the stratabound bands as well as the euhedral to sub-euhedral disseminated variety generally display well-developed, oscillatory zoning. However, in some instances this textural feature is absent; Ramdohr (op. cit.) has suggested that the results obtained by this etching method may not be uniform and there is also the possibility that lack of zoning may be due to slight differences in composition or recrystallisation. The globular pyrite grains are unzoned but etching appears to highlight their concentric mode of growth.

Electron microprobe analyses of trace elements in the pyrite from Glendinning (Appendix III, Tables VI–VII) revealed cobalt values of up to 2140 ppm, nickel up to 4990 ppm, and As values which match the highest to be recorded in pyrite (5% As) by Vaughan and Craig (1978, p. 362). Copper values reach 780 ppm. Silver and selenium were below detection limits but antimony reached 1470 ppm. However, apart from arsenic, trace element values were variable with highest Co and Ni values occurring in the same grains. High arsenic values were also recorded in euhedral pyrite disseminated and in veins, and also in globular pyrite.

Arsenopyrite

Characterised by its silver-white colour, metallic lustre and prismatic habit: (0.2–5.0 mm grain size). In reflected light a polished surface of the mineral displays blue-green-brown anisotropy. Electron microprobe analyses of the arsenopyrite (Appendix III, Table VIII–IX) indicate Co and Ni values comparable with those obtained from pyrite. The antimony level is appreciable (up to 5000 ppm) and copper reached 540 ppm.

Sphalerite

Typified by its translucent brown to yellow colour, resinous lustre, highly perfect cleavage and cubic habit.

Galena

Recognised by its lead-grey colour, metallic lustre, perfect cleavage and cubic habit.

Bournonite ($2PbS. Cu_2S. Sb_2S_3$)
Characterised by its steel-grey colour, brilliant metallic lustre, brittle nature (H=2.5) and distinctive prismatic habit. Individual crystals are often traversed by minute cracks. Under reflected light, a polished surface of the mineral displays a characteristic greenish tint. MacPherson and Livingstone (1982) note the presence of 0.2% Sn in bournonite occurring in sorting floor material.

Semseyite ($9PbS. 4Sb_2S_3$)
This mineral was identified only in one sample (CXD 1533, Appendix III, Table IV) after crushing and X-ray diffraction of tiny dark grey to black prismatic crystals. It is most probably a constituent of a veinlet in the sample.

Stibnite
Typically observed as steel-grey films or 'blooms' on fracture surfaces, many of which are associated with carbonate veinlets. Very rarely seen as confused aggregates of acicular dark grey crystals (CXD 1543, Appendix III, Table III). The mineral has a metallic lustre and is subject to a black tarnish. Under reflected light stibnite exhibits very strong blue anisotropy.

Chalcopyrite
Recognised by its brass-yellow colour which is often tarnished or irridescent, chalcopyrite occurs only rarely in the cores and only as a vein constituent.

Tetrahedrite (Cu_3SbS_3)
Characterised by its appearance in veins as a flint-grey mineral with a typical tetrahedral habit. Identification was confirmed by X-ray powder photography (Ph 6460: CXD 1576).

Tennantite (Cu_3AsS_3)
This mineral is isomorphous with tetrahedrite but was distinguished by X-ray powder photography (Ph 6477: CXD 1592).

Cinnabar
Recognised by its striking cochineal-red colour, adamantine lustre and low hardness (about 2). The mineral was noted as a minor accessory in panned stream sediment concentrates and its previous transport history had removed any distinct crystal morphology.

MINERALISATION

STRATABOUND MINERALISATION

The stratiform pyrite-arsenopyrite mineral assemblage displays textural features supporting a synsedimentary origin. Perhaps the most obvious feature is the frequent concentration, particularly in the fine-grained lithologies, of pyrite and arsenopyrite in individual bands that lie parallel to the original bedding. Further textural evidence for synsedimentary mineralisation is provided by the intraformational breccias which are considered to have formed by penecontemporaneous fragmentation and redeposition of sulphide sediment and sulphide mud as a result of sediment instability and turbidity flow.

The sulphide-rich bands range up to 8 mm in thickness (e.g. BH2, 46.2 m CXD 1536) and the pyrite from these bands displays strong zoning. Wheatley (1977), with reference to sulphides from Avoca Mine in Ireland, suggests that primary, zoned crystalline pyrite implies growth below the sediment-water interface in a low pH environment supersaturated with iron. It seems very probable that the primary zoned pyrite at Glendinning was formed in a euxinic environment and that the arsenopyrite which is intimately associated with the pyrite is also of synsedimentary origin.

It is generally acknowledged that the Co:Ni ratio in pyrite provides an indicator of the origin of the pyrite (Willan and Hall, 1980). Electron microprobe analyses of the Glendinning pyrite show variable levels of Co (up to 2000 ppm) and Ni (up to 5000 ppm) and low Co:Ni ratios (<6). Willan and Hall (1980) plotted average Co:Ni values of pyrite from some stratiform deposits of exhalative-synsedimentary origin and other types of mineralisation (e.g. pyrite from veins, sedimentary and diagenetic pyrite) and plots of the Co:Ni ratios from Glendinning fall within their field of stratiform deposits of exhalative-synsedimentary origin.

The Sb values in the arsenopyrite and, to a lesser extent, the pyrite, indicate that this element was a significant component of the metals present in the mineralising fluids. It thus seems probable that the antimony present in the later fracture-hosted veinlets as stibnite and other sulphides is of local derivation having been remobilised from the stratabound material. However, the possibility that stibnite or other antimony minerals occur as stratiform constituents cannot be ruled out.

The highest metal values may in part at least be due to derivation of cobalt and nickel from basic rocks of the Iapetus oceanic plate. The lower nickel values are imprecise because they occur near or below the analytical limit of detection. The cobalt values remain relatively high and plot close to those of certain exhalative copper and copper-zinc deposits on Willan and Hall's (1980) Co—Ni diagram. However, the arsenic content of the Glendinning sulphide assemblage is much higher than in the deposits considered by Willan and Hall (1980) so that it is not possible to derive a clear indication of genesis from these data.

VEIN MINERALISATION

The second phase of sulphide mineralisation was probably effected by CO_2 and SiO_2-bearing aqueous solutions which invaded fractures in the rocks. The resultant veinlets post-date Caledonian deformation features such as folds and cleavages, but their upper age limit is uncertain. The network of veins is complex and at least three episodes of veining took place (Figure 11): (a) dolomite with a trace of quartz and minor amounts of pyrite, arsenopyrite, galena, bournonite, sphalerite, semseyite, chalcopyrite, tetrahedrite and tennantite; (b) later quartz, with traces of dolomite and minor amounts of pyrite and arsenopyrite, and (c) late-stage fracture-hosted dolomite veins containing stibnite usually in the form of 'blooms' or films, which post-date veins (a) and (b).

The identification of cinnabar in panned concentrates from the area suggests a possible but as yet unobserved association of this mineral with the stibnite. Antimony–mercury mineralisation is well documented, for example Maucher and Höll (1968) describe the antimony ore of Schlaining, Austria which occurs in metamorphosed sedimentary (and volcanic) rocks in which phyllites, limestone, dolomites and quartzites predominate. Arsenopyrite and pyrite are constantly associated with the stibnite ore with local concentrations of cinnabar. Muff (1978) considers this association to be strikingly similar to that in the Murchison Range of the north-eastern Transvaal, South Africa. Despite the metamorphic grade of the above examples, the lithologies at Glendinning are not dissimilar, so an antimony–mercury mineral association is perhaps not entirely out of the question.

The mineralisation observed in the drill core is in some respects similar to that collected from the sorting floors related to the worked vein. The stratiform pyrite-arsenopyrite assemblage is however absent from the sorting floor specimens, in which veins containing stibnite, sphalerite and galena, together with traces of pyrite and arsenopyrite, occur in a quartz-dolomite gangue. The fact that in the drill core stibnite was only seen embedded in carbonate in tiny veinlets which postdate the earlier sphalerite-galena-pyrite-arsenopyrite sulphide mineralised veins suggests either that stibnite formation occurred during two separate events or that in the worked vein the enrichment was more intense and as such masks the order of formation.

CONCLUSIONS

The metal values of the principal mineralised intersections obtained at Glendinning (Table 4) all lie well below present economic grades. Arsenopyrite is the main constituent of economic interest, but only locally does it exceed a few percent of the rocks. The best intersection of arsenopyrite mineralisation is in BH3 where an average grade of 0.69% As is present over 34 m of drillcore, representing a true width of about 12 m. Within this intersection the highest grade is 1.45% As over about 1 m of IFB. The antimony content of this narrow section is only 125 ppm Sb, most of which is probably held in the arsenopyrite lattice. Antimony is highest (0.1%) in the BH4 intersection which is probably related to the worked structure and is accompanied by 1.3% As, 0.3% Pb, 0.08% Zn and 0.1 ppm Au over approximately 0.5 m of greywacke.

The main significance of the results of the limited amount of shallow drilling carried out at Glendinning lies in the recognition of a new type of mineralistion in Britain, namely stratabound arsenopyrite–pyrite mineralisation in a Silurian greywacke sequence. The stratabound sulphides are developed through at least a few tens of metres of succession and over at least a few hundreds of metres of strike-length. They were followed by a subordinate phase of NNE–trending vein mineralisation containing antimony and base metal sulphides.

The mineralisation at Glendinning shares many features in common with that reported from the Clontibret area, County Monaghan, some 250 km south-westwards along the regional Silurian strike in Ireland (Cole, 1922; Anglo United Development Corporation Limited, 1980). Stibnite was worked on a very small scale at Clontibret from a narrow quartz vein in Silurian sediments following its discovery in 1774 and the mines were reopened in 1917. Modern exploration has demonstrated that arsenopyrite mineralisation extends for at least 1.5 km along the regional ENE–WSW strike, as well as occurring in narrow NNE–trending veins. The main interest is in gold with occurs both in the veins and in the strike-related mineralisation.

In view of the considerable mineralised strike-length found at Clontibret and the distinctive gold association, further study of the Glendinning mineralisation and of its possible strike extension is merited. Although antimony minerals of strata-bound type were not observed in the present investigation, the elevated antimony content of the stratiform arsenopyrite and the spatial association of the vein and stratabound mineralisation suggest a common source for the arsenic and antimony. How these metals were concentrated in a turbidite sequence, however, is uncertain. Reimann and Stumpfl (1981) ascribe the formation of stratabound stibnite mineralisation in Lower Palaeozoic rocks of Austria to exhalative activity associated with submarine volcanicity, but in the Glendinning area volcanic rocks are unknown.

ACKNOWLEDGEMENTS

This investigation was made possible by the close cooperation of Lt Col R. P. Johnson-Ferguson of Westerkirk Mains, Bentpath, Langholm. Numerous colleagues in the Institute assisted at various stages in the investigation.

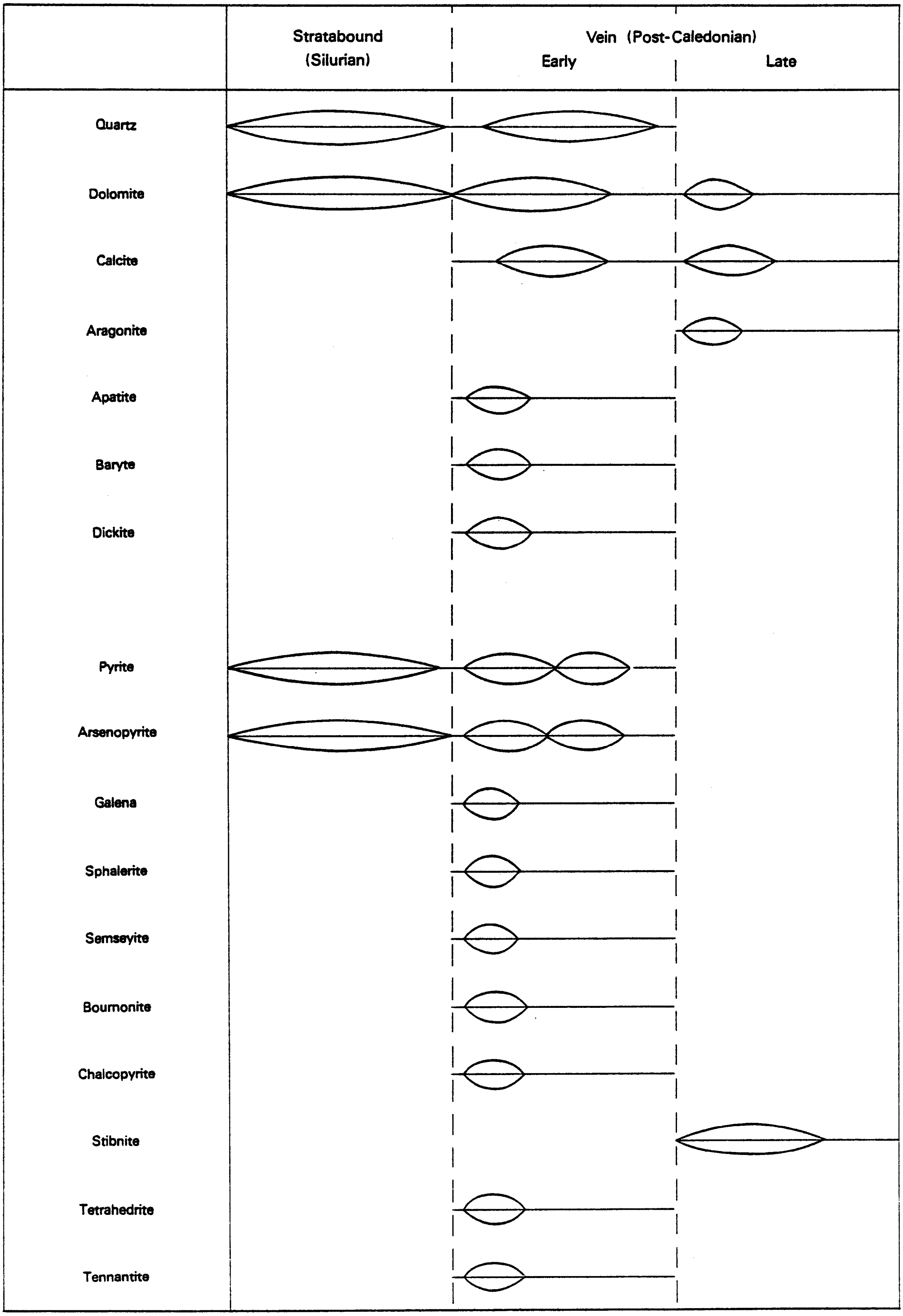

Fig. 11 Mineral paragenesis in the Silurian greywacke sequence and associated mineralisation at Glendinning

REFERENCES

Anglo United Development Corporation Limited. 1980. 31st Annual Report. 20 pp.

Cole, G. A. J. 1922. Memoir and map of localities and minerals of economic importance and metalliferous mines in Ireland. *Mem. Geol. Surv. Ireland*, pp. 14 and 96.

Craig, G. Y. and Walton, E. K. 1959. Sequence and structure in the Silurian rocks of Kirkcudbrightshire. *Geol. Mag.*, Vol. 96, pp. 209–220.

Dewey, H. 1920. Arsenic and antimony ores. *Mem. Geol. Surv. Rep. Min. Res.* GB, Vol. 15, 59 pp.

Dewey, J. F. 1969. Evolution of the Appalachian/ Caledonian Orogen. *Nature*, (London), Vol. 222, pp. 124–129.

— 1974. The geology of the southern termination of the Caledonides. In **Nairn, A. E. M.** (editor), *The ocean basins and their margins.* Vol. 2. The North Atlantic. (New York and London: Plenum Press), pp. 205–231.

Fraser, D. C. 1969. Contouring of VLF–EM data. *Geophysics*, Vol. 34, No. 6, pp. 958–967.

Gallagher, M. J. and others. 1977. Lead, zinc and copper mineralisation in basal Carboniferous rocks at Westwater, south Scotland. *Miner. Reconnaissance Programme Rep. Inst. Geol. Sci.*, No. 17, 80 pp.

Harris, A. L., Baldwin, C. T., Bradbury, H. J., Johnson, H. D. and Smith, R. A. 1978. Ensialic basin sedimentation: the Dalradian Supergroup. In **Bowes, D. R. and Leake, B. E.**, (editors) Crustal evolution in Northwestern Britain and adjacent regions. *Geol. J. Spec. Issue* No. 10, pp. 115–138.

Karous, M. and Hjelt, S. E. 1977. Determination of apparent current density from VLF measurements. *Dept. of Geophysics, University of Oulu. Oulu Contribution No. 89.*

Kennedy, M. J. 1975. The Fleur de Lys Supergroup: stratigraphic comparison of Moine and Dalradian equivalents in Newfoundland with the British Caledonides. *J. Geol. Soc.* (London), Vol. 131, pp. 305–310.

Lagios, E. and Hipkin, R. G. 1979. The Tweeddale Granite – a newly discovered batholith in the Southern Uplands. *Nature*, (London), Vol. 280, pp. 672–675.

Leake, R. C. and Aucott, J. W. 1973. Geochemical mapping and prospecting by use of rapid automatic X-ray fluorescence analysis of panned concentrates. In **M. J. Jones**, (editor) *Geochemical Exploration.* (London: IMM), pp. 389–400.

— **and others.** 1978. A geochemical drainage survey of the Fleet granitic complex and its environs. *Miner. Reconnaissance Programme Rep. Inst. Geol. Sci.*, No. 21, 30 pp.

Leggett, J. K., McKerrow, W. S. and Eales, M. H. 1979. The Southern Uplands of Scotland: a Lower Palaeozoic accretionary prism. *J. Geol. Soc.* (London), Vol. 136, pp. 755–770.

Lumsden, G. I. and others. 1967. The geology of the neighbourhood of Langholm. *Mem. Geol. Surv. Scotland*, 255 pp.

MacPherson, H. G. and Livingstone, A. 1982. Glossary of Scottish mineral species. *Scott. J. Geol.*, Vol. 18, pp. 1–47.

Maucher, A. and Holl, R. 1968. Die Bedeutung geochemisch-stratigraphischer Bezugshorizonte für die Alterstellung der Antimonitlagerstätte von Schlaining im Burgenland, Österreich. *Min. Deposita*, Vol. 3, pp. 272–285.

McKerrow, W. S., Leggett, J. K. and Eales, M. H. 1977. Imbricate thrust model of the Southern Uplands of Scotland. *Nature*, (London), Vol. 267, pp. 237–239.

Middleton, G. V. and Hampton, M. A. 1973. Sediment gravity flows: mechanics of flow and dispersion. In *Turbidites and Deep Water Sedimentation* (S.E.P.M. Pacific Section, Short Course), (Anaheim), pp. 1–38.

Muff, R. 1978. The antimony deposits of the Murchison Range of the North-eastern Transvaal, Republic of South Africa. *Monograph Ser. Min. Deposits*, Vol. 16, (Geb. Born.), pp. 1–90.

Parasnis, D. S. 1971. Physical property guide for rocks and minerals. *ABEM Geophysical Memorandum 4/71.* (Stockholm: Atlas Copco Abem.)

Peach, B. N. and Horne, J. 1899. The Silurian rocks of Britain, Vol. 1, Scotland. *Mem. Geol. Surv.*

Peachey, D., Leake, R. C. and Vickers, B. P. 1982. A rapid field method for the estimation of arsenic in soil and drill sludges. *Rep. Inst. Geol. Sci.*, No. 82/1, pp. 68–70.

Phillips, W. E. A., Stillman, C. J. and Murphy, T. 1976. A Caledonian plate tectonic model. *J. Geol. Soc.* (London), Vol. 132, pp. 579–609.

Ramdohr, P. 1969. *The ore minerals and their intergrowths.* (Pergamon Press), 1174 pp.

Reimann, C. and Stumpfl, E. F. 1981. Geochemical setting of strata-bound stibnite mineralisation in the Kreuzeck Mountains, Austria. *Trans. Instn. Min. Metall. (Sect. B: Appl. Earth. Sci.)*, Vol. 90, pp. 126–132.

Ricci-Luchi, F. 1975. Depositional cycles in two turbidite formations of Northern Italy. *J. Sed. Pet.*, Vol. 45, pp. 3–43.

Rollin, K. E. 1980. IP logging of mineral boreholes at Glendinning antimony Mine, Dumfriesshire. *Inst. Geol. Sci., Appl. Geophys. Unit*, 3 pp.

Rust, B. R. 1965a. The stratigraphy and structure of the Whitehorn area of Wigtownshire, Scotland. *Scott. J. Geol.*, Vol. 1, pp. 101–133.

— 1965b. The sedimentology and diagenesis of Silurian turbidities in South-east Wigtownshire, Scotland. *Scott. J. Geol.*, Vol. 1, pp. 231–246.

Smith, G. F. H. 1919. Semseyite from Dumfriesshire. *Miner. Mag.*, Vol. 18, pp. 354–359.

Smith, A. G. and Briden, T. C. 1977. *Mesozoic and Cenozoic palaeocontinental maps.* (Cambridge University Press.)

Smith, R. T., Gallagher, M. J. and Fortey, N. J. 1978. Controls of lead-zinc mineralisation in basal Carboniferous rocks near Langholm, Scotland. *Trans. Instn. Min. Metall. (Sect. B: Appl. Earth Sci.)*, Vol. 87, pp. 140–143.

Stanton, R. E. 1966. *Rapid methods of trace analysis for geochemical applications.* (London: Edward Arnold) pp. 45–46.

Telford, W. M. and others. 1976. *Applied Geophysics.* (Cambridge University Press.)

Vaughan, D. J. and Craig, J. R. 1978. *Mineral chemistry of metal sulphides.* (Cambridge University Press), 493 pp.

Walker, R. G. 1979. Facies Models 8. Turbidites and associated coarse clastic deposits. *Geosci. Canada, Reprint Series 1*, pp. 91–104.

— **and Mutti, E.** 1973. Turbidite facies and facies associations. In *Turbidites and Deep Water Sedimentation* (S.E.P.M. Pacific Section, Short Course) (Anaheim), pp. 119–158.

Walton, E. K. 1965. Lower Palaeozoic rocks – palaeogeography and structure. In **Craig, G. Y.** (editor) *Geology of Scotland.* (Edinburgh: Oliver and Boyd), pp. 201–227.

Warren, P. T. 1963. The petrography, sedimentation and provenance of the Wenlock rocks near Hawick, Roxburghshire. *Trans. Ed. Geol. Soc.*, Vol. 19, pp. 225–255.

— 1964. The stratigraphy and structure of the Silurian (Wenlock) rocks south-east of Hawick, Roxburghshire, Scotland. *Quart. J. Geol. Soc.*, Vol. 120, pp. 193–222.

Wedepohl, K. H. (Editor) 1972. Handbook of geochemistry. (Berlin: Springer-Verlag), 845 pp.
Weir, J. A. 1974. The sedimentology and diagenesis of the Silurian rocks on the coast west of Gatehouse, . Kirkcudbrightshire. *Scott. J. Geol.,* Vol. 10, pp. 165–186.
Wheatley, C. J. V. 1978. Ore mineral fabrics in the Avoca polymetallic sulphide deposit, south-east Ireland. In **Verwoerd, W. J.** (editor), *Geol. Soc. South Africa Spec. Pub.* No. 4, pp. 529–544.
Willan, R. C. R. and **Hall, A. J.** 1980. Sphalerite geobarometry and trace element studies on stratiform sulphide from McPhun's Cairn, Argyll, Scotland. *Trans. Instn. Min. Metall. (Sect. B: Appl. Earth Sci.),* Vol. 89, pp. 31–40.

APPENDIX I

BOREHOLE LOGS

Note (a). The bedding angle (degrees) is the angle between the observed lithological banding or bedding in the cores and the long axis of the borehole core. In constructing the borehole sections (Figures 8 and 9) it was assumed that the true dip of the beds was sub-vertical. However, this is not necessarily the case, owing to evidence at outcrop of tight folding. Faulting is fairly common and may also invalidate the assumption of subvertical bedding.

Note (b). Sample number is a guide to the geochemical analyses in Appendix II. Where more than one lithological unit is included in a single geochemical sample all but the lowest unit in the borehole is denoted by the same sample number in parentheses.

Inclined depth, m	Intersection, m	Bedding angle°	Lithology	Mineralisation	Sample No. CXD
0.00			Superficial deposits		
13.70	13.70		Boulders, probably gravel		
14.20	0.50		Brown clay with pebbles		1001
20.33	6.13		Mainly loose boulders, probably gravel		
20.97	0.64		Orange-brown clay or silt with pebbles		1002
23.13	2.16		Boulders and orange-brown clay		
23.92	0.79		Orange-brown clay with rock fragments		1003
24.98	1.06		Rock fragments and pebbles in silt or clay		
25.94	0.96		Basal till		1004
			SILURIAN		
30.22	4.28		Mudstone, olive-green, finely-bedded	Numerous quartz veins	
31.15	0.93		Silty sandstone, calcareous with clay-filled fractures at 30.28 m, 30.46 m and 30.83 m	Thin orange-brown carbonate veinlets cut white quartz veinlets	1005
31.80	0.65		Siltstone, muddy, more micaceous towards base; sandstone [CXD 1537] occurs between clay-filled fractures at 31.40 and 31.80 m	Some calcite veining	1006
34.16	2.36		Silty sandstone with small mudstone fragments, e.g. 34.06-34.10 m; somewhat calcareous	Thin calcite veinlets at 30° to core axis averaging 3 mm in thickness, less frequent near base	1007
36.20	2.04		Mudstone, brecciated and limonitic, converted to a clay gouge at top and base indicating faults	Ferruginous veinlets throughout	1008
37.12	0.98		Breccia, possibly a faulted intraformational breccia composed of broken, highly limonitic sediment recognisable in places as silty sandstone [CXD 1538]; mudstone at 37.02-37.12	Some dark capillary-like veinlets in basal mudstone; stibnite on fractures in sandstone	1009
39.17	2.05		Silty sandstone, grey, massive, competent with mudstone clasts; limonite staining is conspicuous at 37.30-37.56 m, 38.09-38.22 m and 38.50-38.65 m	Minor white veinlets	1010
41.18	2.01		Silty sandstone, broken, variably limonite-stained, numerous shear planes	Calcite veinlets and smears of dark (?) sulphide on shear planes	1011
43.79	2.61		Silty sandstone, coarsening in places to a sandstone and with an irregular mudstone parting or clast at 41.64-41.79 m; limonite staining prominent at margins of fractures at 41.30-41.38, 41.92-42.11 m, 42.27-42.51 m and 43.54-43.79 m	Some regular baryte veinlets with pink-stained patches; dark sulphide patches in fracture at 41.30 m	
45.02	1.23		(?) Mudstone, extensively limonite-stained	Some irregular, limonite-stained veinlets	
45.08	0.06		Broken rock and clay denoting fault		(1012)
45.20	0.12		Mudstone, limonite-stained adjacent to veinlets	Numerous quartz veinlets	(1012)
45.55	0.35		Broken rock and clay gouge denoting fault; limonite-stained mudstone at top and base	Quartz veinlets in mudstone	(1012)
46.55	1.00	c10	Siltstone, muddy, somewhat brecciated	Patches of fine-grained iron sulphide; numerous quartz veinlets with stibnite blooms	(1012)
47.15	0.60	c15	Intraformational breccia of banded siltstone clasts in mudstone	Fine-grained pyrite common (c.5%) throughout	1012
48.22	1.07		(?) Mudstone, soft, brown, broken with stringers of clay gouge denoting a fault	Veinlets of quartz up to 4 mm thick (CXD 1577)	1013
49.02	0.80		(?) Mudstone, brown, brecciated	Numerous irregular quartz veinlets and thin veinlets of dark (?) iron oxide	1014
50.75	1.73	15	Mudstone, broken and fine-grained siltstone	Dickite on fractures [CXD 1539]	1015
52.05	1.30		Siltstone		1016
53.72	1.67		Fault breccia and at 53.16-53.72 m a brown-stained sandstone	Breccia intricately and heavily veined with quartz	1017
55.02	1.30	12	Mudstone, compact, grey [CXD 1575]		1018
55.53	0.51		Siltstone, heavily stained by limonite	Minor quartz and calcite veinlets	(1019)
55.78	0.25		Siltstone, grey	Calcite veinlets	(1019)
56.28	0.50		Sandstone, fine-grained	A few veinlets	(1019)
57.08	0.80		Mudstone, limonitic at top	Some calcite veinlets	1019
57.71	0.63		Silty sandstone, grey, hard, limonite-stained along fractures and veins	Quartz veins	(1020)
58.19	0.48		Mudstone parting, dark grey, grading downwards	Pyrite in quartz veins and in dark veinlets; traces of aragonite	(1020)
58.99	0.80		Muddy siltstone with irregular mudstone clasts grading into fine-grained sandstone at 58.55 m	Pyrite in mudstone clast; some calcite veinlets	1020

Inclined depth, m	Intersection m	Bedding angle°	Lithology	Mineralisation	Sample No. CXD
60.80	1.81		Siltstone, grey with limonite stains along fractures and calcite veinlets; breccia zone at 60.04–60.24 m in which one clast contains a thin vein of sulphides	Lobate patches of fine-grained pyrite are cut by calcite veinlets containing pyrite crystals; pyrite and arsenopyrite in veinlet in breccia clast; stibnite in quartz veins at 59.68 m and 60.45 m	1021
62.44	1.64		Siltstone, muddy, highly veined – possibly an intraformational breccia in places; minor sandstone	Disseminated arsenopyrite; numerous dolomite-quartz veinlets containing pyrite and arsenopyrite; stibnite on fractures [CXD 1500]	1022
65.77	3.33		Intraformational breccia varying from a totally brecciated rock to a highly-veined silty sandstone; cement composed of quartz and white clay mineral [CXD 1501-4]	Pyrite and arsenopyrite disseminated throughout; fine-grained pyrite forms lobate patches up to 10 x 60 mm; traces of stibnite on fractures; numerous quartz veins	1023 1024 1025
67.37	1.60	15	Sandstone, fine-grained with clasts of mudstone which are highly limonite-stained in places	Arsenopyrite and pyrite, apparently stratiform at 65.90 m; pyrite also disseminated; numerous quartz veins	1030
69.52	2.15		Siltstone, strongly limonite-stained with unstained mudstone partings	Quartz veinlets; no sulphides observed	1031
71.87	2.35		Sandstone, fine-grained, compact, grey except at 70.67–71.43 m where limonite staining is common and well-developed shear planes run 10° to the core axis denoting a fault	Veinlets of quartz and dark calcite; soft clay mineral (?dickite) at 71.47–71.87 m	1032
72.92	1.05		Sandstone, fine-grained, highly brecciated, limonitised in part	Veinlets of quartz	1033
75.87	2.95	20	Laminated siltstone, pale mudstone then sandstone, limonite-stained along veinlets; disseminated micaceous hematite	Veinlets of quartz; traces of disseminated pyrite [CXD 1505]	1034
77.92	2.05		Sandstone, grey, competent, minor limonite staining [CXD 1506]; mudstone clasts near base	Quartz veinlets up to 10 mm thick running mainly at 60–80° to the core axis	1035
79.12	1.20		Sandstone, initially limonite-stained; sheared and veined at 78.52–78.64 m with shear planes at 30° to the core axis; somewhat broken siltstone near base	Quartz veinlets in sheared sandstone; calcite veinlets in limonite-stained sandstone	1036
81.96	2.84	c40	Mudstone, dark grey with bands of white mudstone and sub-rounded sandstone clasts; also sandstone with mudstone clasts	Pyrite in mudstone, quartz veinlets in sandstone clasts, calcite veinlets in mudstone clasts [CXD 1507]	1037
82.66	0.70		Sandstone, fine-grained, highly limonite-stained at 81.96–82.26 m	Numerous quartz veinlets up to 1 cm thick in at least two generations	1038
83.22	0.56	40	Mudstone, very fine-grained, pale green with interbanded grey mudstone	A few veinlets	1039
85.27	2.05		Siltstone, grey, laminated with bands of pale grey mudstone [CXD 1576]; thin band of green mudstone at 85.20–85.22 m	Some quartz veinlets up to 2 cm thick; fine-grained pyrite occurs at margin of green mudstone	1040

END OF BOREHOLE AT 85.27 m

Inclined depth, m	Intersection m	Bedding angle°	Lithology	Mineralisation	Sample No. CXD
0.00			SILURIAN		
7.62	7.62	(?)20	Weathered sandstone, siltstone, very minor mudstone		
9.00	1.38	25	Siltstone, minor mudstone; sheared and veined at 8.50 m		
10.89	1.89	15	Siltstone with interdigitations of fine-grained sandstone; conspicuous band of green mudstone at 9.35-9.37 m; ferruginous fractures at 10.3, 10.9 and 11.3 m	Traces of disseminated pyrite in the sandstone; calcite veinlets; (?) stibnite bloom on one fracture	
14.47	3.58		Siltstone, compact, medium grey, poorly bedded; large mudstone clast at 13.5-13.8 m; ferruginous fracture surfaces	Some irregular calcite veinlets	
14.90	0.47		Mudstone, shaly with a siltstone band at 14.60-14.80 m		
17.62	2.72		Siltstone with mudstone clasts; ferruginous fractures	Quartz veinlets common at 15.3-15.6 m	
20.17	2.55	15	Siltstone, pale coloured with well-developed maroon laminae along bedding; fine-grained sandstone at 19.31-19.44 m contains micaceous hematite grains	Anastomosing calcite veinlets in at least two generations	
23.80	3.63		Sandstone, fine-grained, calcareous with siltstone laminae; pale siltstone and mudstone at 21.61-21.81 m	Occasional calcite veinlets and pyrite grains	
25.10	1.30		Mudstone, grey, weakly laminated having its contact with sandstone unit above preserved for 0.5 m along the core; sheared in plane of core axis		
27.75	2.65	c0	Sandstone, fine-grained, calcareous with a thin mudstone at 26.2 m; core broken at 27.0 m	Calcite veinlets, especially at 26.4 m	
28.42	0.67	c0	Sandstone as above with numerous elongated clasts (up to 10 x 12 mm) of dark muddy siltstone orientated parallel to the core axis	Traces of fine-grained pyrite	
32.00	3.58	c0	Sandstone as above, with elongated mudstone clasts at 30.7-31.0 m	Calcite veinlets	
33.00	1.00	10	Siltstone, alternating light and dark coloured, non-calcareous; core broken to 32.1 m		
35.90	2.90		Sandstone, initially fine but coarsening downwards; non-calcareous; sheared and broken on either side of a thin green mudstone at 34.50-34.51 m	Quartz veinlets	
36.26	0.36		Fault zone in siltstone and soft mudstone; calcareous		
36.80	0.54	45	Sandstone, non-calcareous with angular clast of pale siltstone at 36.64-36.69 m	Quartz veinlets in siltstone clast	
38.70	1.90		Sandstone with interdigitating siltstone and mudstone; mudstone clasts in other lithologies, sandstone clasts in mudstone; sheared and veined siltstone at 38.3-38.6 m		
42.60	3.90		Siltstone, locally varying to fine-grained sandstone with mudstone clasts; some mudstone bands	Pyrite disseminated in siltstone at 42.5 m; pyrite and (?) stibnite in quartz veinlet at 42.2 m [CXD 1592]; calcite vein on shear plane at 39.6-39.9 m	
42.77	0.17		Fault in sandstone		(1128)
44.38	1.78	20-40	Siltstone, pale, massive; core broken at 44.0 m indicating fault; some red staining in mudstone near base [CXD 1545-6; 1560]	Minor stratiform pyrite and arsenopyrite at 43.8 and 44.3 m; pyrite, arsenopyrite and traces of stibnite in quartz veinlets	1128
46.44	2.06	25-35	Sandstone, massive, non-calcareous followed by mudstone with sandstone clasts at 45.86-45.99 m, then by siltstone and finally mudstone at 46.17-46.44 m [CXD 1547, 1561]	Disseminated pyrite and arsenopyrite locally form 5% in sandstone; stratiform pyrite and arsenopyrite in basal mudstone; pyrite in veinlets; arsenopyrite prisms and stibnite bloom on fractures	1129
48.07	1.63	35	Breccia vein composed largely of siltstone banded by quartz veins which incorporate clasts of mineralised sandstone; in places an intraformational breccia of siltstone clasts set in a matrix of quartz; fault gouge at 47.42-47.54 m	Disseminated pyrite and lesser arsenopyrite average 5%; pyrite common in some siltstone clasts; red-brown (?) semseyite at 48.06-48.07 m; (?) aragonite in cavity at 46.93 m; some late calcite veinlets	1130
48.97	0.90		Breccia vein as above, the siltstone clasts forming 60% and sometimes highly pyritic; matrix is quartz	Sulphides common as above; (?) semseyite at 48.64-48.82 m [CXD 1585]; calcite and (?) aragonite in cavities	1131
51.40	2.43		Breccia vein as above; micaceous hematite abundant in siltstone clasts; highly veined sandstone clasts also present [CXD 1562]; total thickness of breccia vein is 4.96 m	Sulphides common as above; stibnite on fracture at 50.8-51.0 m; calcite-lined cavity at 49.05-49.07 m; quartz veins abundant	1132
52.97	1.57		Siltstone, broken and veined but not a true breccia; mudstone at 52.24-52.26 m	Pyrite and arsenopyrite in wisps, irregularly disseminated and in quartz veinlets; red-brown (?) semseyite on fractures	1133
54.50	1.53		Siltstone, unbedded, highly veined	Pyrite and arsenopyrite minor in quartz-calcite veinlets	1134
56.02	1.52		Siltstone, muddy and intermingled mudstone; fault gouge at 55.66-55.86 m	Numerous veinlets containing pyrite and arsenopyrite; brick-red (?) hematite and/or (?) semseyite in wispy veinlets at 54.98 m [CXD 1589] and around 55.46 m [CXD 1590] with red staining up to 4 mm on margins	1135

Inclined depth, m	Intersection m	Bedding angle°	Lithology	Mineralisation	Sample No. CXD
57.75	1.73		Siltstone, unbedded, locally muddy; reddish-coloured hematitic alteration in places [CXD 1549, 1563]	Disseminated pyrite and arsenopyrite particularly common in highly veined siltstone at 57.37-57.57 m; sulphides also in veinlets with dickite; stibnite bloom on fractures at 56.94 m	1136
58.82	1.07		Sandstone, massive with broken mudstone at 58.11-58.41 m then siltstone to 58.82 m	Traces of pyrite in sandstone; pyrite and arsenopyrite along bedding, in veinlets and disseminated in siltstone	1137
59.72	0.90		Siltstone, muddy, core broken; subsequently brecciated sandstone [CXD 1550]	Disseminated arsenopyrite common and lesser pyrite especially at 58.95-59.02 m; also with stibnite in veinlets	1138
61.69	1.97	25	Siltstone, massive, poorly bedded	Pyrite and arsenopyrite in stratiform impregnations as at 60.09-60.20 m [CXD 1564] and in veinlets	1139
63.55	1.86		Siltstone, locally a fine-grained sandstone, compact; dark mudstone parting at 62.19-62.23 m; pale muddy siltstone at 62.78-63.08 m	Pyrite on bedding planes accompanied by dark staining; minor sulphides in quartz veinlets; slickensided calcite veinlets at 63.08-63.40 m	1140
65.49	1.94		Siltstone, muddy and pale coloured, changing to grey siltstone at 63.85 m; this alternates with darker silty mudstone, irregularly-bedded and clast-like at 64.12-64.65 m; remainder is massive sandstone with occasional mudstone clasts	Pyrite on bedding planes accompanied by dark staining; minor pyrite in quartz veinlets	1141
67.42	1.93	40	Siltstone, muddy and compact, varying to grey siltstone with mudstone clasts	Small lenses of fine pyrite and (?) grey sulphide [CXD 1593]	1142
69.11	1.69		Sandstone, fine-grained, changing at 68.29 m to mudstone then at 68.89 m to siltstone; graded bedding at 67.94-68.19 m; convoluted laminae in mudstone, the base of which is sheared with many fine veinlets of quartz	Pyrite disseminations in the sandstone, especially at 67.9 m and with (?) grey sulphide in veinlets [CXD 1573]; also in small patches and in quartz veins in the mudstone; arsenopyrite in quartz veinlets at 69.0 m	1143
71.50	2.39		Sandstone, fine-grained, changing to mudstone at 70.26 m with fine quartz veinlets	Pyrite disseminated and on fractures; (?) stibnite in veinlets	1144
73.37	1.87		Mudstone and siltstone, poorly bedded	Pyrite disseminations in siltstone and on fractures in mudstone	1145
75.25	1.88		Siltstone, muddy with darker mudstone lenses; basal 40 cm is essentially a red-stained mudstone	Disseminated and vein pyrite; (?) stibnite on fractures; (?) chalcopyrite veinlets in basal mudstone [CXD 1588]	1146
76.37	1.12		Mudstone, siltstone and fine-grained sandstone, poorly-bedded with minor red staining; fractured	Pyrite and arsenopyrite in small patches and disseminations	1147
78.90	2.53		Siltstone, pale with darker mudstone laminae; core broken at 76.57-77.22 m indicating a fault	Pyrite and lesser arsenopyrite in patches and disseminations; extensive quartz veining	1148
81.50	2.60	30	Siltstone, compact with lesser mudstone; fine-grained sandstone 80.50-81.50 m	Pyrite in veinlets; traces of stibnite on fractures	1149
82.88	1.38		Mudstone with sandstone clasts and much irregular quartz veining at 82.21 m, followed by fine-grained sandstone	Pyrite and stibnite on fractures in mudstone; pyrite also in sandstone clasts; disseminated pyrite in the basal sandstone	1150
85.27	2.39		Mudstone, siltstone and fine-grained sandstone	Pyrite disseminated in siltstone, less commonly in sandstone; also with (?) galena in veinlets	1151
86.72	1.45	20	Siltstone, poorly bedded, micaceous matrix, brecciated near base; some mudstone laminae	Sulphides on fractures; quartz-(?) baryte veinlets common, in places regular and 2-5 cm thick	1152
88.70	1.98	15-20	Siltstone, poorly bedded with dark grey mudstone laminae	Pyrite disseminated and in veinlets; stibnite bloom on fractures	1153
90.77	2.07	c0	Siltstone, hard, competent with undulating bedding; red staining commencing at 90.32 m consists of patches, anastomosing veinlets and developments at the margins of quartz veinlets	Pyrite in small patches throughout and with traces of (?) stibnite in quartz veinlets	1154
91.70	0.93		Siltstone, grey, hard and generally red-stained; fractured at 90.77-90.87 m	Pyrite and arsenopyrite on fractures; pyrite also in patches	1155
93.17	1.47		Breccia vein of siltstone fragments in a purplish siltstone matrix with much grey and white quartz; thin seams of rock gouge	Disseminated pyrite and arsenopyrite with traces of (?) grey sulphide	1156
95.12	1.95		Siltstone, dark and fine-grained alternating with paler and coarser siltstone; quartz veinlets locally concentrated in a small shear zone at 94.17 m	Pyrite and arsenopyrite common as disseminations and in veinlets with traces of stibnite	1157
96.54	1.42		Siltstone and fine sandstone, brecciated in places with development of quartz and a soft, pale green (?) clay mineral; silty mudstone at base	Arsenopyrite and pyrite common as disseminations; (?) chalcopyrite in quartz veinlets	1158
98.41	1.87		Sandstone, fine-grained, hard and competent with dark mudstone clasts and laminae; large patches of pale green dickite [CXD 1587]	Arsenopyrite and pyrite common as disseminations; also in veinlets [CXD 1586]	1159

Inclined depth, m	Intersection m	Bedding angle°	Lithology	Mineralisation	Sample No. CXD
98.73	0.32		Intraformational breccia consisting of light grey siltstone clasts in a darker grey siltstone matrix	Pyrite and arsenopyrite common; veinlets of pyrite; much dark quartz [CXD 1558]	(1160)
98.99	0.26		Siltstone; veinlets of dark quartz containing pyrite are cut by irregular veinlets of white quartz	Disseminated pyrite; stibnite blooms on fractures	(1160)
99.09	0.10		Intraformational breccia, as at 98.41-98.73 m	As at 98.41-98.73 m	(1160)
100.35	1.26		Siltstone, commonly red stained	Disseminated arsenopyrite and pyrite [CXD 1559]	1160
102.16	1.81		Siltstone, matrix weakly reddened	Pyrite in patches and in veinlets with a trace of (?) stibnite	1161
104.32	2.16		Siltstone as above with red staining decreasing towards base; sulphides decrease concomitantly with degree of staining	Pyrite in patches and in veinlets with arsenopyrite and (?) stibnite	1162
106.67	2.35		Intraformational breccia, mainly of siltstone fragments, some of mudstone; light green mudstone parting at 106.63 m	Pyrite and arsenopyrite as disseminations, in patches and in veinlets	1163
107.75	1.08	20	Siltstone, muddy, alternating from light grey to dark grey in colour	Pyrite and stibnite on fractures	1164
109.47	1.72		Intraformational breccia of sandstone, siltstone, mudstone and quartz; red-stained patches and veinlets common	Pyrite and arsenopyrite disseminated in areas of red staining; (?) stibnite on fractures	1165
111.09	1.62	c0	Sandstone, grey and structureless with some siltstone laminae; some fractures are developed parallel to the laminae which probably mark the bedding	Pyrite and arsenopyrite disseminated and on fractures; stibnite on fractures; quartz veins	1166
113.15	2.06	c0	Probably an intraformational breccia consisting of sandstone, siltstone and mudstone with abundant regular and irregular quartz veins; elsewhere the three lithologies are interdigitated with undulatory bedding	Pyrite and arsenopyrite as disseminations in sandstone, as elongate stratiform patches in mudstone [as at 112.90 m, CXD 1567], and in quartz veinlets; stibnite on fractures	1167
114.73	1.58		Intraformational breccia at 113.15-113.25 m, pale green to light red fault gouge at 113.25-113.50 m with some brecciation of adjacent rocks; remainder is sandstone, with interdigitating mudstone laminae to 114.01 m	Pyrite, arsenopyrite and (?) stibnite in breccia; traces of pyrite in gouge; finely disseminated pyrite in sandstone; pyrite in veinlets and (?) bournonite in quartz veinlet at 113.64 m	1168
116.30	1.57		Siltstone, lesser sandstone and mudstone; mudstone clasts in siltstone; core badly broken 114.73-115.25 m indicating a fault	Pyrite and minor arsenopyrite in section of broken core; veinlets and small patches of pyrite in siltstone	1169
118.80	1.50		Sandstone; siltstone and mudstone, commonly brecciated; some large patches of quartz	Pyrite, minor arsenopyrite and traces of (?) bournonite in quartz patches and veinlets; also large patches of pyrite	1170

END OF BOREHOLE AT 118.80 m

Inclined depth, m	Intersection, m	Bedding angle°	Lithology	Mineralisation	Sample No. CXD
0.00					
4.44	4.44		Superficial deposits		
			SILURIAN		
7.62	3.18		Sandstone with dark lithic fragments, weathered	Calcite veinlets	
9.30	1.68		Mudstone, olive-green and siltstone	Irregular quartz veinlets	
9.80	0.50		Core loss		
13.96	4.16	20	Siltstone with mudstone partings and clasts, locally brecciated	Quartz veins, pyrite stringers and at 13.3 m pyrite lenses	1048
16.86	2.90	20	Siltstone, broken in places	Minor quartz veins	1049
20.72	3.86	15	Mudstone and siltstone, laminated; units of silty sandstone; shear zone at 19.34 m	Green mica on fractures [CXD 1542]; quartz veins	
21.57	0.85		Mudstone; broken, soft clay gouge in places		
23.40	1.63		Sandstone, compact with disseminated micaceous hematite; siltstone band at 22.52-22.56 m	(?) grey sulphide on fractures woth pyrite and (?) chalcopyrite	
24.79	1.39		Mudstone, lesser siltstone and sandstone, fractured near base	Minor disseminated sulphide	
26.61	1.82	40	Siltstone and interbedded mudstone, bedding in places undulating and exhibiting fold structures; clay gouge at 25.84 m	Quartz veinlets	
28.04	1.43		Sandstone with minor mudstone clasts and laminae	Calcite veinlets; disseminated sulphide	
30.16	2.12		Mudstone coarsening downwards into siltstone which exhibits cross-bedding; limonitic fractures		
31.32	1.16		Siltstone coarsening downwards into sandstone	Quartz veinlets common	
32.72	1.40		Intraformational breccia of sandstone fragments and lesser siltstone and mudstone fragments; irregular quartz patches common	Pyrite as disseminations, in veinlets and on fractures	1171
33.47	0.75		Sandstone, strongly quartz-veined	Minor disseminated pyrite	1182
36.05	2.58		Intraformational breccia of mudstone fragments and lesser siltstone and sandstone fragments; quartz patches common	Pyrite disseminated and on fractures; quartz veinlets common	1183
38.48	2.43		Sandstone with mudstone clasts and laminae over lowermost 60 cm; broken and fractured in places	Pyrite disseminated and in veinlets throughout; grey sulphide crystal on fracture at 36.28 m [CXD 1584]	1172 1173
39.72	1.24		Sandstone with mudstone laminae and clasts, also siltstone; core broken	Numerous pyrite veinlets	1174
41.08	1.36	5	Siltstone, well-bedded mudstone partings; core broken	Numerous pyrite veinlets and patches; minor quartz veinlets	1175
43.26	2.18	5-30	Sandstone to 41.58 m then interbedded with siltstone and subsidiary mudstone	Pyrite disseminated in sandstone, on fractures in mudstone	1176
44.79	1.53	35	Siltstone with lesser interbedded mudstone and sandstone	Disseminated pyrite; quartz veinlets with (?) bournonite at 44.24 m	1177
46.22	1.43	60	Siltstone and interbedded mudstone	Disseminated pyrite in siltstone; stibnite on fractures [CXD 1580]	1178
47.50	1.28		Siltstone with mudstone laminae, especially at 46.9-47.5 m where core is broken with pyrite stringers	Disseminated pyrite in siltstone; stibnite in quartz veinlets	1179
49.20	1.70		Sandstone and siltstone, poorly bedded with quartz veinlets cut by dolomite veinlets [CXD 1569]	Pyrite, arsenopyrite and (?) grey sulphide disseminated; pyrite and stibnite on fractures	1180
51.10	1.90		Sandstone, siltstone and laminae of mudstone	Disseminated pyrite; arsenopyrite and pyrite on fractures	1181
53.67	2.57		Siltstone with dark mudstone clasts; shear plane at 20° to core axis	Traces of pyrite and arsenopyrite in siltstone; quartz veinlets	1050
55.88	2.21		Siltstone, laminated with paler siltstone and darker mudstone	Pyrite disseminated and in veinlets with aragonite [CXD 1508]	1051
57.05	1.17		Sandstone, silty with mudstone laminae	Traces of disseminated pyrite	1052
59.55	2.50		Mudstone initially then silty sandstone, highly brecciated and irregularly veined by quartz which forms patches up to 10 cm in diameter	Sulphides not observed; greenish mica in altered breccia [CXD 1570]	1053
61.70	2.15	20	Siltstone with mudstone laminae; calcite-filled shears are aligned with the laminae	Traces of disseminated pyrite and (?) arsenopyrite	1054
64.65	2.95	10	Sandstone, lesser siltstone and mudstone laminae	Traces of disseminated pyrite	1055
66.47	1.82		Sandstone, siltstone and mudstone, strongly brecciated in places	Disseminated pyrite and arsenopyrite; stibnite on fractures [CXD 1509]; quartz veinlets common	1056
68.19	1.72		Siltstone and silty sandstone, minor mudstone	Minor disseminated pyrite and arsenopyrite; acicular stibnite in quartz vein [CXD 1543] and stibnite on fracture in mudstone [CXD 1510]	1057

Inclined depth, m	Intersection, m	Bedding angle°	Lithology	Mineralisation	Sample No. CXD
70.01	1.82	30	Sandstone with mudstone laminae	Minor disseminated pyrite and arsenopyrite; quartz veins	1058
72.04	2.03		Mudstone and subordinate siltstone	Minor disseminated pyrite in siltstone; stibnite bloom on fracture in mudstone [CXD 1511]	1059
73.52	1.48	30	Sandstone with conspicuous pale green mudstone of 72.42–72.46 m	Disseminated pyrite and arsenopyrite in sandstone	1060
75.22	1.70		Siltstone, highly veined and broken	Disseminated pyrite and arsenopyrite common	1061
83.12	7.90		Intraformational breccia consisting of fragments of siltstone, lesser sandstone and minor mudstone; later shearing common	Pyrite and arsenopyrite common as disseminations, in stratiform trails and in veinlets; stibnite bloom on fractures [CXD 1544,1512]	1062–1066
85.02	1.90		Siltstone, lesser mudstone and sandstone; quartz veins common especially at 84.60–84.80 m	Stratiform arsenopyrite and pyrite [CXD 1513]	1067
			Siltstone and mudstone	Arsenopyrite (crystals up to 2 mm in length) and pyrite as disseminations; dickite in quartz-carbonate veinlets [CXD 1514]	1068
89.20	2.25		Siltstone and mudstone, strongly brecciated especially at 88.3–88.6 m	Pyrite in elongated patches and disseminated with arsenopyrite	1069
91.97	2.77		Siltstone containing dark lithic fragments and occasional mudstone partings especially at 91.89–91.97 m where arsenopyrite is common	Arsenopyrite in patches; bournonite in quartz veinlets [CXD 1582]	1070
93.76	1.79		Sandstone, fine-grained, maroon staining present; highly brecciated at 92.55–93.15 m where sandstone is intermixed with more fine-grained sediment	Disseminated pyrite and arsenopyrite common; sphalerite in veinlets [CXD 1583]	1071
95.58	1.82		Sandstone and siltstone, brecciated; some thin dark mudstone partings, particularly at 94.80 m and at 95.38–95.58 m	Disseminated pyrite and arsenopyrite throughout; (?) bournonite on fracture at 94.06 m; numerous quartz veinlets and some calcite veinlets	1072
97.62	2.04	10	Siltstone, broken but less brecciated than in unit above; a few mudstone partings	Minor pyrite and arsenopyrite as disseminations	1073
100.57	2.95		Mudstone, silty and highly fractured, grading at 99.8 m into a competent quartz-rich siltstone	Pyrite, stibnite and (?) bournonite on fractures; quartz veinlets rare	1074
103.10	2.53	30	Mudstone, silty	Pyrite, stibnite and (?) dickite on fractures; quartz veinlets uncommon except at 103.0 m	1075
104.49	1.39		Mudstone to 103.50 then fractured siltstone	Stratiform pyrite and arsenopyrite; pyrite, stibnite and bournonite on fractures and in veinlets [CXD 1515]	1076
107.62	3.13		Sandstone, silty, grey and compact with minor mudstone; brecciated at 107.32–107.62 m	Stratiform arsenopyrite and pyrite, especially in mudstone; stibnite and dickite [CXD 1516] in anastomosing quartz veinlets	1077
109.78	2.16		Siltstone, well bedded, with some thin mudstone partings and gradational sandstone layers; locally brecciated; yellowish-coloured, fine-grained (?) dickite coats fracture surfaces at 107.62–107.72 m	Sparsely disseminated pyrite and arsenopyrite; pyrite fringes carbonate veins; stibnite on fractures [CXD 1517]	1078
111.69	1.91		Mudstone, pale coloured and interbedded with darker siltstone	Pyrite in patches and in quartz veinlets; stibnite on fractures	1079
115.00	3.31		Siltstone with some mudstone partings	Disseminated pyrite; stibnite and (?) bournonite in quartz veinlets	1080
117.20	2.20	20	Mudstone, finely laminated in places; locally sheared especially at 115.3–115.4 m	Pyrite disseminated and in veinlets throughout; traces of stibnite on fractures	1081
120.10	2.90	15	Sandstone, fine-grained, grey and massive, interbedded with lesser mudstone; brecciated with quartz veinlets at 118.4 m and 119.1 m	Pyrite weakly disseminated and in veinlets	1082
121.99	1.89	20	Sandstone with interbedded mudstone and siltstone; the mudstone appears to be in the form of clasts	Pyrite weakly disseminated in sandstone; also in veinlets	1083
124.22	2.23	15	Siltstone and mudstone varying abruptly from one to another; lithological landing finely developed	Pyrite disseminated and in quartz veinlets; latter are sheared with planes 10–20° to core axis	1084
126.22	2.00		Sandstone with minor mudstone, probably as a clast, at 125.30–125.40 m	Minor disseminated pyrite; quartz veinlets uncommon	1085
129.22	3.00		Sandstone, silty and minor mudstone; irregular bedding in sandstone is displayed by wispy mud layers	Disseminated pyrite throughout; irregular quartz veins; patches and single grains of bournonite in carbonate veinlet [CXD 1518]	1086
131.62	2.40		Sandstone and minor mudstone, probably as clasts; veinlets of opaline quartz at 40° to core axis	Pyrite and arsenopyrite as wisps, disseminated and in veinlets; patch of fine-grained pyrite 12 mm across in clast at 130.85 m	1087
133.17	1.55		Sandstone with irregular clasts of mudstone; strongly veined, especially at 132.77–133.17 m	Pyrite disseminated and with (?) grey sulphide on fractures and at veinlet margins	1088

Inclined depth, m	Intersection m		Lithology	Mineralisation	Sample No. CXD
134.71	1.54		Siltstone, finely banded	Stratiform pyrite; disseminated pyrite and arsenopyrite; sulphides also in and marginal to quartz veinlets; the latter are sometimes cut by sulphide veinlets	1089
140.62	5.91		Intraformational breccia composed of a grey, compact admixture of sandstone and mudstone clasts set in a dark, sulphide-rich matrix containing dickite [CXD 1520]; well-developed, sub-angular clasts of sandstone can measure up to 5 cm across; some clasts exhibit veining; the breccia is locally sheared, especially at 137.06-137.36 m	Disseminated pyrite and subordinate arsenopyrite in matrix [CXD 1519, 1521]; patches of pyrite up to 2 cm across; pyrite occasionally present in clasts; pyrite and dickite in quartz-carbonate veinlets with (?) bournonite on fracture at 136.3 m	1090-1093
142.64	2.02	10	Siltstone, very finely flow-banded	Minor stratiform pyrite; stibnite intergrown with (?) bournonite in veinlet at 141.82-141.93 m	1094
144.27	1.63		Siltstone, flow-banded, and sandstone; very brecciated	Pyrite along bedding and in veinlets; arsenopyrite at 144.15 m; baryte veinlets at 143.52-143.54 m; bournonite in baryte veinlet at 143.62 m [CXD 1573]	1095
145.52	1.25	10	Siltstone and mudstone, finely-banded	Stratiform, disseminated and veinlet pyrite and arsenopyrite, especially at 145.2 m; bournonite on fractures [CXD 1522, 1565]	1096
146.67	1.15	20	Sandstone, weakly banded with subordinate siltstone; contains micaceous hematite grains and is unusually coarse-grained at 146.04-146.23 m	Pyrite and arsenopyrite as disseminations, on bedding planes and in sparse quartz veinlets	1097
148.07	1.40	20	Siltstone, finely-banded, muddy in places	Pyrite, arsenopyrite and (?) grey sulphide disseminated and in fine stratiform layers up to 1 mm thick; also in veinlets with quartz, baryte and at 146.92 m, dickite	1098
148.24	0.17		Intraformational breccia composed of clasts of sandstone up to 25 mm across and of darker siltstone; the clasts are angular to sub-angular and are set in a dark, sulphide-rich matrix; the clast:matrix ratio is approximately 70:30	Matrix of breccia consists essentially of arsenopyrite and quartz; globular pyrite occurs in clasts, [CXD 1566]	(1099)
148.95	0.71	15	Siltstone, finely-banded; bedding is parallel with contact against intraformational breccia above	Pyrite and arsenopyrite as disseminations and on fractures	1099
150.45	1.50		Siltstone, muddy in places, relatively coarse-grained and sulphide-rich in others	Pyrite, arsenopyrite and (?) grey sulphide disseminated and on fractures	1100
151.77	1.32		Siltstone, dark grey, compact, poorly-bedded	Pyrite in patches up to 15 mm across; pyrite and arsenopyrite disseminated, in veinlets and at margins of quartz veins up to 2 cm thick	1101
153.05	1.28		Siltstone, weakly banded, incorporating clasts of sandstone and mudstone; probably an intra-formational breccia at 152.34-153.05; somewhat sheared	Pyrite and arsenopyrite disseminated, within sandstone clasts and in veinlets; quartz veins common	1102
154.97	1.92	30	Siltstone, weakly banded, core very broken	Quartz veins	1103
156.07	1.10		Siltstone, finely banded with some mudstone partings	Pyrite locally exceeds 10% of rock; with arsenopyrite stratiform at 155.80-155.90	1104
157.62	1.55	c0	Siltstone, very finely banded with darker sulphidic bands	Pyrite very fine-grained in darker bands; anastomosing quartz veinlets at 157.28-157.41 m	1105
159.55	1.93	c0	Siltstone and mudstone, finely banded	Disseminated pyrite; quartz veins with pyrite and baryte at 157.62-157.74 m [CXD 1523]	1106
160.95	1.40	10	Siltstone, finely banded	Disseminated pyrite; quartz-carbonate veinlets	1107
162.27	1.32	10	Siltstone, finely banded	Disseminated pyrite; thick quartz vein at 162.15-162.27 m	1108
164.20	1.93		Siltstone, compact, finely banded in places	Disseminated pyrite; quartz veins up to 2 cm thick	1109
165.81	1.61		Siltstone, finely banded with mudstone	Disseminated pyrite, especially at 165.40-165.55 m [CXD 1524, 1552]	1110
167.10	1.29		Siltstone, fine banded	Stratiform pyrite in darker bands of siltstone; stibnite on fractures [CXD 1571]	1111
168.73	1.63	10	Siltstone, finely banded; core broken at 168.22-168.73 m	Stratiform pyrite and arsenopyrite; bright, globular pyrite in stringers; aggregate of bournonite 4 mm across in veinlet [CXD 1525, 1553, 1572]	1112
170.04	1.31		Siltstone, finely banded; strongly veined at 168.66-169.27 m and at 169.83-169.95 m	Stratiform pyrite and arsenopyrite; thicker veinlets zoned with outer carbonate and central quartz; bournonite in dolomite [CXD 1581]	1113
171.59	1.55		Siltstone, finely banded; pale siltstone at 170.57-170.77 m containing stratiform pyrite is in contact with a darker mudstone in which pyrite patches measure up to 1 cm across	Pyrite and arsenopyrite disseminated and in veinlets; quartz vein 7 mm thick at 170.80 m	1114
173.11	1.52	15	Siltstone, finely banded, cross-laminated; brecciated dark mudstone at 173.27-173.34 m with abundant pyrite	Stratiform and vein pyrite and arsenopyrite; sulphides locally concentrated in siltstone at vein margins	1115

Inclined depth, m	Intersection m	Bedding angle°	Lithology	Mineralisation	Sample No. CXD
174.96	1.85		Siltstone, cross-laminated with well defined alternating dark and light laminae	Stratiform dark grey (?) sulphide at 173.76 m; stratiform pyrite and arsenopyrite especially at 174.70-174.96 m	1116
176.35	1.39		Siltstone, cross-laminated, varying locally to sandstone	Disseminated pyrite and minor arsenopyrite; pyrite in quartz veins	1117
178.58	2.23		Breccia vein of mudstone and siltstone rock fragments set in a quartz-dolomite matrix; the matrix is usually hard, grey and fine-grained but at 178.35 m the quartz is relatively coarse and cream coloured; the absence of fractures suggests the assemblage is an intraformational breccia	Patches of massive pyrite up to 2 cm across in matrix; pyrite and minor arsenopyrite disseminated through some rock fragments [CXD 1526,1527, 1528,1530]	1118
180.54	1.96		Siltstone, grey, passing into fine-grained sandstone at 178.72 m; mudstone at 179.10-179.45 m then fine-grained sandstone with rounded patches of mudstone; reverts to siltstone at 179.96 m	Stratiform and disseminated pyrite and arsenopyrite in upper siltstone [CXD 1568], persisting weakly into the sandstone; rare pyrite in lower units; some pyrite in veinlets	1119
182.82	2.28	45	Siltstone, medium grey, poorly bedded, grading in places into fine-grained sandstone and into mudstone	(?) stibnite in calcite veinlets; quartz veins common at 181.7-182.4 m	1120
186.82	4.00	45	Siltstone, muddy, poorly bedded with abrupt variations to mudstone and fine-grained sandstone	(?) stibnite on fractures; veins uncommon with only a trace of pyrite	1121 1122
188.33	1.51		Initially a fine-grained sandstone, then siltstone laminated with dark mudstone and terminating in fine-grained sandstone, sheared at 188.3 m	Traces of disseminated pyrite in the sandstones	1123
191.33	3.00		Sandstone, compact, massive, dark grey, rarely veined or fractured	Persistent traces of pyrite; ruggy calcite veinlet cuts a quartz veinlet at 190.07 m	1124
193.93	2.60	15	Sandstone, fine-grained, massive and uniform with abundant flakes of red micaceous hematite [CXD 1531]	Traces of pyrite in hairline veinlets at 198.22 m and 193.75 m with (?) stibnite	1125
196.06	2.13	10	Siltstone, muddy, with fine-grained sandstone at 194.13-194.38 m	Minor disseminated pyrite; few veinlets; stibnite bloom [CXD 1532]	1126
197.82	1.73		Mudstone, lesser siltstone, grading into siltstone towards the base	(?) stibnite bloom on fracture	1127

END OF BOREHOLE AT 197.82 m

Inclined depth, m	Intersection m	Bedding angle°	Lithology	Mineralisation	Sample No. CXD
0.00					
5.06	5.06		Superficial deposits		
			SILURIAN		
6.52	1.46		Sandstone, limonite-stained and soft green mudstone	Quartz and calcite veinlets	
7.47	0.95		Siltstone with broken mudstone partings	Calcite veinlets in mudstone	
8.02	0.55		Mudstone with siltstone clast at 7.54 m; maroon coloured lenticles subparallel to bedding at 7.90-7.96 m	Orange-stained calcite veinlets	
9.00	0.98		Siltstone with disseminated micaceous hematite; mudstone with maroon coloured bands, notably at 8.58-8.62 m		
11.47	2.47		Siltstone with numerous mudstone partings, contacts usually abrupt but sometimes gradational	Calcite veinlets in mudstone and at 11.32-11.35 m in siltstone	
12.80	1.33		Sandstone, fine-grained, calcareous with micaceous hematite	Rare thin calcite veinlets	
13.40	0.60	30	Mudstone with a siltstone band at 13.15-13.26 m	Limonite-stained calcite veinlets	
15.06	1.66	45	Siltstone, massive, coarser at top with an irregular dark grey mudstone parting at 13.70 m	A few regular calcite veinlets up to 8 mm thick	
16.19	1.13		Intraformational breccia, mainly of mudstone clasts initially, passing into mainly siltstone clasts, many of which are veined	Calcite veining common except in areas of siltstone	
16.62	0.43	40	Siltstone, massive, dark to light grey in colour, calcareous; some thin mudstone partings	A few calcite veinlets at 45° to core axis	
19.63	3.01	35	Siltstone to 17.37 m, then mudstone; cut by thin breccia and by clay-filled fracture at 18.23-18.28 m	Numerous, irregular, orange-stained calcite veinlets	1041
22.22	2.59		Siltstone, grey and compact grading into olive-green silty mudstone containing some elongated clasts	Minor quartz veins and some (?) dolomite veins	1042
24.39	2.17		Mudstone and siltstone with elongated clasts of dark mudstone within the siltstone; locally brecciated, some clay-filled fractures	Numerous irregular calcite veinlets and some quartz veinlets	1043
25.52	1.13		Siltstone, grey, hard and competent except at 24.39-25.09 m where it is broken with slickensided surfaces	Pyrite impregnates broken section, extending into hard siltstone with arsenopyrite	1044
27.17	1.65		Siltstone, grey, very fractured, limonitised at base; sandstone from 26.38 m, sheared at 26.70 m with numerous quartz and calcite veinlets	Pyrite and arsenopyrite disseminated through lower sandstone; stibnite on fractures [CXD 1540]	1026
28.29	1.12		Sandstone, fine-grained, initially broken and friable	Pyrite and arsenopyrite disseminated through broken rock and with semseyite and sphalerite [CXD 1533; 1574] probably in veinlets	1027
29.41	1.12		Sandstone with thick developments of quartz resulting in a hard, competent rock despite brecciation	Thin quartz veins with minor pyrite and arsenopyrite	1028
30.82	1.41		Sandstone, massive strongly brecciated [CXD 1534; 1541]	Arsenopyrite and pyrite as disseminations and in veinlets with bournonite at 29.5 m	1029
32.62	1.80		Siltstone, compact and grey with mudstone partings	Quartz veinlets; calcite veinlet at 31.41 m with (?) grey sulphide	1045
34.10	1.48		Siltstone with mudstone partings; somewhat brecciated at 32.62-33.62 m [CXD 1535]	Pyrite and arsenopyrite as disseminations and in quartz veinlets; (?) grey sulphide in veinlet at 33.17 m	1046
36.67	2.57		Siltstone, grading in places into fine-grained sandstone containing lithic fragments and micaceous hematite; some mudstone partings; brecciated and reddened at 35.34-35.70 m	Regular calcite veinlets up to 13 mm thick but no visible sulphide	1047
38.18	1.51		Mudstone, silty and calcareous	Numerous quartz veins	
39.02	0.84		Sandstone, massive	Minor quartz veins	
44.35	1.33	40	Silty mudstone, initially laminated, pale to dark grey then uniform; maroon laminae parallel to bedding in basal 10 cm signifying oxidation of sandstone in next unit		
46.84	2.49		Sandstone, grey, hard and massive	Regular calcite veinlets common	
48.97	2.13		Mudstone with extensive maroon staining	Calcite and quartz veinlets fairly common	
53.15	4.18		Sandstone grading in places into silty sandstone; mudstone clasts apparently broken in situ at 49.82 m	Calcite veinlets especially at 51.82-51.86 m, red stained	
55.31	2.16	40	Mudstone and silty mudstone with some maroon staining parallel to bedding	Red stained calcite veinlets up to 3 cm thick	
59.96	4.65	50	Sandstone, hard, compact, massive with some micaceous hematite; mudstone partings contain deformed calcite veinlets at 59.30 m; some soft sediment deformation	Calcite veinlets up to 1 cm thick	
63.17	3.21		Siltstone grading into sandstone in places; intraformational clasts of dark mudstone are present; minor maroon staining along bedding planes		

Inclined depth, m	Intersection m	Bedding angle°	Lithology	Mineralisation	Sample No. CXD
65.67	2.50	40	Mudstone and siltstone exhibiting soft sediment deformation; a thin light green mudstone parting with some maroon staining; possible concretionary structure at 64.33 m	Many irregular calcite veinlets; chalcopyrite in light green mudstone; stibnite "bloom" and maroon pyrite on fractures with calcite	
68.72	3.05		Mudstone and siltstone, less deformed than in preceding unit	Stibnite "bloom" on fractures with calcite	
71.17	2.45		Siltstone grading in places into sandstone; somewhat calcareous; micaceous hematite throughout; a few mudstone partings	A few regular calcite veinlets, sometimes pink in colour	
72.27	1.10		Mudstone, olive-green with bands of light green mudstone with which maroon staining is associated; a small sandstone clast at 71.8 m	Calcite veinlets	
76.05	3.78		Sandstone, silty, calcareous with disseminated micaceous hematite; grades into siltstone in places with a few mudstone partings	Calcite veinlets	
84.87	8.82		Mudstone and siltstone, brecciated in places; pale coloured siltstone is calcareous	Extensive calcite veinlets, irregular, especially at 80.43-80.52 m at right-angles to core axis	

END OF BOREHOLE AT 84.87 m

APPENDIX II

GEOCHEMICAL ANALYSES OF DRILLCORE

Note (a). For more detailed lithological descriptions the sample number and sample depth should be cross-referenced to the corresponding borehole table in Appendix I; IFB denotes infraformational breccia.

Note (b). In the column headed 'Feature', B signifies the development of brecciation, D the presence of characteristics suggestive of debris flow development and F the occurrence of faulting.

Note (c). The incidence of vein and stratabound mineralisation was estimated visually during logging and classified as significant, trace or absent. For an explanation of the abbreviations refer to the list given in Appendix III.

APPENDIX II TABLE I BOREHOLE 1

Sample No. CXD	Depth From (m)	To (m)	Inter-section (m)	Generalised lithology	Feature	Mineralisation Stratabound Trace	Stratabound Sig.	Vein Trace	Vein Sig.	Ca (%)	Ti (%)	Fe (%)	Cu (ppm)	Zn (ppm)	As (ppm)	Sr (ppm)	Zr (ppm)	Sb (ppm)	Ba (ppm)	Pb (ppm)
1001	13.70	14.20	0.50	Clay,pebbles						1.71	0.56	5.64	28	84	60	80	275	13	222	16
1002	20.33	20.97	0.64	Clay,pebbles						1.74	0.57	6.25	33	91	190	67	240	22	266	39
1003	23.13	23.92	0.79	Clay,rock fragments						0.19	0.60	6.56	31	97	114	51	250	14	288	17
1004	24.98	25.94	0.96	Basal till						0.40	0.58	6.11	28	86	229	57	255	20	283	27
1005	30.22	31.15	0.93	Sandstone						3.50	0.50	5.29	12	73	63	130	266	12	308	11
1006	31.15	31.80	0.65	Siltstone						2.86	0.49	5.39	11	75	38	101	222	9	219	5
1007	31.80	34.16	2.36	Sandstone						4.61	0.42	4.91	25	62	29	124	248	15	358	5
1008	34.16	36.20	2.04	Mudstone	F					4.24	0.50	4.88	41	48	186	77	175	44	305	6
1009	36.20	37.12	0.92	Breccia, (?) IFB	B(?)D			St		5.13	0.46	4.68	28	45	98	69	239	24	278	8
1010	37.12	39.17	2.05	Sandstone	D					4.64	0.41	4.53	18	41	32	91	231	12	221	6
1011	39.17	41.18	2.01	Sandstone	F					4.57	0.43	4.07	8	23	87	66	223	11	224	3
1012	45.02	47.15	2.13	IFB,siltstone	D		Py	St		4.27	0.45	4.58	61	29	1557	162	182	58	260	17
1013	47.15	48.22	1.07	(?)Mudstone	F					1.46	0.46	5.87	76	37	2643	76	178	53	362	32
1014	48.22	49.02	0.80	(?)Mudstone	B					3.14	0.56	5.43	31	31	464	120	172	49	369	15
1015	49.02	50.75	1.73	Mudstone				Dk		4.09	0.50	4.43	41	34	82	162	175	46	240	14
1016	50.75	52.05	1.30	Siltstone						4.94	0.46	4.85	42	46	157	148	206	36	255	6
1017	52.05	53.72	1.67	Fault breccia,sandst.	F					5.15	0.43	4.52	33	41	74	221	177	30	257	6
1018	53.72	55.02	1.30	Mudstone						4.76	0.47	4.17	30	47	57	130	191	36	1039	8
1019	55.02	57.08	2.06	Mudst.,siltst.,sandst.						5.83	0.42	5.04	50	55	262	138	188	46	289	10
1020	57.08	58.99	1.91	Siltst.,sandst.,mudst.		Py		Py,Ar		4.97	0.43	4.50	18	27	376	141	215	33	224	40
1021	58.99	60.80	1.81	Siltstone		Py		Py,Ap,St		4.31	0.46	4.79	44	31	2578	153	165	66	251	293
1022	60.80	62.44	1.64	Siltstone,(?)IFB	?D		Ap	St	Py,Ap	2.81	0.45	3.46	23	20	3215	156	165	59	215	209
1023	62.44	63.44	1.00	IFB	D		Py,Ap	St	Dk	4.37	0.46	4.22	25	16	1935	306	248	58	189	443
1024	63.44	64.44	1.00	IFB	D		Py,Ap		Dk	4.05	0.46	3.92	20	20	960	371	323	35	207	246
1025	64.44	65.77	1.33	IFB	D		Py,Ap		Dk	4.24	0.46	5.13	19	17	7894	404	185	60	170	329
1030	65.77	67.37	1.60	Sandstone	D	Ap	Py			4.35	0.47	4.58	27	29	467	200	178	45	225	146
1031	67.37	69.52	2.15	Siltstone						4.47	0.47	4.46	31	40	258	148	182	28	278	16
1032	69.52	71.87	2.35	Sandstone	F				(?)Dk	5.59	0.43	4.65	24	55	154	169	183	28	292	10
1033	71.87	72.92	1.05	Sandstone	B					5.10	0.44	4.57	9	57	64	172	171	23	282	10
1034	72.92	75.87	2.95	Siltst.,mudst.,sandst.		Py				4.84	0.42	4.55	16	42	11	141	198	12	407	8
1035	75.87	77.92	2.05	Sandstone	D					4.75	0.45	4.80	13	51	65	134	188	12	270	10
1036	77.92	79.12	1.20	Sandstone	F					3.92	0.49	4.84	34	38	35	137	176	42	299	7
1037	79.12	81.96	2.84	Mudstone,sandstone	D	Py				4.04	0.50	4.84	34	38	58	132	174	44	270	9
1038	81.96	82.66	0.70	Sandstone						4.50	0.47	4.41	34	37	90	120	199	46	185	13
1039	82.66	83.22	0.56	Mudstone						2.46	0.55	4.54	120	56	106	144	192	127	243	8
1040	83.22	85.27	2.05	Siltstone,mudstone		Py				3.05	0.55	4.47	48	40	92	147	202	56	204	10

APPENDIX II TABLE II BOREHOLE 2

Sample No. CXD	Depth From (m)	To (m)	Inter-section (m)	Generalised lithology	Feature	Mineralisation Stratabound Trace	Stratabound Sig.	Vein Trace	Vein Sig.	Ca (%)	Ti (%)	Fe (%)	Cu (ppm)	Zn (ppm)	As (ppm)	Sr (ppm)	Zr (ppm)	Sb (ppm)	Ba (ppm)	Pb (ppm)
1128	42.60	44.38	1.78	Siltstone	F	Py,Ap		Py,St		5.07	0.43	4.51	37	42	295	145	188	38	200	7
1129	44.38	46.44	2.06	Sandst.,siltst.,mudst.	D		Py,Ap	Py,Ap,St		4.42	0.43	4.27	27	34	2783	122	262	32	211	11
1130	46.44	48.07	1.63	Breccia vein	D		Py,Ap	(?)Sm,(?)Ar		1.27	0.26	3.39	15	10	2177	52	93	60	103	20
1131	48.07	48.97	0.90	Breccia vein	D		Py,Ap	(?)Sm,(?)Ar		0.31	0.21	5.12	21	9	2508	23	72	118	81	26
1132	48.97	51.40	2.43	Breccia vein	D		Py	St		0.15	0.27	7.42	11	7	2467	31	116	151	100	59
1133	51.40	52.97	1.57	Siltstone	B		Py,Ap	Py,Ap,(?)Sm		1.41	0.43	4.75	25	17	4584	75	140	73	188	16
1134	52.97	54.50	1.53	Siltstone				Py,Ap		3.39	0.48	3.89	30	30	3601	114	167	43	240	20
1135	54.50	56.02	1.52	Siltstone	F			Py,Ap,(?)Sm		3.66	0.51	4.69	70	30	2955	139	146	61	259	30
1136	56.02	57.75	1.73	Siltstone			Ap,Py	St,Ap,Py,Dk		1.37	0.51	4.26	55	30	4665	86	148	68	207	30
1137	57.75	58.82	1.07	Sandst.,mudst.,siltst.			Py,Ap			3.44	0.46	4.08	40	20	3238	121	168	39	191	40
1138	58.82	59.72	0.90	Siltstone,sandstone	F	Py	Ap	St	Py,Ap	4.18	0.32	5.29	25	40	22300	131	108	100	137	70
1139	59.72	61.69	1.97	Siltstone		Py,Ap		Py,Ap		4.33	0.42	4.57	25	20	3461	146	176	27	178	60
1140	61.69	63.55	1.86	Siltstone,mudstone			Py	Py		4.10	0.49	4.95	40	30	219	170	180	41	204	120
1141	63.55	65.49	1.94	Siltstone,mudstone	D		Py	Py		4.16	0.47	5.51	30	30	167	156	173	43	206	150
1142	65.49	67.42	1.93	Siltstone	D	Py,(?)GS				4.82	0.42	5.40	30	30	249	138	169	32	183	190
1143	67.42	69.11	1.69	Sandst.,mudst.,siltst.	D		Py	Ap,Py,(?)GS		4.07	0.49	4.30	30	20	1978	117	231	39	151	190
1144	69.11	71.50	2.39	Sandstone,mudstone			Py	Py,St		3.48	0.49	5.60	35	30	476	121	170	41	189	120
1145	71.50	73.37	1.87	Mudstone,siltstone		Py		Py		4.23	0.48	5.09	25	20	500	173	153	24	472	90
1146	73.37	75.25	1.88	Siltstone,mudstone			Py	Py,(?)St,(?) Cp		3.73	0.50	5.06	40	30	481	134	187	38	206	150
1147	75.25	76.37	1.12	Mudst.,siltst.,sandst.	B		Py,Ap			3.18	0.52	4.76	25	20	2853	108	214	26	340	30
1148	76.37	78.90	2.53	Siltstone	F	Ap	Py			4.19	0.47	5.05	25	20	1081	142	169	26	296	50
1149	78.90	81.50	2.60	Siltstone,sandstone				Py,St		3.99	0.49	4.47	30	20	201	114	199	38	252	40
1150	81.50	82.88	1.38	Mudstone	D		Py	Py,St		3.85	0.53	4.61	40	20	219	144	218	44	197	50
1151	82.88	85.27	2.39	Mudst.,siltst.,sandst.			Py	Py,(?)Gl		3.35	0.59	4.42	65	30	341	143	220	61	250	180
1152	85.27	86.72	1.45	Siltstone	B			Py,(?)Br		4.82	0.47	4.27	65	40	320	141	199	49	1628	20
1153	86.72	88.70	1.98	Siltstone		Py		Py,St		4.29	0.50	4.33	40	30	397	148	180	39	205	30
1154	88.70	90.77	2.07	Siltstone		Py		Py,(?)St		4.59	0.47	4.30	25	30	322	121	185	29	170	30
1155	90.77	91.70	0.93	Siltstone	F		Py	Py,Ap		3.65	0.48	4.60	20	30	1903	134	181	35	224	30
1156	91.70	93.17	1.47	Breccia vein	D,F	(?)GS	Py,Ap			3.39	0.37	4.83	15	40	3664	139	149	81	163	30
1157	93.17	95.12	1.95	Siltstone			Py,Ap	St	Py,Ap	3.38	0.45	4.16	95	20	7147	116	168	52	216	30
1158	95.12	96.54	1.42	Siltstone,sandstone	B		Ap,Py	Cp		2.21	0.41	4.08	60	20	11900	94	157	62	162	30
1159	96.54	98.41	1.87	Sandstone	D		Ap,Py	Ap,Py,Dk		1.74	0.41	3.32	35	20	13900	77	169	59	144	30
1160	98.41	100.35	1.94	Siltstone,IFB	D		Py,Ap	Py,St		3.69	0.38	4.37	45	20	4032	125	169	35	153	20
1161	100.35	102.16	1.81	Siltstone		Py		Py,(?)St		4.52	0.40	4.29	15	20	81	130	199	27	139	20
1162	102.16	104.32	2.16	Siltstone		Py		Py,Ap,(?)St		4.26	0.42	4.81	25	20	2080	138	183	47	316	20
1163	104.32	106.67	2.35	IFB	D		Py,Ap	Py,Ap		3.49	0.54	4.10	35	20	3693	169	192	47	277	30
1164	106.67	107.75	1.08	Siltstone				Py,St		3.22	0.51	4.73	50	30	638	148	201	50	225	100
1165	107.75	109.47	1.72	IFB	D		Py,Ap	(?)St		4.71	0.46	4.91	30	30	4740	192	176	41	170	110
1166	109.47	111.09	1.62	Sandstone			Py,Ap	Py,Ap,St		4.15	0.56	4.29	20	20	3508	171	418	40	132	70
1167	111.09	113.15	2.06	IFB	D		Py,Ap	Py,Ap,St		3.52	0.49	4.60	35	20	5615	172	176	57	209	30
1168	113.15	114.73	1.58	Sandstone,IFB	D,F	Ap	Py	Py,St,(?)Bn		3.83	0.42	4.01	30	20	1311	166	255	36	156	150
1169	114.73	116.30	1.57	Siltstone	D,F	Py		Py,Ap		3.70	0.50	4.55	40	30	446	177	176	46	237	120
1170	116.30	118.80	2.50	Sandst.,siltst.,mudst.	B		Py	Py,Ap,(?)Bn		4.68	0.47	4.90	25	30	873	216	184	36	284	90

APPENDIX II TABLE III BOREHOLE 3

Sample No. CXD	Depth From (m)	To (m)	Inter-section (m)	Generalised lithology	Feature	Mineralisation Stratabound Trace	Stratabound Sig.	Vein Trace	Vein Sig.	Ca %	Ti %	Fe %	Cu ppm	Zn	As	Sr	Zr	Sb	Ba	Pb
1048	10.79	13.14	2.35	Siltstone	D			Py		4.63	0.43	4.27	13	28	1154	112	183	23	169	19
1049	13.14	13.96	0.82	Siltstone	D		Py			2.31	0.57	4.32	37	34	1169	116	199	54	255	21
1171	31.32	32.72	1.40	IFB	D		Py	Py		4.86	0.45	5.21	25	20	399	177	160	56	240	90
1182	32.72	33.47	0.75	Sandstone		Py				4.77	0.45	5.00	20	30	242	184	171	50	271	70
1183	33.47	36.05	2.58	IFB	D		Py	Py		3.12	0.53	4.66	35	10	616	149	174	72	318	110
1172	36.05	37.59	1.54	Sandstone	D		Py	GS,Py		4.47	0.32	3.82	20	10	314	150	157	44	205	70
1173	37.59	38.48	0.89	Sandstone	D		Py		Py	4.60	0.41	4.40	15	10	570	167	209	33	165	50
1174	38.48	39.72	1.24	Sandstone	D				Py	5.06	0.43	4.98	15	20	579	164	213	33	154	50
1175	39.72	41.08	1.36	Siltstone			Py		Py	3.35	0.55	4.33	45	10	495	146	202	80	211	90
1176	41.08	43.26	2.18	Sandst.,siltst.,mudst.		Py		Py		4.51	0.48	4.75	40	30	221	171	215	53	255	70
1177	43.26	44.79	1.53	Siltst.,mudst.,sandst.			Py	(?)Bn		5.23	0.39	5.05	15	20	285	240	178	41	219	60
1178	44.79	46.22	1.43	Siltstone,mudstone			Py	(?)St		4.31	0.47	5.02	35	20	298	173	168	99	277	110
1179	46.22	47.50	1.28	Siltstone	F		Py	St		4.50	0.45	3.92	30	20	229	395	172	81	223	100
1180	47.50	49.20	1.70	Sandstone,siltstone		(?)GS	Py,Ap	Py,St		4.29	0.47	4.32	35	20	3562	163	226	82	433	110
1181	49.20	51.10	1.90	Sandstone,siltstone			Py	Py,Ap		4.55	0.35	3.96	20	20	665	158	184	62	166	70
1050	51.10	53.67	2.57	Siltstone	D,F	Py,Ap				4.58	0.46	4.82	31	42	287	170	171	87	188	122
1051	53.67	55.88	2.21	Siltstone,mudstone			Py	Py,Ar		3.32	0.58	4.34	37	31	1195	186	191	87	241	103
1052	55.88	57.05	1.17	Sandstone		Py				4.44	0.48	4.00	32	21	296	284	209	85	267	129
1053	57.05	59.55	2.50	Mudstone,sandstone	B					4.25	0.38	4.00	14	21	1000	254	195	41	203	34
1054	59.55	61.70	2.15	Siltstone	F	Py,(?)Ap				4.23	0.49	3.89	30	16	372	216	187	84	257	126
1055	61.70	64.65	2.95	Sandstone,siltstone		Py				4.09	0.50	4.22	28	19	894	198	179	76	531	109
1056	64.65	66.47	1.82	Sandst.,siltst.,mudst.	B		Py,Ap	St,?GS		3.75	0.51	5.05	44	23	2739	189	167	127	408	170
1057	66.47	68.19	1.72	Siltstone,sandstone		Py,Ap		St		4.81	0.43	4.93	37	29	652	179	162	120	223	152
1058	68.19	70.01	1.82	Sandstone		Py,Ap				4.59	0.44	5.05	21	31	613	175	163	60	193	83
1059	70.01	72.04	2.03	Mudstone,siltstone		Py		St		3.41	0.55	5.61	28	33	600	165	160	121	254	121
1060	72.04	73.52	1.48	Sandstone		Py,Ap				3.32	0.53	4.34	20	24	1645	146	196	62	215	76
1061	73.52	75.22	1.70	Siltstone	F		Py,Ap			3.66	0.51	4.82	46	22	5552	170	170	113	302	160
1062	75.22	76.77	1.55	IFB	D,F		Py,Ap	Py,Ap,St		2.77	0.48	4.58	34	15	6419	226	180	90	227	111
1063	76.77	78.67	1.90	IFB	D,F		Py,Ap	Py,Ap,St		3.16	0.51	5.09	35	13	12300	174	189	109	170	130
1064	78.67	79.91	1.24	IFB	D,F		Py,Ap	Py,Ap,St		2.49	0.51	4.56	40	11	17900	164	168	150	175	249
1065	79.91	81.36	1.45	IFB	D,F		Py,Ap	Py,Ap,St		2.82	0.50	4.42	49	15	9897	173	174	138	344	233
1066	81.36	83.12	1.76	IFB	D,F		Py,Ap	Py,Ap,St		3.81	0.51	4.86	23	18	8021	225	177	93	188	75
1067	83.12	85.02	1.90	Siltst.,mudst.,sandst.			Py,Ap			3.29	0.51	4.82	43	14	4850	182	179	106	228	151
1068	85.02	86.95	1.93	Siltstone,mudstone			Py,Ap	Dk		2.39	0.57	4.13	27	18	6604	158	216	82	228	79
1069	86.95	89.20	2.25	Siltstone,mudstone	B		Py,Ap			2.04	0.53	4.56	31	12	8293	167	235	102	183	105
1070	89.20	91.97	2.77	Siltstone	D		Ap,(?)GS	Py,Ap		2.55	0.50	4.04	20	156	9160	138	257	549	454	1143
1071	91.97	93.76	1.79	Sandstone	B		Py,Ap	(?)Sp		1.73	0.47	3.46	36	1804	12200	119	216	198	968	1966
1072	93.76	95.58	1.82	Sandstone,siltstone	B		Py,Ap	(?)Bn		2.22	0.45	5.18	25	13	15200	136	192	112	510	105
1073	95.58	97.62	2.04	Siltstone		Py,Ap				4.71	0.46	4.33	38	32	689	207	151	112	251	176
1074	97.62	100.57	2.95	Mudstone,siltstone	B			Py,St,(?)Bn		3.70	0.51	4.36	51	22	1012	81	171	130	266	209
1075	100.57	103.10	2.53	Mudstone				Py,St,(?)Dk		3.62	0.51	4.56	23	24	1243	177	165	86	259	109
1076	103.10	104.49	1.39	Siltstone,mudstone	B	Py,Ap		Py,St,Bn		4.17	0.49	4.38	19	21	2154	185	270	51	190	67
1077	104.49	107.62	3.13	Sandstone	B		Py,Ap	St,Dk		3.58	0.51	4.68	29	22	4847	172	165	95	240	115
1078	107.62	109.78	2.16	Siltstone		Py,Ap		Py,St		4.61	0.46	4.51	31	21	681	237	186	84	220	126
1079	109.78	111.69	1.91	Mudstone,siltstone		Py		Py,St		3.74	0.54	5.39	22	30	402	262	174	102	231	109
1080	111.69	115.00	3.31	Siltstone			Py	St,(?)Bn		4.66	0.47	4.97	27	29	136	220	198	85	288	123
1081	115.00	117.20	2.20	Mudstone			Py	St	Py	4.00	0.50	5.03	35	32	439	202	161	105	268	167
1082	117.20	120.10	2.90	Sandstone,mudstone		Py		Py		5.62	0.45	4.77	31	29	158	216	265	88	291	128
1083	120.10	121.99	1.89	Sandst.,mudst.,siltst.	D	Py		Py		4.96	0.46	4.36	10	27	130	211	222	29	199	29
1084	121.99	124.22	2.23	Siltstone,mudstone	D	Py		Py		4.32	0.51	4.16	13	23	1451	296	201	59	299	54
1085	124.22	126.22	2.00	Sandstone	D	Py				4.43	0.45	4.57	57	25	3233	12	261	121	144	167
1086	126.22	129.22	3.00	Sandstone,mudstone			Py	Bn		3.84	0.42	3.53	20	22	886	200	247	61	436	76
1087	129.22	131.62	2.40	Sandstone	D		Py,Ap	Py,Ap		3.35	0.43	3.86	23	13	4712	250	217	86	146	90
1088	131.62	133.17	1.55	Sandstone	D		Py	Py,(?)GS		3.40	0.47	4.46	48	14	4634	241	198	126	214	161
1089	133.17	134.71	1.54	Siltstone			Py,Ap	Py,Ap		2.99	0.51	4.74	30	15	5701	203	216	84	648	85
1090	134.71	136.35	1.64	IFB	D		Py,Ap	Py,Bn		2.34	0.30	5.72	40	10	5435	102	119	110	109	120
1091	136.35	137.92	1.57	IFB	D,F		Py,Ap	Py		2.69	0.40	5.43	25	10	14300	130	159	116	147	80
1092	137.92	139.23	1.31	IFB	D		Py,Ap	Py		2.75	0.33	3.68	35	10	5081	98	144	114	95	120
1093	139.23	140.62	1.30	IFB	D		Py,Ap	Py		2.87	0.22	5.62	25	10	5747	95	97	87	179	80
1094	140.62	142.64	2.02	Siltstone	D	Py		St,(?Bn)		4.00	0.48	3.88	41	31	1304	179	206	116	273	179
1095	142.64	144.27	1.63	Siltstone,sandstone	D,B	Ap	Py	Py,Br,Bn		3.97	0.43	4.31	20	21	3767	152	185	74	705	96
1096	144.27	145.52	1.25	Siltstone,mudstone			Py,Ap	Py,Ap,Bn		3.75	0.48	4.71	45	19	7207	191	171	118	757	164
1097	145.52	146.67	1.15	Sandstone,siltstone		Ap	Py	Py,Ap		4.87	0.42	4.21	17	17	1710	151	250	48	198	62
1098	146.67	148.07	1.40	Siltstone			Py,Ap,(?)GS	Py,Ap,Br,Dk		3.30	0.49	4.34	34	17	6459	153	176	91	244	121
1099	148.07	148.95	0.88	IFB,siltstone			Ap,Py	Py,Ap		3.83	0.46	5.54	23	21	12200	209	180	93	243	69
1100	148.95	150.45	1.50	Siltstone			Py,Ap,(?)GS	Py,Ap,(?)GS		4.48	0.44	4.94	44	24	8918	209	145	134	273	172
1101	150.45	151.77	1.32	Siltstone			Py,Ap	Py,Ap		4.23	0.45	4.44	46	22	5225	196	145	117	257	170
1102	151.77	153.05	1.28	Siltstone,IFB	D	Ap	Py	Py,Ap		3.71	0.51	4.04	57	43	1753	181	168	93	222	49
1103	153.05	154.97	1.92	Siltstone	F					5.12	0.47	4.83	16	51	57	172	174	31	204	6
1104	154.97	156.07	1.10	Siltstone			Py,Ap			4.78	0.47	4.93	7	47	1837	162	183	26	197	15
1105	156.07	157.62	1.55	Siltstone			Py			5.24	0.46	5.17	18	63	57	191	176	20	255	7
1106	157.62	159.55	1.93	Siltstone			Py	Py,Br		5.35	0.47	5.24	23	64	74	226	185	35	6505	13
1107	159.55	160.95	1.40	Siltstone			Py			3.94	0.54	5.71	20	73	28	172	190	29	281	6
1108	160.95	162.27	1.32	Siltstone			Py			3.77	0.55	5.72	36	74	42	163	200	44	254	6
1109	162.27	164.20	1.93	Siltstone			Py			4.16	0.54	5.74	25	70	28	165	197	45	300	23
1110	164.20	165.81	1.61	Siltstone			Py			5.69	0.43	4.95	26	46	22	160	193	54	226	92
1111	165.81	167.10	1.29	Siltstone			Py	St		4.40	0.48	4.77	31	30	967	166	191	55	243	47
1112	167.10	168.73	1.63	Siltstone	B	Ap	Py	Py,Bn		4.10	0.52	4.25	26	25	101	168	221	80	395	99
1113	168.73	170.04	1.31	Siltstone			Py,Ap			5.47	0.41	4.52	26	39	1062	165	192	45	210	37
1114	170.04	171.59	1.55	Siltstone			Py,Ap	Py,Ap		4.14	0.47	4.37	32	23	3192	156	220	38	221	24
1115	171.59	173.11	1.52	Siltstone			Py,Ap	Py,Ap		4.09	0.41	3.97	29	26	2474	143	186	40	220	6
1116	173.11	174.96	1.85	Siltstone			Py,Ap,(?)GS			3.96	0.47	4.15	45	33	3161	163	180	46	279	9
1117	174.96	176.35	1.39	Siltstone		Ap	Py	Py		4.20	0.38	4.16	31	28	1336	145	196	33	158	6
1118	176.35	178.58	2.23	Breccia vein,(?)IFB	(?)D	Ap	Py			2.48	0.23	4.53	15	16	3200	102	81	39	164	14
1119	178.58	180.54	1.96	Siltst.,sandst.,mudst.	D	Py,Ap		Py		4.31	0.46	4.85	36	42	218	153	164	43	371	48
1120	180.54	182.82	2.28	Siltstone				(?)St		4.49	0.47	5.09	34	59	64	177	154	39	255	46
1121	182.82	184.94	2.12	Siltstone				(?)St,Py		4.49	0.46	4.88	42	51	53	149	161	52	239	14
1122	184.94	186.82	1.88	Siltstone				(?)St,Py		4.84	0.45	5.23	42	65	43	154	155	45	231	11
1123	186.82	188.83	2.01	Sandstone,siltstone	F	Py				4.17	0.48	5.39	14	72	20	120	184	16	265	6
1124	188.83	191.33	2.50	Sandstone		Py				4.71	0.42	5.16	22	57	5	94	198	7	313	1
1125	191.33	193.93	2.60	Sandstone				Py,(?)St		5.31	0.46	4.58	20	57	10	162	271	7	438	8
1126	193.93	196.06	2.13	Siltstone		Py		St		3.85	0.50	5.67	20	92	13	118	177	27	385	10
1127	196.06	197.82	1.76	Mudstone,siltstone				(?)St		3.99	0.50	5.89	13	98	28	145	155	14	402	18

APPENDIX II TABLE IV BOREHOLE 4

Sample No. CXD	Depth From (m)	To (m)	Inter-section (m)	Generalised lithology	Feature	Mineralisation Stratabound Trace	Stratabound Sig.	Vein Trace	% Ca	% Ti	% Fe	ppm Cu	ppm Zn	ppm As	ppm Sr	ppm Zr	ppm Sb	ppm Ba	ppm Pb
1041	16.64	19.63	2.99	Mudstone,siltstone	F				3.45	0.53	6.94	43	110	74	79	165	120	275	7
1042	19.63	22.22	2.59	Siltstone	D				3.69	0.51	5.92	33	103	26	101	172	66	209	11
1043	22.22	24.39	2.17	Mudstone,siltstone	D				2.57	0.57	6.86	47	102	52	68	199	105	196	26
1044	24.39	25.52	1.13	Siltstone	F	Ap	Py		2.95	0.49	5.36	36	25	643	77	183	97	190	151
1026	25.52	27.17	1.65	Siltstone,sandstone	F		Py,Ap	Ap,Py	3.12	0.47	3.69	20	125	2468	83	218	133	175	265
1027	27.17	28.29	1.12	Sandstone			Py,Ap	Py,Ap,Sm,Sp	2.72	0.41	5.38	38	839	12848	75	180	1067	175	3136
1028	28.29	29.41	1.12	Sandstone	B			Py,Ap	7.03	0.24	5.90	27	38	1234	83	113	114	104	109
1029	29.41	30.82	1.41	Sandstone	B		Py,Ap	Py,Ap,Bn	3.54	0.43	5.09	28	48	3877	80	207	156	171	173
1045	30.82	32.62	1.80	Siltstone				(?)GS	3.93	0.49	5.22	32	70	74	105	174	116	224	144
1046	32.62	34.10	1.48	Siltstone	B			Py,Ap,(?)GS	3.40	0.50	5.58	34	52	2642	93	184	97	170	105
1047	34.10	36.67	2.57	Siltstone	B				4.13	0.48	5.27	20	86	10	120	190	44	210	13

APPENDIX II TABLE V

Analyses for additional elements in selected core samples

Sample No. CXD	From (m)	To (m)	Inter-section (m)	Generalised lithology	Feature	Stratabound Trace	Stratabound Sig.	Vein Trace	Vein Sig.	Ni	Mo	Ag	Sn	W	Au	Hg	Bi	U
										ppm								
Borehole 1 [see also Table I]																		
1021	58.99	60.80	1.81	Siltstone		Py		Py,Ap,St		112	2	2	1	5	0.052	0.12	2	5
1022	60.80	62.44	1.64	Siltstone, (?)IFB	(?)D		Ap	St	Py,Ap	73	6	0	0	5	0.11	0.08	0	3
1023	62.44	63.44	1.00	IFB	D		Py,Ap	St	Dk	76	0	1	0	7	0.010	0.13	1	3
1024	63.44	64.44	1.00	IFB	D		Py,Ap		Dk	65	1	0	2	6	<0.01	0.22	0	4
1025	64.44	65.77	1.33	IFB	D		Py,Ap		Dk	88	2	1	3	9	<0.01	0.16	4	4
Borehole 4 [see also Table IV]																		
1026	25.52	27.17	1.65	Siltstone, sandstone	F		Py,Ap	Ap,Py		54	0	0	3	4	<0.01	0.15	1	2
1027	27.17	28.29	1.12	Sandstone			Py,Ap	Py,Ap,Sm,Sp		73	2	1	3	0	0.100	0.45	6	2
1028	28.29	29.41	1.12	Sandstone	B			Py,Ap		44	2	0	2	0	<0.01	0.14	1	0
1029	29.41	30.82	1.41	Sandstone	B,Py,Ap			Py,Ap,Bn		59	1	2	0	4	<0.01	0.16	2	4

APPENDIX III

PETROGRAPHY AND MINERALOGY OF SELECTED CORE SAMPLES AND MINE DUMP SAMPLES, AND ELECTRON MICROPROBE ANALYSES OF SULPHIDES

Introduction

Specimens were examined in polished thin section and investigated by X-ray diffraction, X-ray fluorescence analysis, electron microprobe analysis and carbonate staining using Alizarin-red solution. The diffraction technique employed was powder photography and the results given in the tables bear the powder film numbers. Analyses by XRF were effected by scans of polished thin sections, panning concentrates and powder camera diffraction mounts using a Siemen's VRS manual spectrometer. The results are expressed in Tables I—IV, corresponding to samples from BHs 1—4 respectively, and in Table V which deals with dump specimens from the sorting floors associated with the old mine workings.

Microprobe analyses were carried out by B. Beddoe-Stephens with a Cambridge Instruments Microscan 5 on 14 pyrite grains and 14 arsenopyrite grains and the results are given in Tables VI—IX.

Mineral abbreviations used in Tables I—V

Ap	arsenopyrite	PF	potassic feldspar
Ar	aragonite	Pl	plagioclase
At	apatite	Py	pyrite
Br	baryte	Qz	quartz
Bn	bournonite	RF	rock fragments
Ca	calcite	St	stibnite
Cp	chalcopyrite	Sm	semseyite
Cy	clay minerals	Sp	sphalerite
Dk	dickite	Tm	tourmaline
Do	dolomite	Tn	tennantite
Gl	galena	Tt	tetrahedrite
Gs	unidentified grey sulphide	Zc	zircon
Hm	hematite		

TABLE I

Petrography of core specimens, BH1

Sample Number (CXD)	Depth (m)	PTS No	Name	Mineral Constituents Major	Minor	Comments
1537	31.75-31.79	5859	Sandstone	Qz Hm	Pl Tm RF Zc	Matrix consists of chlorite, clay minerals, muscovite, sericite and hematite; original biotite altered to hematite; veinlets contain dolomite
1538	36.50-36.56	5860	Sandstone	Qz Hm	St Py RF	Turbid matrix consists of clay minerals, muscovite, sericite, hematite, trace chlorite; veinlets contain hematite; stibnite on fracture surfaces
1577	47.54-47.62	6359	Siltstone	Qz Hm	Py	Intensely altered; replacement by carbonate and hematite; disseminated pyrite largely replaced by hematite
1539	50.02-50.08		Siltstone	Qz	Py Dk	Dickite abundant along fracture surfaces; trace of disseminated pyrite
1575	54.86-54.94	6357	Sandstone	Qz Hm	Tm RF Py	Matrix strongly altered with traces of hematite, biotite, muscovite and carbonate; minor disseminated pyrite; calcite in veinlets
1500	61.91-62.00		Sandstone	Qz	Py Ap St	Veinlets contain pyrite, arsenopyrite, quartz and dolomite; trace of stibnite on fracture surfaces
1501	62.60-62.64		Breccia	Qz	Ap Py St RF Cy	Specimen from possible fault zone; strong alteration to dickite; trace disseminated pyrite and arsenopyrite; stibnite on fracture surfaces
1502	64.04-64.10		Breccia	Qz	RF Cy	As for CXD 1501 except no apparent sulphide mineralisation
1503	64.26-64.31		Breccia	Qz	RF Py Ap	As for CXD 1501 but no stibnite apparent
1504	65.19-65.22		Breccia	Qz	RF Do Cy Py Ap	Alteration less intense than CXD 1501-1503; disseminated pyrite and arsenopyrite
1505	75.42-75.49	5852	Sandstone	Qz	RF Pl PF Py Tm Zc	Feldspar clasts strongly sericitised; matrix consists of clay minerals, sericite, muscovite shreds, chlorite and amorphous iron oxide; traces of disseminated pyrite
1506	76.94-76.97	5853	Sandstone	Qz	RF Pl Do Py Tm Zc	Feldspar clasts strongly sericitised; matrix consists of clay minerals, sericite, muscovite shreds, dolomite, traces of chlorite and amorphous iron oxide; trace of disseminated pyrite
1507	79.16-79.22	5861	Mudstone		Py	Trace of disseminated globular pyrite
1576	83.56-83.75	6358	Siltstone	Qz	Do	Turbid matrix largely comprised of dolomite; veins contain pyrite and tetrahedrite (confirmed by XRD: Ph 6460); finely disseminated pyrite also present; trace of stibnite on fracture surfaces

TABLE II

Petrography of core specimens, BH2

Sample Number (CXD)	Depth (m)	PTS No	Name	Mineral Constituents Major	Minor	Comments
1592	42.09-42.27					Dark grey sulphide in quartz veinlets identified as tetrahedrite and tennantite by XRD analysis (Ph 6477)
1545	44.20-44.23		Mudstone		Py Ap St	Non-laminated; traversed by at least two generations of veinlets (i) contains traces of pyrite and arsenopyrite (ii) intersects type (i) and contains minute crystals of pyrite; stibnite on fracture surfaces
1560	44.25-44.30	6024	Mudstone		Py Ap Hm Do	Strong sericitisation; stratiform pyrite and arsenopyrite concentrated in narrow bands parallel to original bedding; distinctive red colouration due to late-stage veins of dolomite and hematite (confirmed by XRD, Ph 6416, 6417)
1546	44.30-44.32		Sandstone	Qz	Py Ap St	Contains "flames" of mudstone; single traversing vein contains pyrite and arsenopyrite; trace of stibnite on fracture surfaces
1536	46.17-46.25		Mudstone		Py Ap St	Pyrite and arsenopyrite in bands parallel to original bedding; trace of stibnite on fracture surfaces
1561	46.25-46.29	6025	Mudstone		Py Ap	Strongly sericitised; stratiform pyrite and arsenopyrite exhibit slight hematatic alteration
1585	48.68-48.77	6361	Breccia	Qz RF	Do Hm Dk	Fragments of mudstone or siltstone contain patches of hematite (Ph 6485) possibly replacing pyrite; matrix of quartz and trace dolomite; veins contain quartz and dickite; traces of pyrite altered to hematite; stibnite on fracture surfaces
1548	48.97-49.00		Sandstone	Qz	Do Py Ap St	Masked alteration associated with antense quartz-carbonate veining; sparsely disseminated pyrite and arsenopyrite; trace of stibnite on fracture surfaces
1562	49.11-49.18	6026	Breccia	Qz RF	Hm	Coarse sandstone fragments set in a quartz matrix; fragments contain abundant aggregates of prismatic crystals of hematite probably replacing arsenopyrite (XRF scan indicated major Fe)
1589	54.96-55.04					Red veins identified as hematite plus a mica mineral by XRD analysis (Ph 6475)
1590	55.30-55.37					Red mineral identified by XRD analysis as hematite plus mica mineral (Ph 6476)
1549	56.12-56.14		Mudstone		Py St Hm	Reddish hematitic alteration obscures much of the mineralogy; pyrite sparsely disseminated; trace of stibnite on fracture surfaces
1563	57.42-57.47	6027	Siltstone	Qz Ap Py	Do Dk Ap Py	Abundant disseminated arsenopyrite with subordinate globular pyrite; complex vein network; infilling minerals are quartz, dolomite, dickite and traces of pyrite and arsenopyrite

TABLE II (continued)

Sample Number (CXD)	Depth (m)	PTS No	Name	Mineral Constituents Major	Minor	Comments
1550	59.08-59.17		Breccia	Qz RF Do	Py Ap	Sandstone or siltstone fragments set in a quartz-dolomite matrix; finely disseminated pyrite and arsenopyrite
1564	60.14-60.20	6028	Sandstone	Qz	Do Py Ap	Strong sericitisation; disseminated pyrite with subordinate arsenopyrite; veinlets contain dolomite with trace pyrite
1573	68.13-68.23					Grey sulphides in veinlets identified as galena plus tetrahedrite (Ph 6454)
1588	74.94-74.99					Grey sulphide in veinlets identified as chalcopyrite (Ph 6474)
1558	98.57-98.62	6022	Breccia	RF Qz Do	Py Ap	Rock fragments consist of mudstone, siltstone and sandstone and all contain disseminated pyrite and arsenopyrite; quartz-dolomite matrix contains disseminated pyrite arsenopyrite; fine, sinuous veinlets contain traces of pyrite and arsenopyrite
1559	100.23-100.30	6023; 6023A	Siltstone	Qz Do	Py Hm (Ap)	Fabric masked by intense carbonate alteration; where alteration is most intense, arsenopyrite is almost completely replaced by hematite and dolomite; pyrite appears to have suffered little or no alteration
1567	112.87-112.97	6031	Mudstone	Do	Py Ap	Nature of original rock difficult to evaluate as carbonate is alteration intense; banded pyrite and arsenopyrite probably stratiform

TABLE III

Petrography of core specimens, BH3

Sample Number (CXD)	Depth (m)	PTS No	Name	Mineral Constituents Major	Minor	Comments
1542	19.42					Small green flakes from vein identified by XRD analysis as a dioctahedral mica mineral (Ph 6324)
1584	36.28-36.38					Grey sulphide in veinlets identified by XRD analysis as bournonite (Ph 6461)
1580	45.69-45.77					Dark grey sulphide in vein identified by XRD analysis as bournonite (Ph 6458)
1569	49.05-49.13	6033	Sandstone	Qz	RF Do Py Zc	Quartz and undifferentiated rock fragments set in a matrix of clay minerals, sericite, dolomite and a trace of chlorite; disseminated pyrite; two generations of veining: (i) dolomite with traces of pyrite, and (ii) quartz; the quartz veins cross-cut and postdate the dolomite veins
1508	55.5				Ar	Clear tabular crystal from a late-stage fracture identified by XRD analysis as aragonite (Ph 6313)
1570	57.85-57.95	6034	Breccia	RF Qz Do	Py	Fragments of sandstone and mudstone strongly altered to sericite and chlorite; matrix consists of quartz and dolomite; a fine network of quartz-carbonate veins have provided localised sites for strong carbonate alteration; trace of globular pyrite in matrix; greenish mineral associated with altered rock fragments identified by XRD analysis as a dioctahedral mica mineral (Ph 6407)
1509	64.78-68.85		Mudstone		Py Ap St	Specimen very friable; abundant disseminated pyrite and arsenopyrite; trace of stibnite on fracture surfaces
1593	65.93-66.05	6362	Mudstone		Py Qz Do	Discrete patches of disseminated pyrite; quartz-dolomite veins containing traces of pyrite
1543	66.78-66.83		Sandstone	Qz	St	Fine acicular stibnite on fracture surfaces confirmed by XRD analysis (Ph 6322)
1510	67.92-68.02		Mudstone		St	Stibnite blooms on fracture surfaces confirmed by XRD analysis (Ph 6320)
1511	70.36-70.42		Mudstone		Py St	Blooms of stibnite on fracture surfaces; trace of disseminated pyrite
1544	79.38-79.42		Breccia	RF Qz Do	Ap Py	Siltstone or sandstone fragments set in a quartz-carbonate matrix; although the rock is strongly sheared stratiform arsenopyrite with subordinate pyrite are still recognisable
1512	80.87-80.90	5854; 5854A	Siltstone	Qz	Zc Py Ap	Occasional zircon grains present in matrix; arsenopyrite and pyrite in bands; trace of stibnite on fracture surfaces; two generations of veining: (i) dolomite with traces of pyrite and (ii) quartz with traces of dolomite and arsenopyrite; the quartz veins cross-cut the dolomite veins

TABLE III (continued)

Sample Number (CXD)	Depth (m)	PTS No	Name	Mineral Constituents Major	Minor	Comments
1513	83.35-83.41		Mudstone		Ap	Despite shearing, bands of arsenopyrite with traces of pyrite are roughly parallel to the original bedding
1514	86.93-87.02	5863	Sandstone	Qz	Py Ap RF Do Dk	Despite obliteration of most primary features by shearing, bands of arsenopyrite and pyrite lying roughly parallel to the original bedding can still be seen; two generations of veining, (i) dolomite veins and (ii) later veins containing quartz, dolomite and dickite; veins are devoid of sulphide minerals
1582	90.92-91.17				Bn Ap Sp	Grey sulphides identified by XRD analysis as bournonite, arsenopyrite and a trace of sphalerite (Ph 6457; 6473)
1583	92.35-92.49	6360	Breccia	RF Qz	Py Ap Do Sp	Fragments of sandstone or siltstone containing traces of disseminated pyrite and arsenopyrite; matrix consists of coarse crystalline quartz with a trace of dolomite; veins contain coarse platy dolomite with a trace of pyrite and cross cutting quartz veins containing pyrite, arsenopyrite and sphalerite: confirmed by XRD analysis (Ph 6459)
1515	103.83-103.91		Mudstone		Ap Py Bn St	Arsenopyrite and pyrite in bands parallel to original bedding; trace of bournonite in veins and stibnite on fracture surfaces
1516	106.19-106.26	5855	Mudstone		Ap Py Qz Do Dk St	Arsenopyrite is disseminated in varying amounts through the rock; differential distribution of disseminated arsenopyrite; however, together with minor pyrite it is also concentrated in a band running parallel to the original bedding; veinlets contain quartz, dolomite and dickite (confirmed by XRD analysis: Ph 6318); stibnite blooms on fracture surfaces
1517	109.23-109.31	5864	Sandstone	Qz	Py Ap St RF Pl Tm Zc	Sparse distribution of disseminated pyrite and arsenopyrite; stibnite on fracture surfaces; two generations of veining, (i) dolomite veins (ii) late veins of quartz with traces of dolomite and pyrite
1518	128.49-128.61	5865	Sandstone	Qz	Py Bn RF Pl Tm Zc	Finely disseminated pyrite; narrow dolomitic vein contains tiny crystals of bournonite
1519	134.73-134.79	5866	Breccia	Qz Do RF	Dk Py	Fragments of mudstone, sandstone and quartz set in a matrix containing quartz, carbonate, dickite and abundant disseminated pyrite; narrow quartz-carbonate veins contain minor amounts of pyrite
1520	137.49-137.56		Breccia	Qz Do RF	Dk Py	Similar to specimen CXD 1519; dickite identified by XRD analysis (Ph 6318)
1521	139.63-139.74	5867	Breccia	Qz Do RF	Py Ap Dk	Similar to CXD 1519 except that a trace of arsenopyrite is present while dickite is uncommon
1573	143.62-143.67		Sandstone	Qz	RF Do Bn Br Py	Associated with a thin brecciated zone; a dolomite rich vein contains bournonite and baryte, confirmed by XRD analysis (Ph 6386); trace of disseminated pyrite

TABLE III (continued)

Sample Number (CXD)	Depth (m)	PTS No	Name	Mineral Constituents Major	Minor	Comments
1522	145.05-145.11	5868	Mudstone		Py Ap Bn Do	Pyrite and arsenopyrite occur in bands parallel to the original bedding whereas bournonite (Ph 6323) is confined to fracture surfaces; the veinlets present are composed of dolomite, with traces of pyrite and arsenopyrite
1565	145.17-145.24	6029	Mudstone		Py Ap Do	Pyrite and arsenopyrite occur in two distinctive bands about 1 mm wide which lie parallel to the original bedding, and also in minor amounts in dolomite-rich veinlets
1566	148.07-148.24	6030	Breccia	RF Qz Ap	Py	Fragments consist of sericitised mudstone or siltstone which contain globular pyrite and bands of pyrite roughly parallel to the original bedding; matrix contains quartz and arsenopyrite in roughly equal proportions together with traces of dolomite and pyrite; veinlets are comprised of dolomite with traces of pyrite
1523	157.63-157.69	5869	Mudstone		Py Ap Qz Do Cp Br Gl	Finely disseminated pyrite and arsenopyrite with rare flecks of chalcopyrite; complex network of veining: infilling minerals include dolomite, baryte, quartz and traces of pyrite and galena
1522	165.40-165.55	6021	Mudstone		Py Qz Do Gl	Microscopic pyrite located along limbs and crests of small folds; veins contain quartz, dolomite and galena (confirmed by XRD analysis, Ph 6387)
1524	165.75-165.80	5870	Siltstone	Qz	Py Do Gl St	Trace of disseminated pyrite; dolomite-quartz veins contain small crystals of galena; stibnite blooms on fracture surfaces
1571	166.64-166.81	6096	Siltstone	Qz	Py Hm St	Finely disseminated pyrite with concentrations in narrow zones parallel to the original bedding; hair veinlets contain hematitic dust; stibnite on fracture surfaces
1525	168.01					Tiny black crystals in a dolomite vein identified by XRD analysis as bournonite (Ph 6312)
1553	168.44-168.48		Mudstone		Py Ap	Abundant disseminated arsenopyrite with stringers of globular pyrite
1572	168.62-168.73	6035	Siltstone	Qz	Py Ap	Pyrite and arsenopyrite occur in bands parallel to the original bedding; arsenopyrite is the dominant sulphide; globular pyrite has formed around the arsenopyrite crystal boundaries
1581	169.60-169.66					Black sulphide in dolomite veinlet is bournonite (Ph 6456)
1526	175.27-175.30	5871	Sandstone	Qz	Pl Tm Zc RF Py Hm	Finely disseminated pyrite altering to hematite; two generations of veining, (i) dolomite-quartz veins with subhedral to euhedral crystals of pyrite and (ii) later quartz veins devoid of sulphide minerals

TABLE III (continued)

Sample Number (CXD)	Depth (m)	PTS No	Name	Mineral Constituents Major	Mineral Constituents Minor	Comments
1527	176.82-176.92	5856	Breccia	RF Qz Py	Do Dk	Rock fragments are predominantly mudstone, strongly sericitised and carrying abundant disseminated pyrite; the quartz-dolomite matrix contains areas of massive pyrite seemingly confined to certain zones; trace of dickite in matrix; complex network of quartz and dolomite veins
1528	177.08-177.15	5857	Breccia	RF Qz	Ap Py Do	Similar to specimen CXD 1527 except that traces of disseminated arsenopyrite occur in some of the rock fragments whereas the zones of massive pyrite are absent
1530	177.70-177.75		Breccia	RF Qz	Ap Py Do	Trace of disseminated pyrite and arsenopyrite in a quartz-dolomite matrix
1529	177.76-177.81		Breccia	RF Qz Py	Do Dk	Similar to specimen CXD 1527
1568	178.64-178.69	6032	Siltstone	Qz	Py Ap Do	Incorporates irregular flame-shaped masses of mudstone which contain isolated crystals of arsenopyrite and pyrite; arsenopyrite and pyrite are disseminated throughout the siltstone; veinlets contain dolomite with a trace of pyrite
1531	193.12-193.20		Sandstone	Qz	RF Hm	Abundant, bronze-coloured flaky mineral identified as hematite which appears to be replacing biotite
1532	194.88-194.98		Mudstone		Py St	Finely laminated; sparse dissemination of pyrite; stibnite blooms on fracture surfaces

TABLE IV

Petrography of core specimens, BH4

Sample Number (CXD)	Depth (m)	PTS NO	Name	Mineral Constituents Major	Minor	Comments
1540	26.92-26.96	5873	Sandstone	Qz	Pl Py Ap St RF	Minor disseminated arsenopyrite and pyrite; veinlets contain dolomite and hematite; stibnite on fracture surfaces
1533	27.50-27.55		Breccia	Qz RF	Py Ap Sp Sm At	Very friable rock with abundant pyrite and arsenopyrite in matrix; from the crushed sample the following were identified by XRD analysis: sphalerite (Ph 6306, 6310); semseyite (Ph 6308, 6309, 6311); arsenopyrite (Ph 6281); apatite (Ph 6317) and quartz (Ph 6307)
1574	27.62-27.67	6356	Sandstone	Qz	Py Ap St Gl Do	Matrix consists of clay minerals, carbonate, a trace of chlorite, shreds of muscovite and minor biotite; disseminated pyrite and arsenopyrite; quartz-carbonate veins contain pyrite, arsenopyrite and galena; stibnite blooms on fracture surfaces
1541	29.41-29.50	5874	Sandstone	Qz	Pl Zc RF Py Ap Bn	Disseminated pyrite; pyrite, arsenopyrite and trace of bournonite in quartz-carbonate veins
1534	29.53-29.56		Sandstone	Qz	Py Ap	Comments as for CXD 1541 but no bournonite detected
1535	33.17-33.22	5875	Sandstone	Qz		Disseminated arsenopyrite and minor pyrite; veinlets contain quartz, dolomite and traces of chlorite and hematite but no sulphides

TABLE V

Petrographic data for specimens from the sorting floors of Glendinning Mine

Sample Number DBR	PTS Number	Mineral Constituents Major	Mineral Constituents Minor	% Quartz-Carbonate Gangue
501	4886	St Sp		30
502	4887	Sp Gl	St Py	35
503	4888	Sp Gl	Py	15
504	4889	St Sp	Py Gl	60
505	4890	St Sp	Gl Py	45
506	4891	St Sp Gl	Py	35
507	4892	Sp Gl	Py Ap St	30
508	4893	Gl	Sp Py Gl	80
509	4894		Gl St Sp	85

TABLE VI

Electron microprobe analysis of stratiform pyrite

	1	2	3	4	5	6	7	8	9	LLD[≠]
Wt %										
Fe	41.73	41.20	44.93	44.70	46.07	45.24	45.98	45.27	45.17	
S	49.97	48.55	49.35	49.38	51.77	50.46	53.32	51.59	50.50	
As	2.83	1.35	5.31	4.87	1.98	4.05	1.25	3.25	3.62	
Total	94.53*	91.10*	99.59	98.95	99.82	99.75	100.55	100.11	99.29	
Atomic formulae (3.000)										
Fe	0.957	0.975	1.000	0.998	1.004	0.997	0.987	0.987	0.998	
S	1.995	2.001	1.912	1.921	1.964	1.937	1.993	1.960	1.943	
As	0.048	0.024	0.088	0.081	0.032	0.067	0.020	0.053	0.060	
ppm										
Ni	4990	3140	(10)	230	1710	40	-	190	(40)	200
Co	2140	1300	930	900	1210	730	-	850	820	260
Sb	1220	1200	(0)	(120)	(0)	(0)	no	190	(40)	210
Ag	(0)	(0)	(0)	(0)	(0)	(0)	data	(0)	(0)	220
Se	(0)	(70)	(100)	(0)	(0)	(0)	-	(0)	(0)	680
Cu	620	600	370	660	780	(190)	-	(0)	440	300
PTS No	6027	6027	6029	6029	6030	6030	6030	6035	6035	
CXD No	1563	1563	1565	1565	1566	1566	1566	1572	1572	
BH No	2	2	3	3	3	3	3	3	3	
Depth: (m)	57.42 -57.47	57.42 -57.47	145.17 -145.24	145.17 -145.24	148.07 -148.24	148.07 -148.24	148.07 -148.24	168.62 -168.73	168.62 -168.73	

Notes: Values in brackets are below 99% confidence detection limits. (≠ lower limit of detection: 80-100 sec. counts).
* Low totals probably due to poor specimen surfaces related to abundant microscopic inclusions in grains.

TABLE VII

Electron microprobe analyses of vein pyrite

	1	2	3	4	5
Wt %					
Fe	45.38	45.30	45.93	44.77	46.02
S	50.76	52.99	51.11	51.85	53.53
As	5.18	0.62	1.83	3.34	1.36
Total	101.32	98.91	98.97	99.96	100.91
Atomic formulae (3.000)					
Fe	0.989	0.984	1.011	0.976	0.984
S	1.927	2.006	1.959	1.969	1.994
As	0.084	0.010	0.030	0.054	0.022
ppm					
Ni	(0)	(0)	(0)	(0)	(0)
Co	480	(190)	280	940	720
Sb	(0)	1470	(0)	670	60
Ag	(70)	(100)	(0)	290	(0)
Se	(180)	(0)	(130)	(250)	(0)
Cu	760	680	380	570	560
PTS No	5854	6027	6027	5854A	5854A
CXD No	1512	1563	1563	1512	1512
BH No	3	2	2	3	3
Depth: (m)	80.87 -80.90	57.42 -57.47	57.42 -57.47	80.87 -80.90	80.87 -80.90

TABLE VIII

Electron microprobe analyses of stratiform arsenopyrite

	1	2	3	4	5	6	7
Wt %							
Fe	34.44	34.09	34.46	34.62	34.74	34.99	34.66
S	20.77	21.16	20.97	21.41	21.41	21.46	22.13
As	42.92	42.95	44.32	44.19	43.32	42.86	43.05
Total	98.13	98.20	99.75	100.22	99.47	99.31	99.84
Atomic formulae (3.000)							
Fe	1.007	0.993	0.994	0.991	0.999	1.006	0.988
S	1.058	1.074	1.053	1.067	1.072	1.075	1.098
As	0.935	0.933	0.953	0.942	0.929	0.919	0.914
ppm							
Ni	1060	4820	(90)	(0)	-	240	190
Co	950	1290	700	690	-	840	760
Sb	2150	570	(0)	1360	no	1380	3280
Ag	(0)	(0)	-	-	data	(0)	(0)
Se	400	-	-	-	-	500	-
Cu	380	430	420	(170)	-	260	390
PTS No	6029	6029	6030	6030	6030	6035	6035
CXD No	1565	1565	1566	1566	1566	1572	1572
BH No	3	3	3	3	3	3	3
Depth (m)	145.17 -145.24	145.17 -145.24	148.07 -148.24	148.07 -148.24	148.07 -148.24	168.62 -168.73	168.62 -168.73

TABLE IX

Electron microprobe analyses of vein arsenopyrite

	1	2	3	4	5	6	7	
Wt %								
Fe	34.67	34.75	34.27	34.06	34.72	34.44	35.38	
S	21.22	21.80	21.18	21.67	20.96	22.49	23.84	
As	43.05	42.38	41.91	41.38	41.88	41.05	41.05	
Total	98.94	98.93	97.36	97.11	97.56	97.98	100.27	
Atomic formulae (3.000)								
Fe	1.003	0.999	1.004	0.995	1.017	0.992	0.987	
S	1.069	1.092	1.081	1.103	1.069	1.127	1.159	
As	0.928	0.909	0.915	0.902	0.914	0.881	0.854	
ppm								LLD≠
Ni	(60)	(40)	(140)	(0)	(110)	(80)	670	210
Co	710	640	640	460	430	(200)	780	270
Sb	220	1620	4520	(0)	560	(40)	5080	220
Ag	(0)	(0)	(0)	(0)	(0)	(0)	(0)	230
Se	(0)	(0)	(610)	(220)	(550)	1550	(690)	1000
Cu	480	360	430	480	320	540	(60)	310
PTS No	6027	6027	5854	5854	5854	5854A	5854A	
CXD No	1563	1563	1512	1512	1512	1512	1512	
BH No	2	2	3	3	3	3	3	
Depth (m)	57.42 -57.47	57.42 -57.47	80.87 -80.90	80.37 -80.90	80.87 -80.90	80.87 -80.90	80.87 -80.90	

≠ Lower limit of detection: 80-100 sec. counts

APPENDIX IV

GEOPHYSICAL PROFILES

In the geophysical survey of the Glendinning mine area, IP measurements were made along five NW–SE profiles. The detailed results are presented here as Figures 1–5. Apparent resistivity and chargeability results are given in the form of pseudosections and VLF–EM results are plotted as profiles of the percentage in-phase and out-of-phase component. The apparent VLF current-density was calculated by the method of Karous and Hjelt (1977) and is presented as pseudosections. The corresponding topographic profiles and the available geological information are also shown in Figures 1–5. The location of each traverse is shown on Appendix VI, Figure 1.

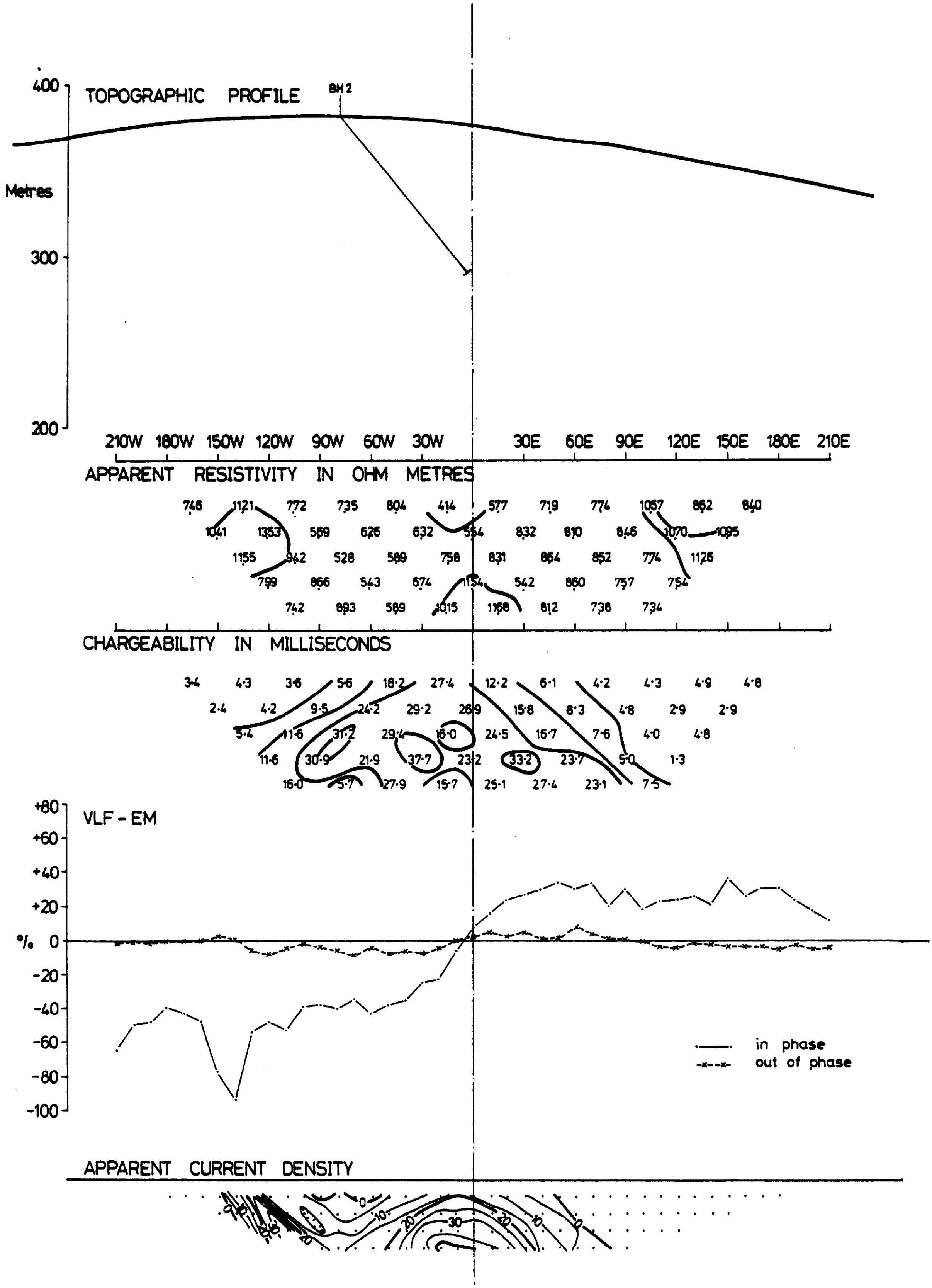

APPENDIX IV, Fig1 GEOPHYSICAL PROFILES FOR LINE 300N

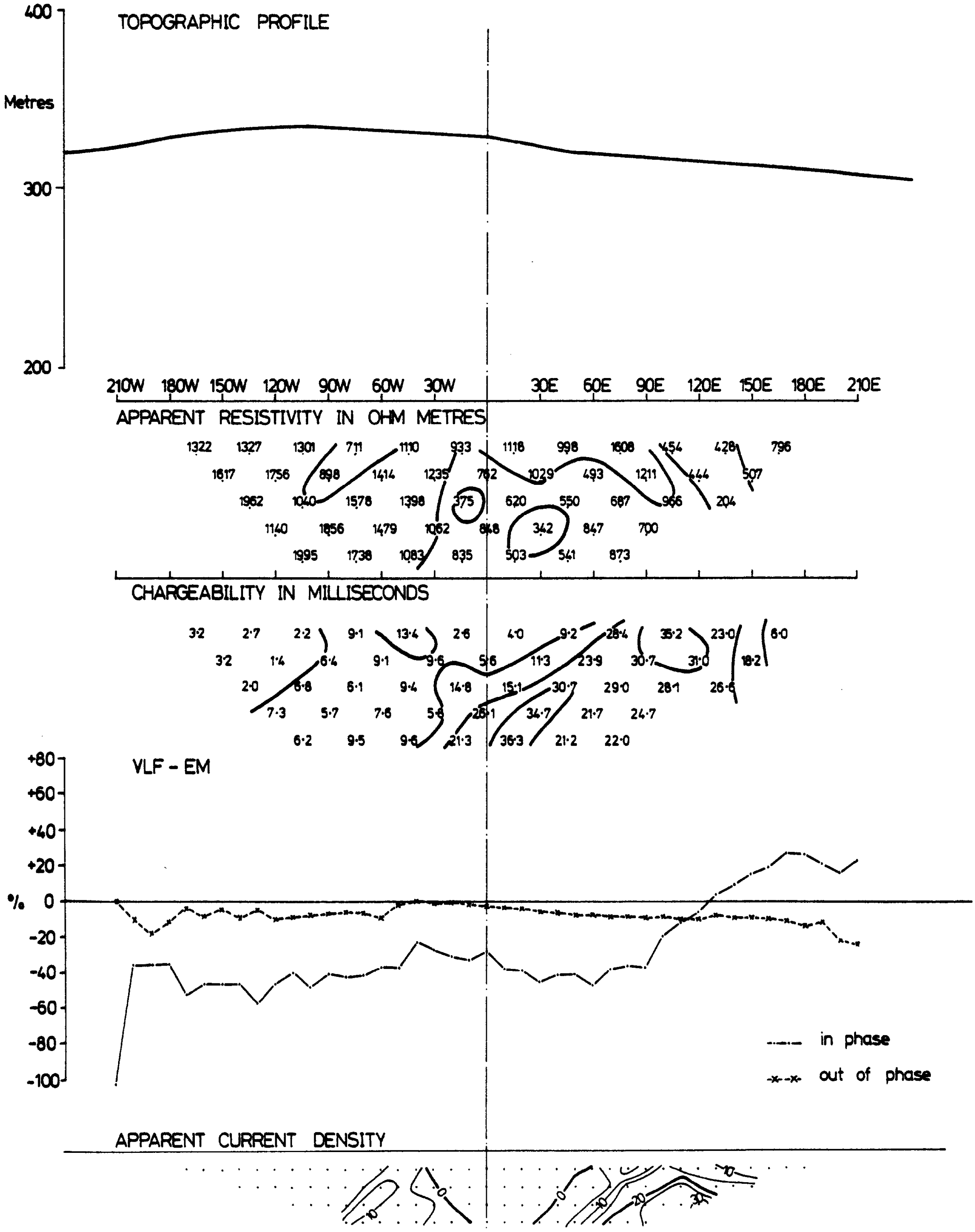

APPENDIX IV, Fig 2 GEOPHYSICAL PROFILES FOR LINE 100N

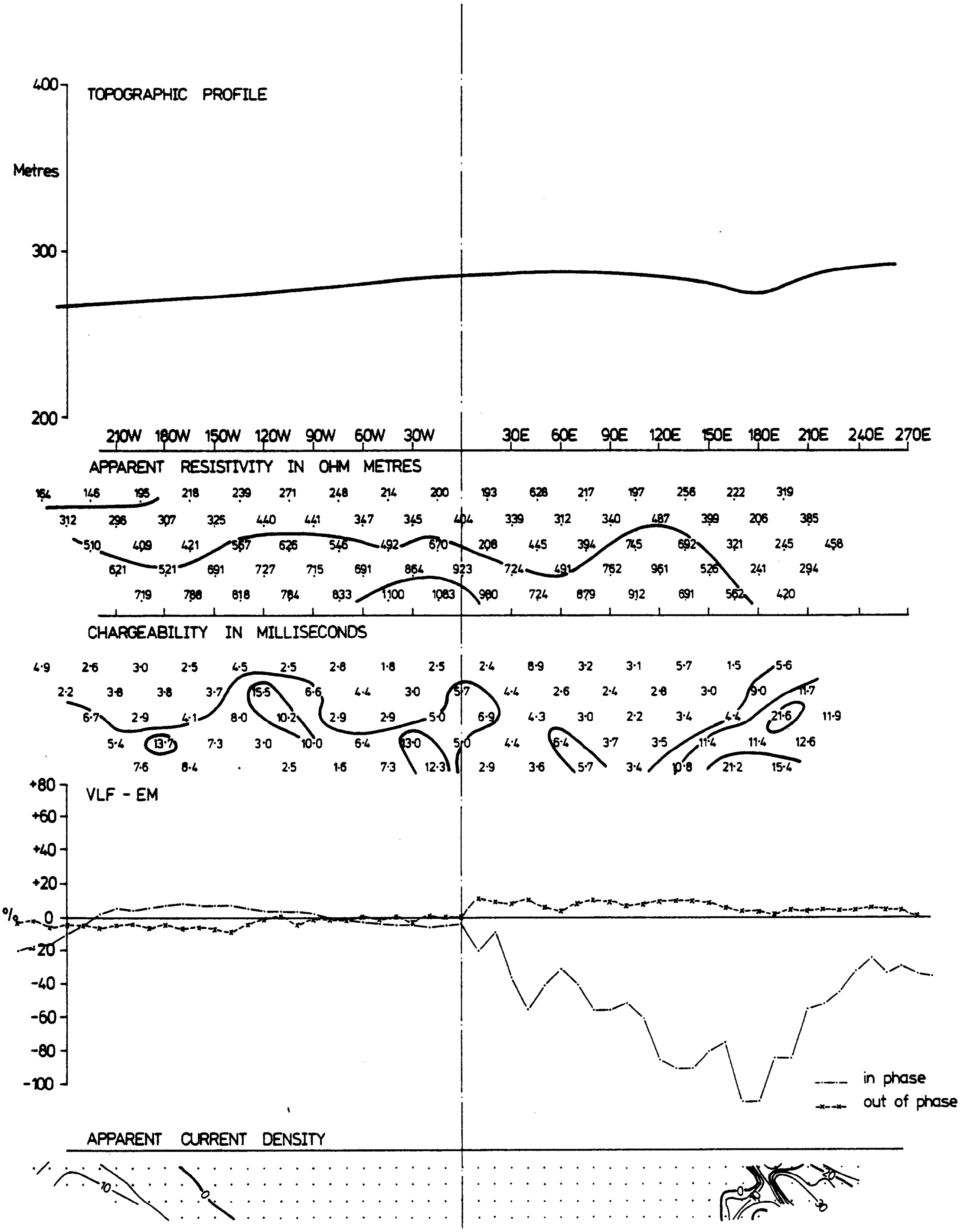

APPENDIX IV, Fig 3 GEOPHYSICAL PROFILES FOR LINE 100S

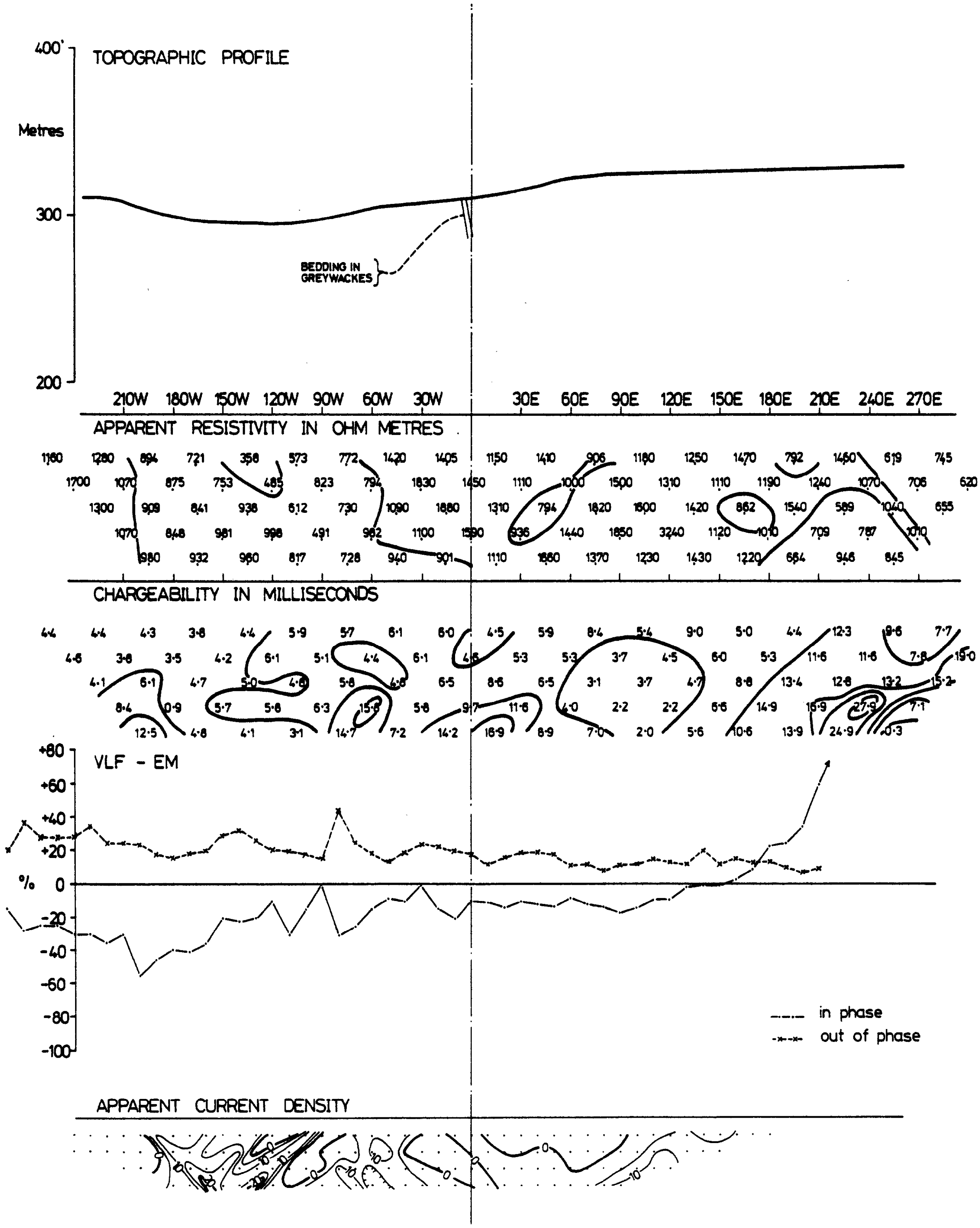

APPENDIX IV, Fig 4 GEOPHYSICAL PROFILES FOR LINE 300S

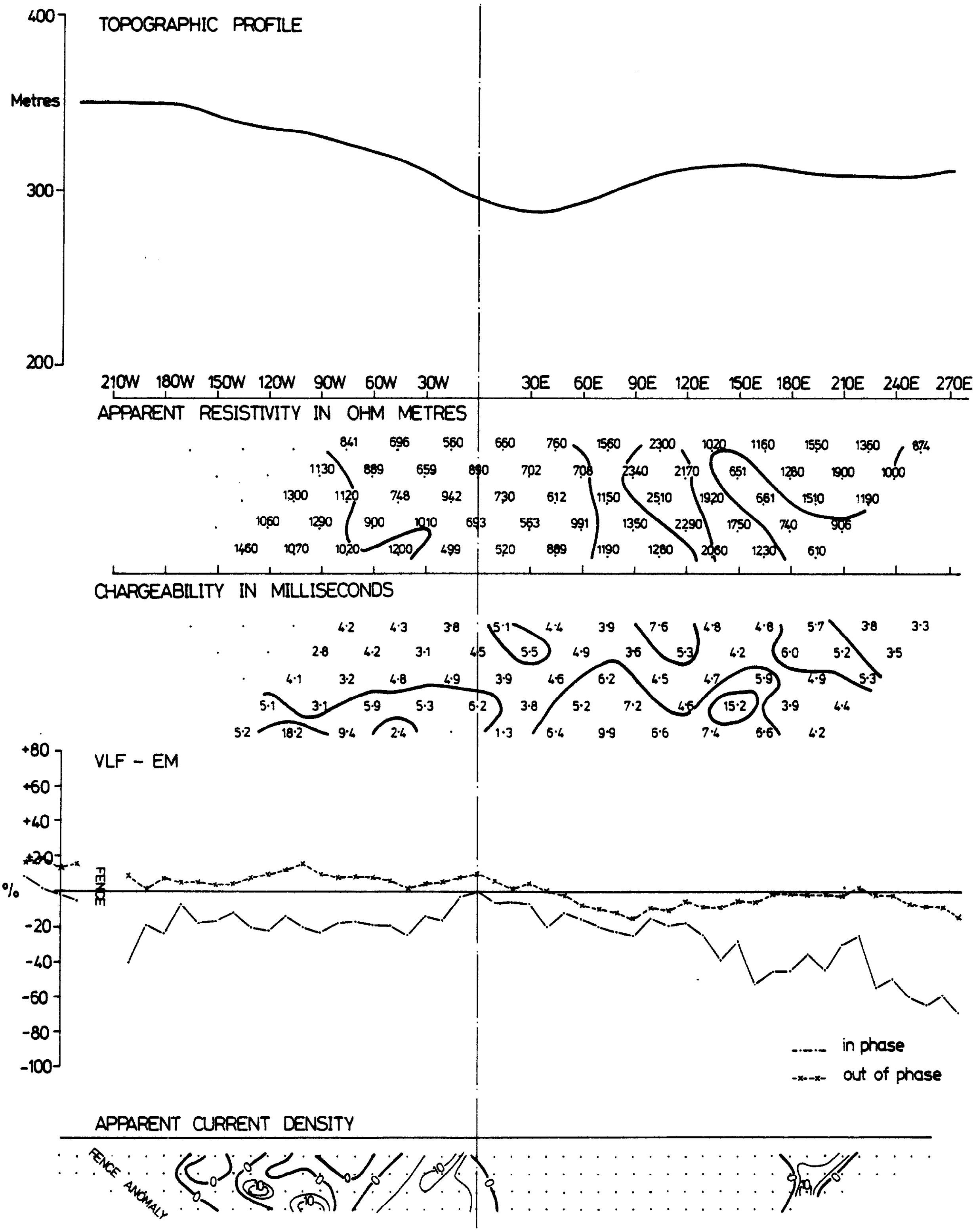

APPENDIX IV, Fig 5 GEOPHYSICAL PROFILES FOR LINE 500S

APPENDIX V

DISTRIBUTION OF METALS IN HEAVY MINERAL CONCENTRATES FROM DRAINAGE NEAR GLENDINNING

Geochemical maps showing the distribution of iron, zinc, lead, copper, nickel, barium, tin and arsenic in panned concentrates are presented in Figures 1 –8.

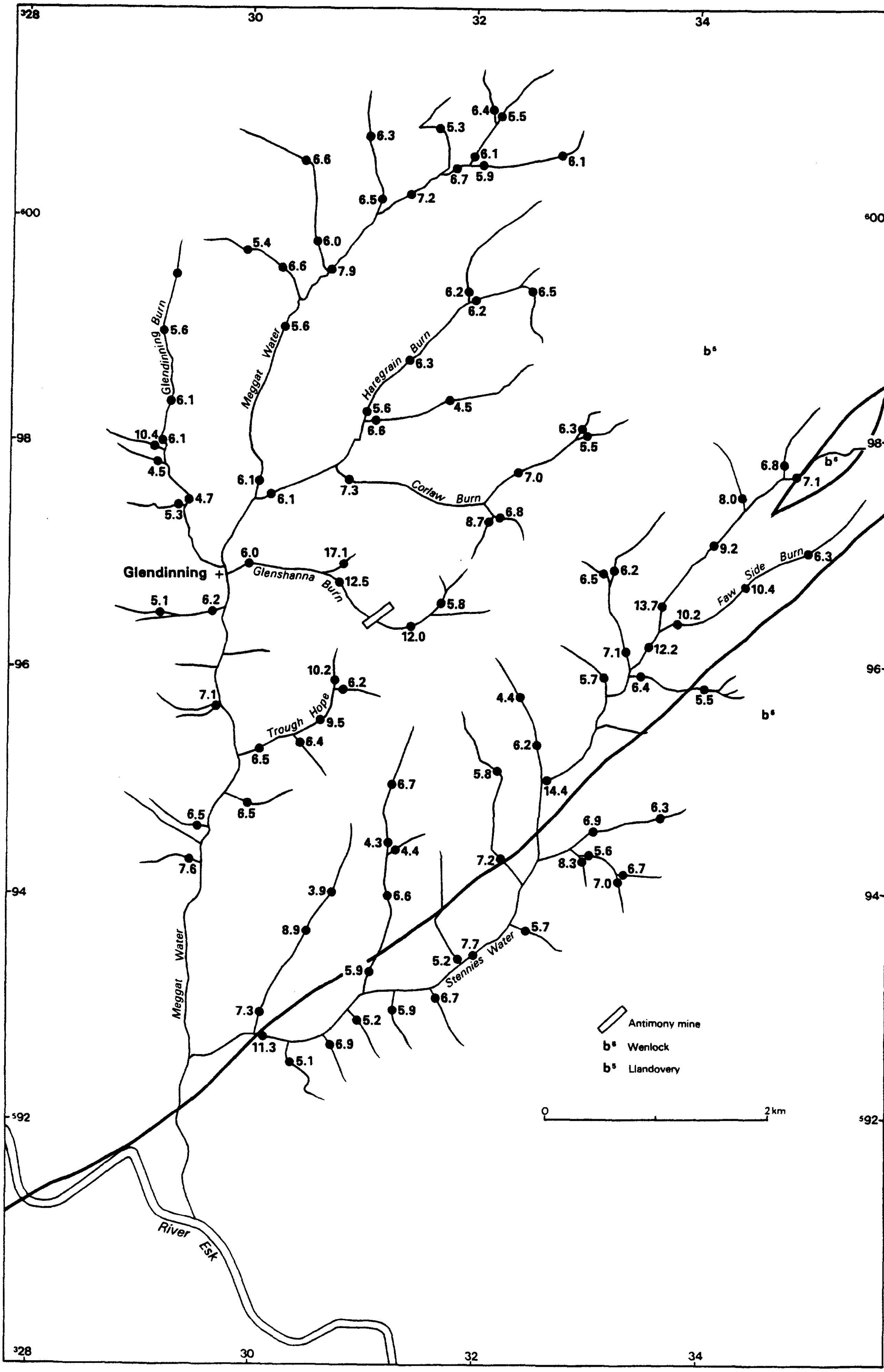

Appendix V, Fig. 1 Distribution of iron (%) in heavy mineral concentrates from drainage near Glendinning

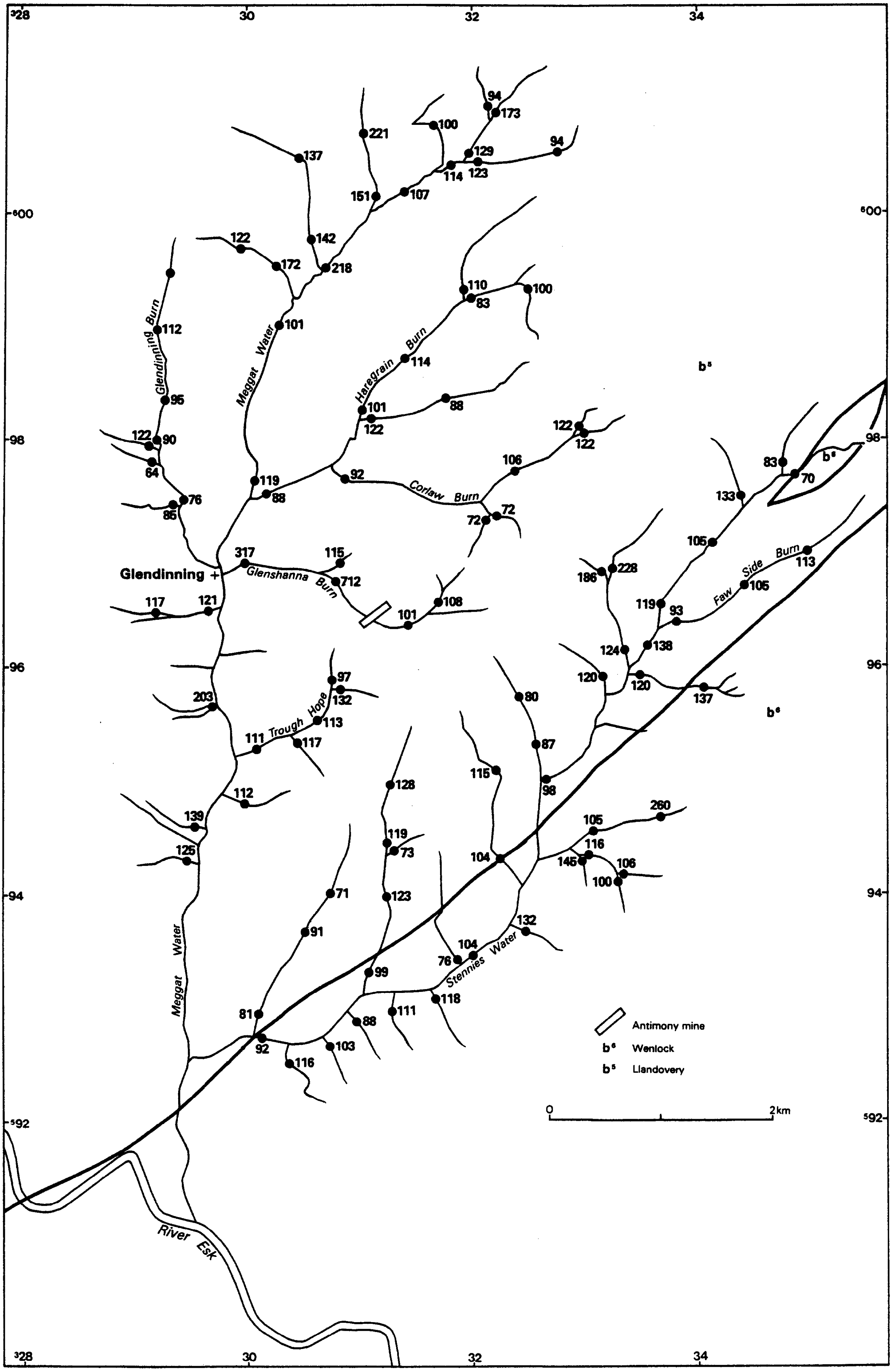

Appendix V, Fig. 2 Distribution of zinc (ppm) in heavy mineral concentrates from drainage near Glendinning

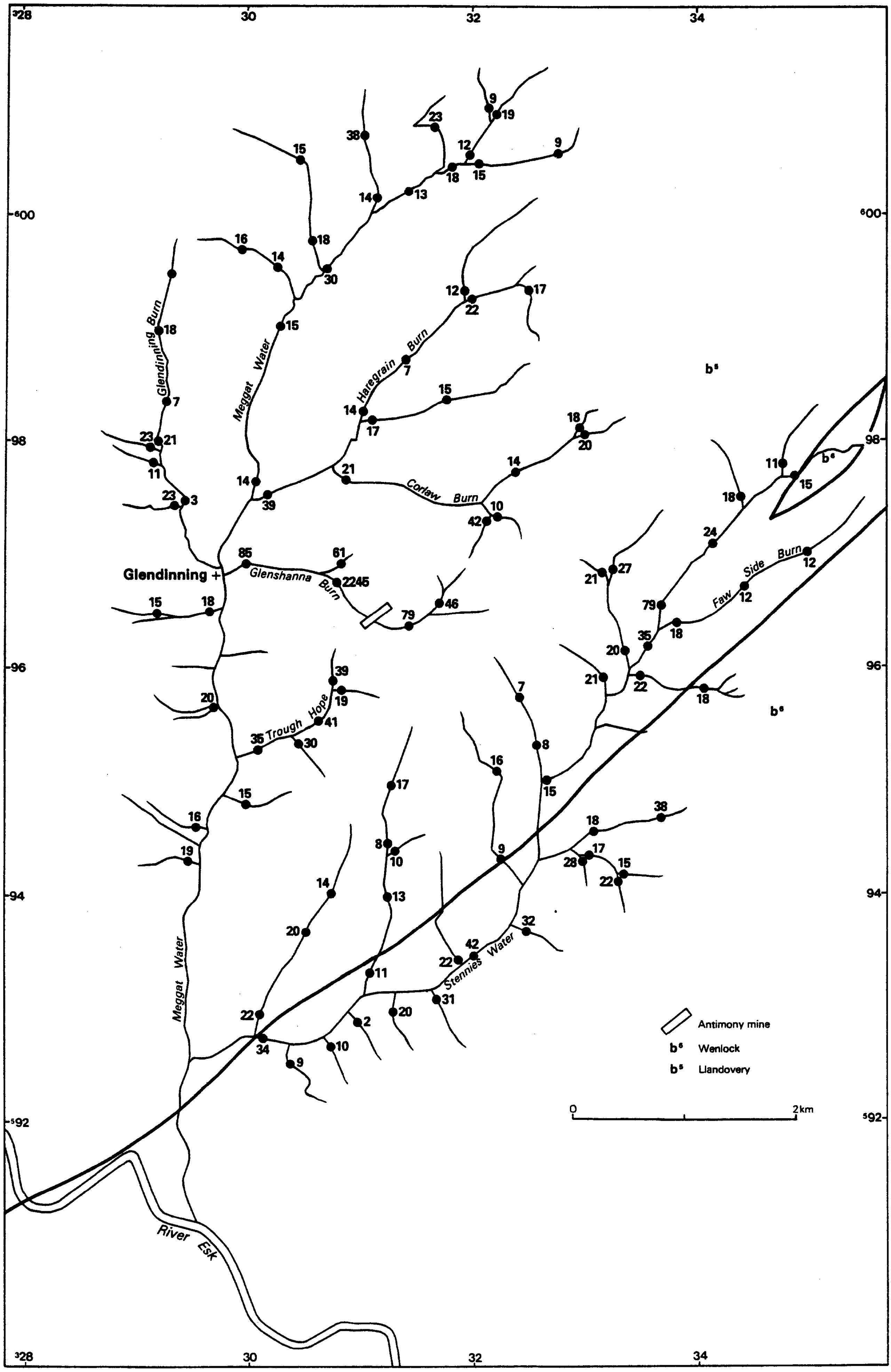

Appendix V, Fig. 3 Distribution of lead (ppm) in heavy mineral concentrates from drainage near Glendinning

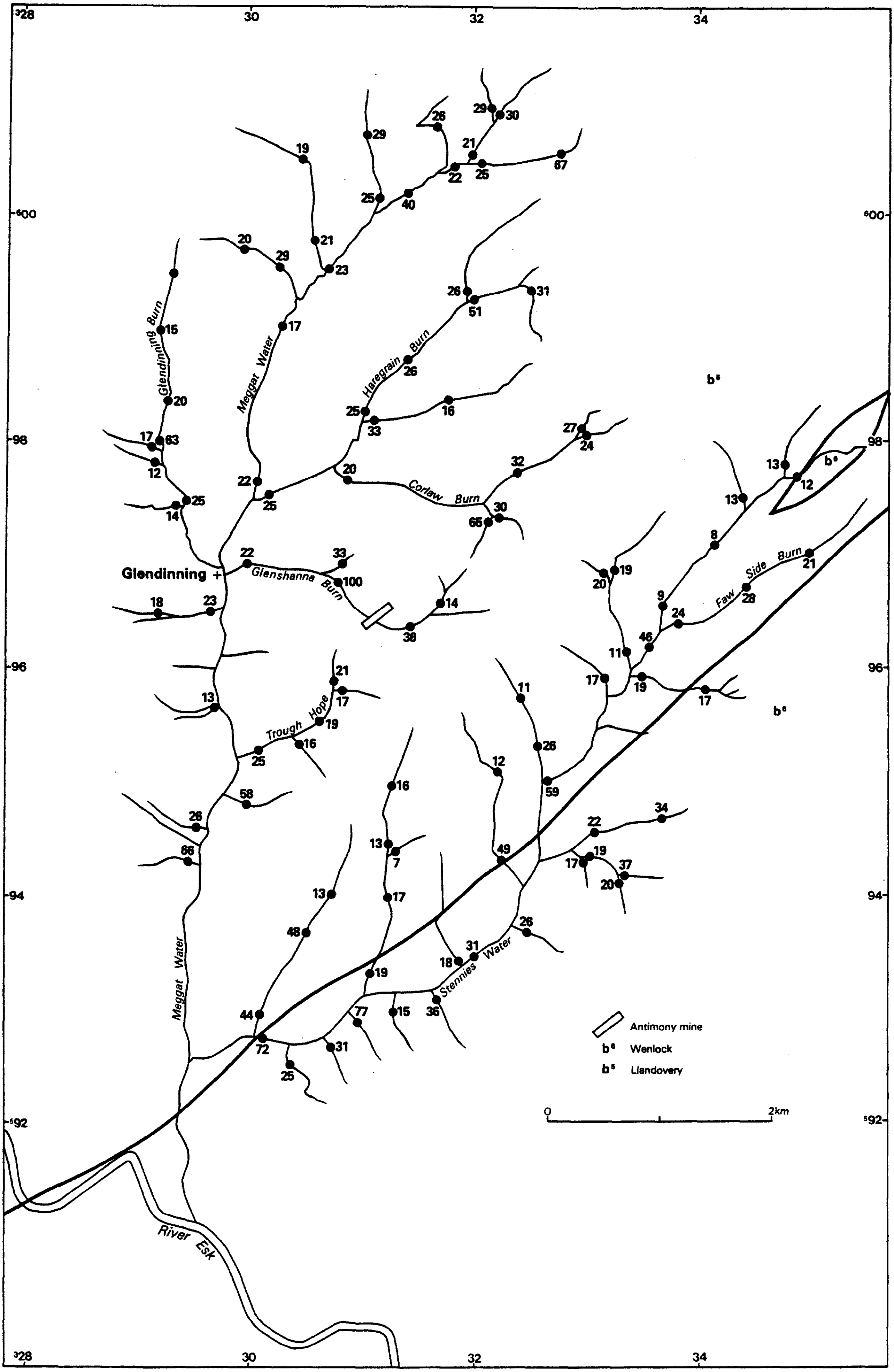

Appendix V, Fig. 4 Distribution of copper (ppm) in heavy mineral concentrates from drainage near Glendinning

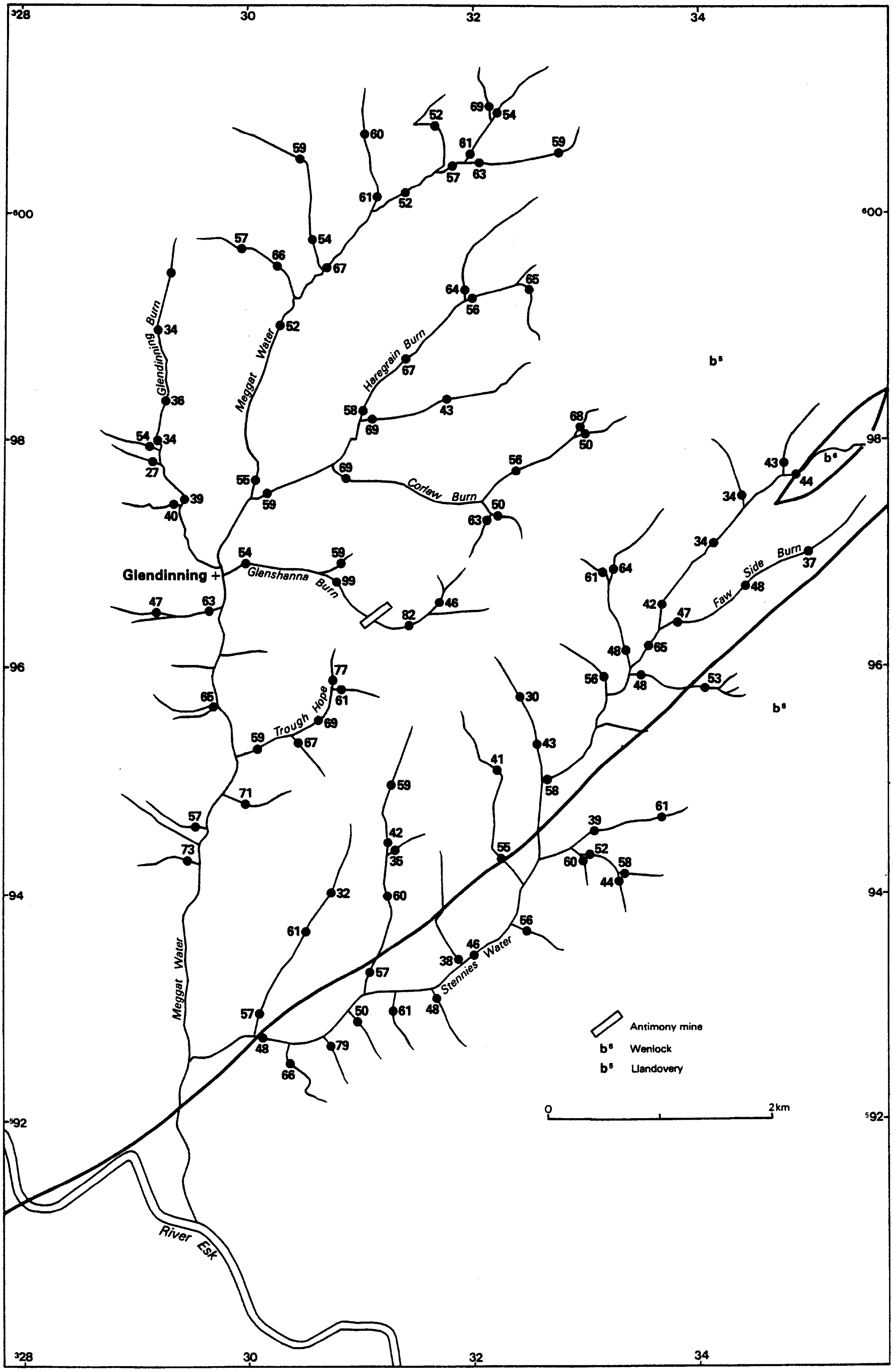

Appendix V, Fig. 5 Distribution of nickel (ppm) in heavy mineral concentrates from drainage near Glendinning

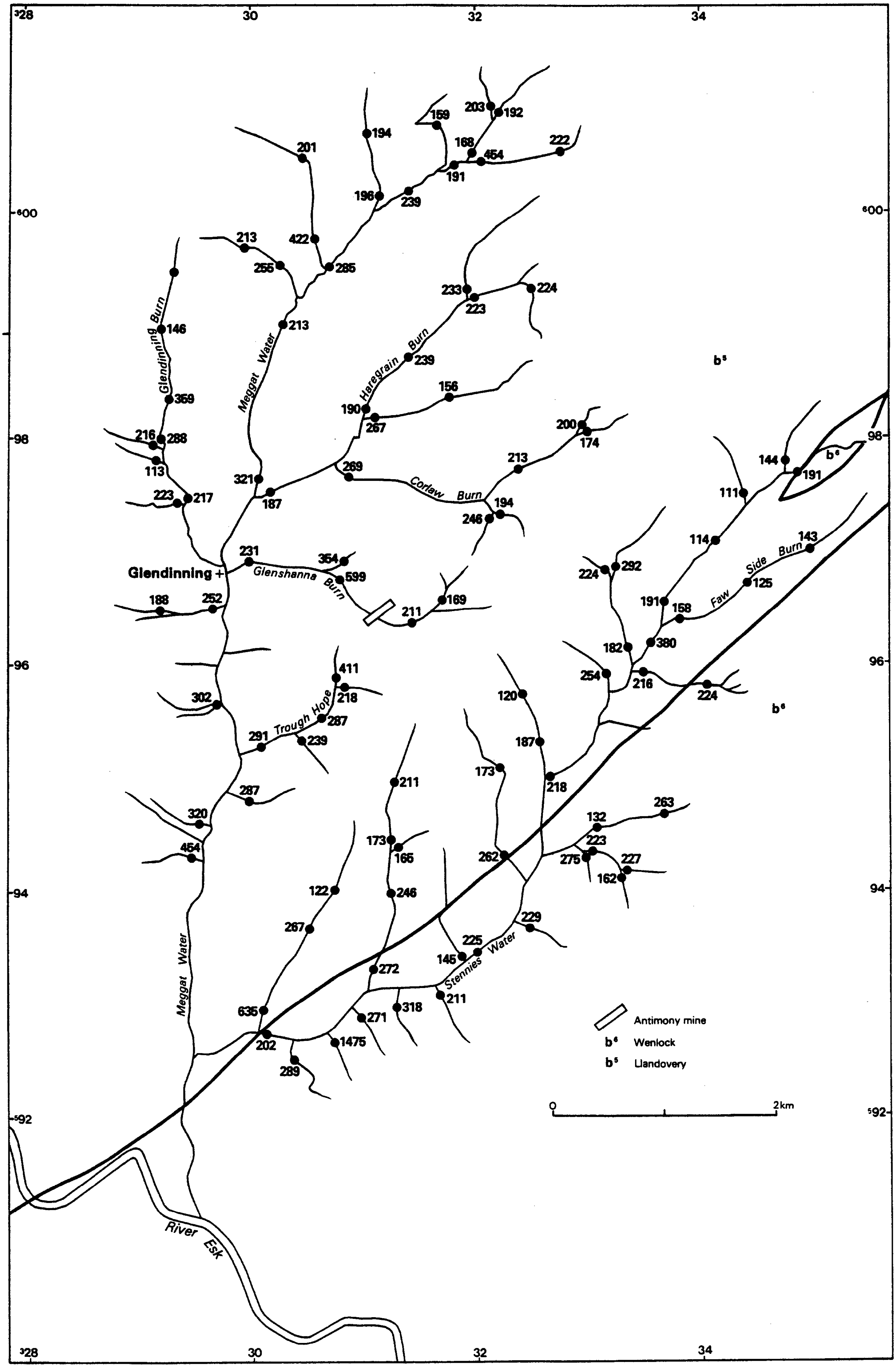

Appendix V, Fig. 6. Distribution of barium (ppm) in heavy mineral concentrates from drainage near Glendinning

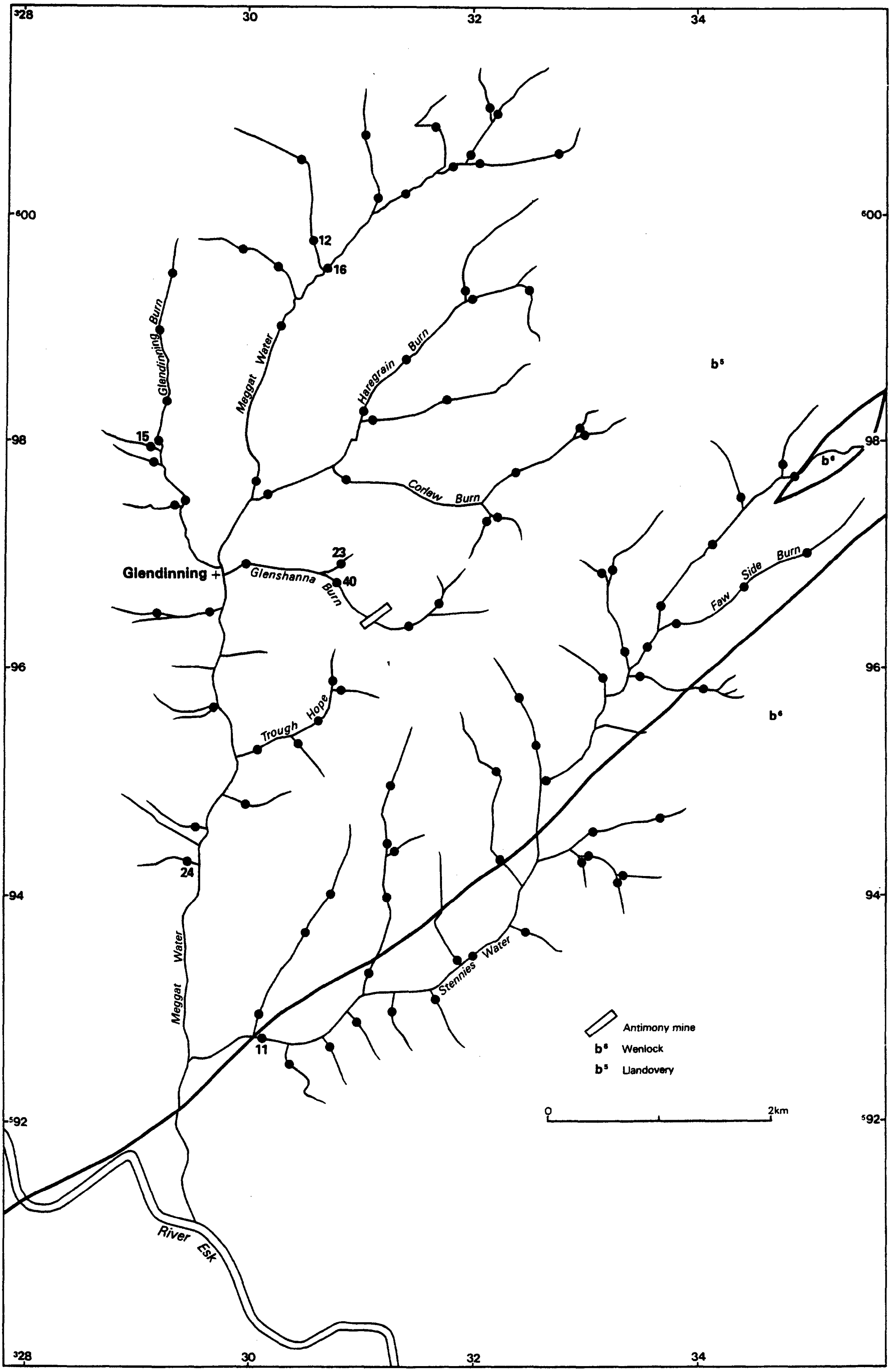

Appendix V, Fig. 7 Distribution of tin (ppm) in heavy mineral concentrates from drainage near Glendinning

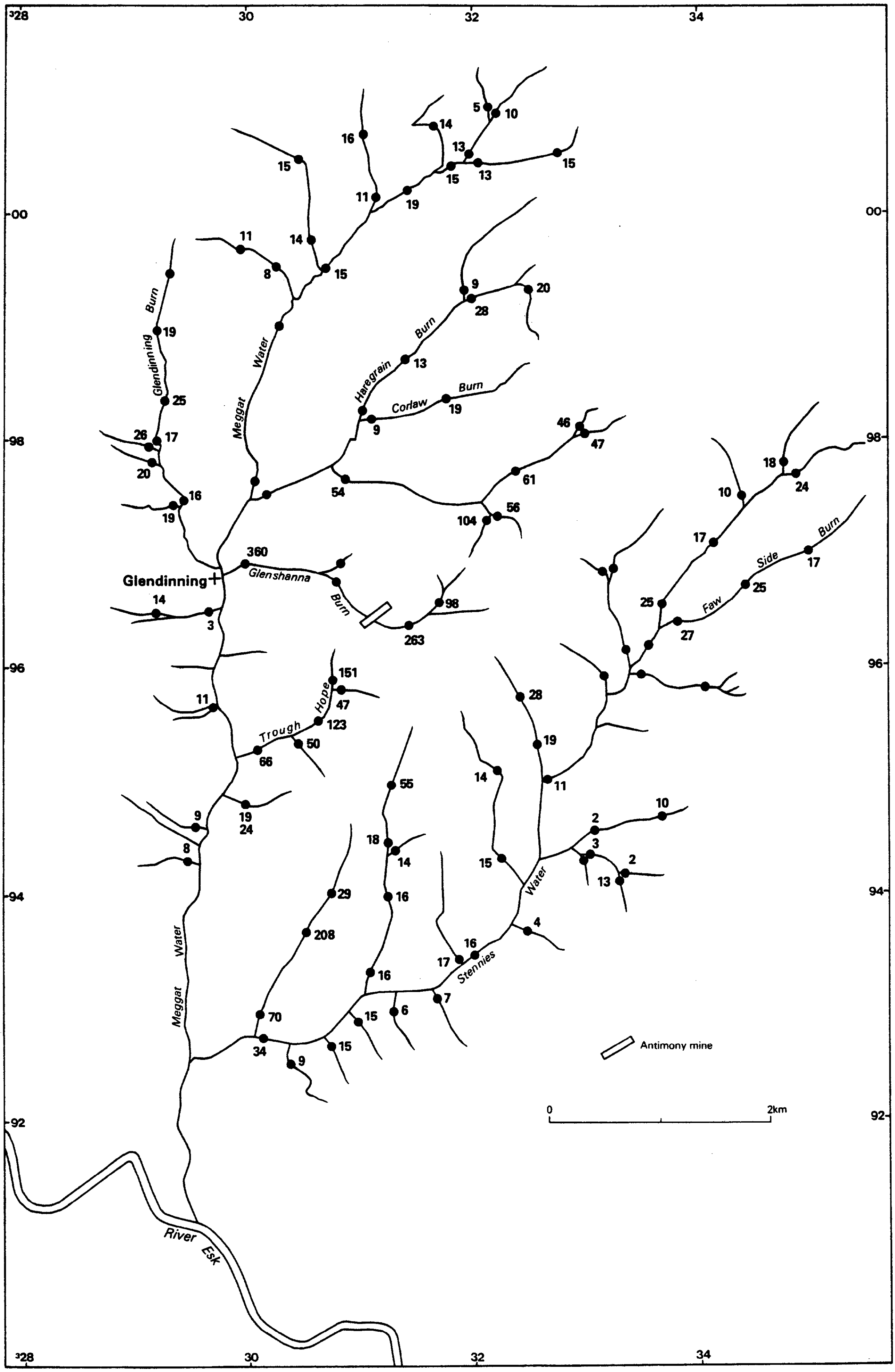

Appendix V, Fig. 8 Distribution of arsenic in heavy mineral concentrates from the Glendinning area

APPENDIX VI

GEOPHYSICAL MAP AND MAPS OF METAL DISTRIBUTION IN OVERBURDEN IN THE GLENDINNING MINE – TROUGH HOPE AREA

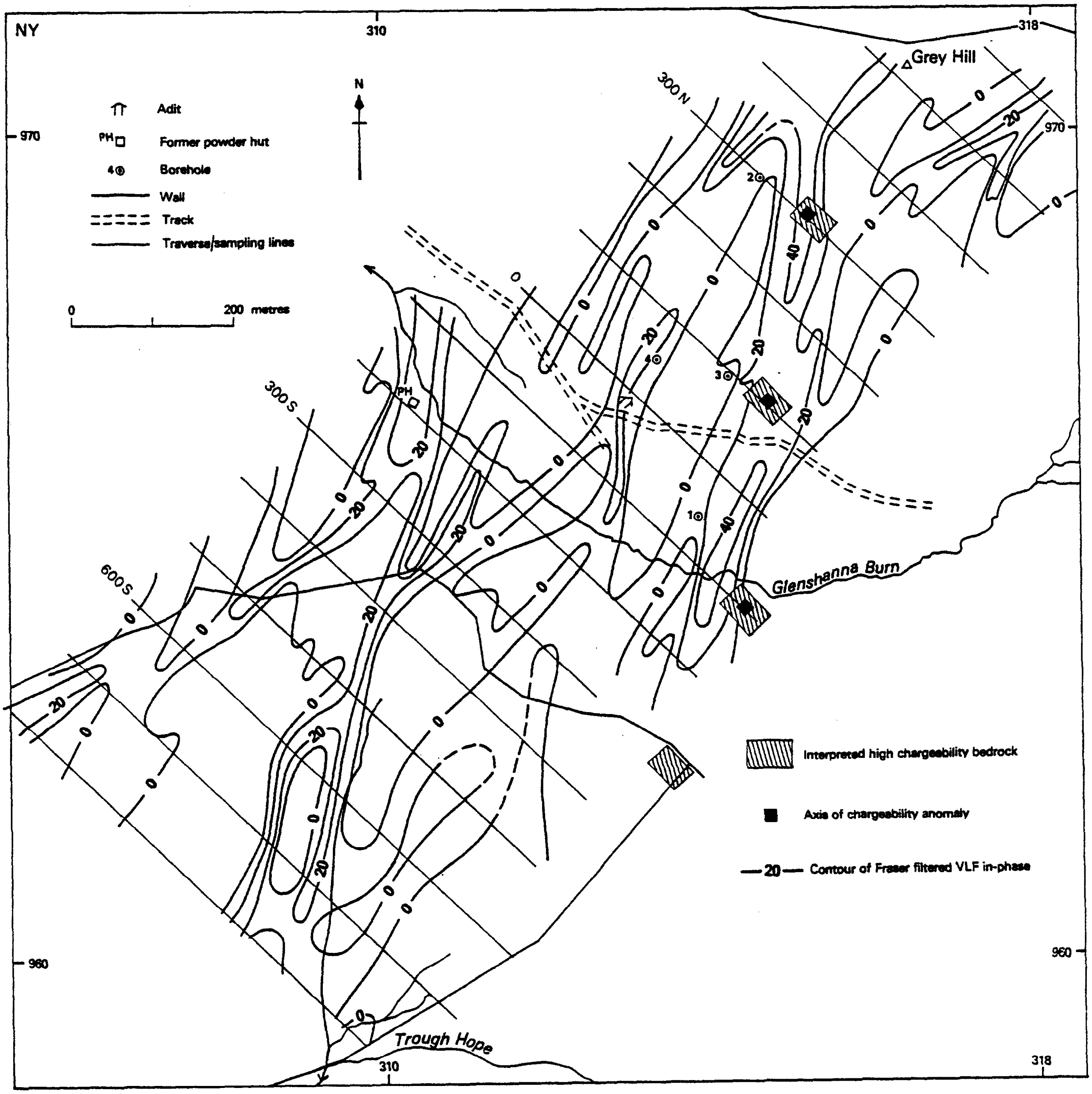

Appendix VI, Fig.1 VLF-EM map of the area around Glendinning mine; IP maxima are also shown

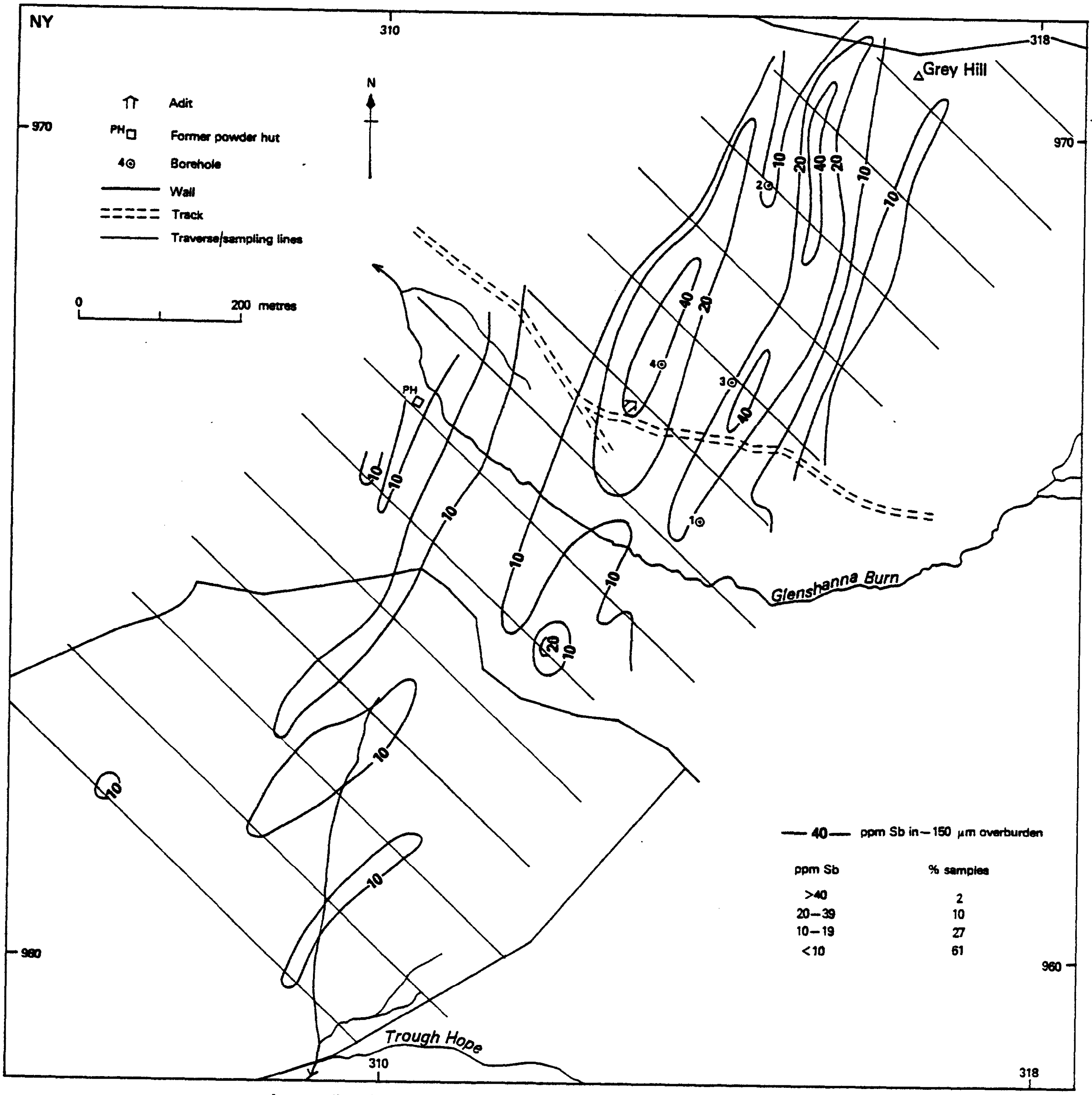

Appendix VI, Fig. 2 Distribution of antimony in shallow overburden

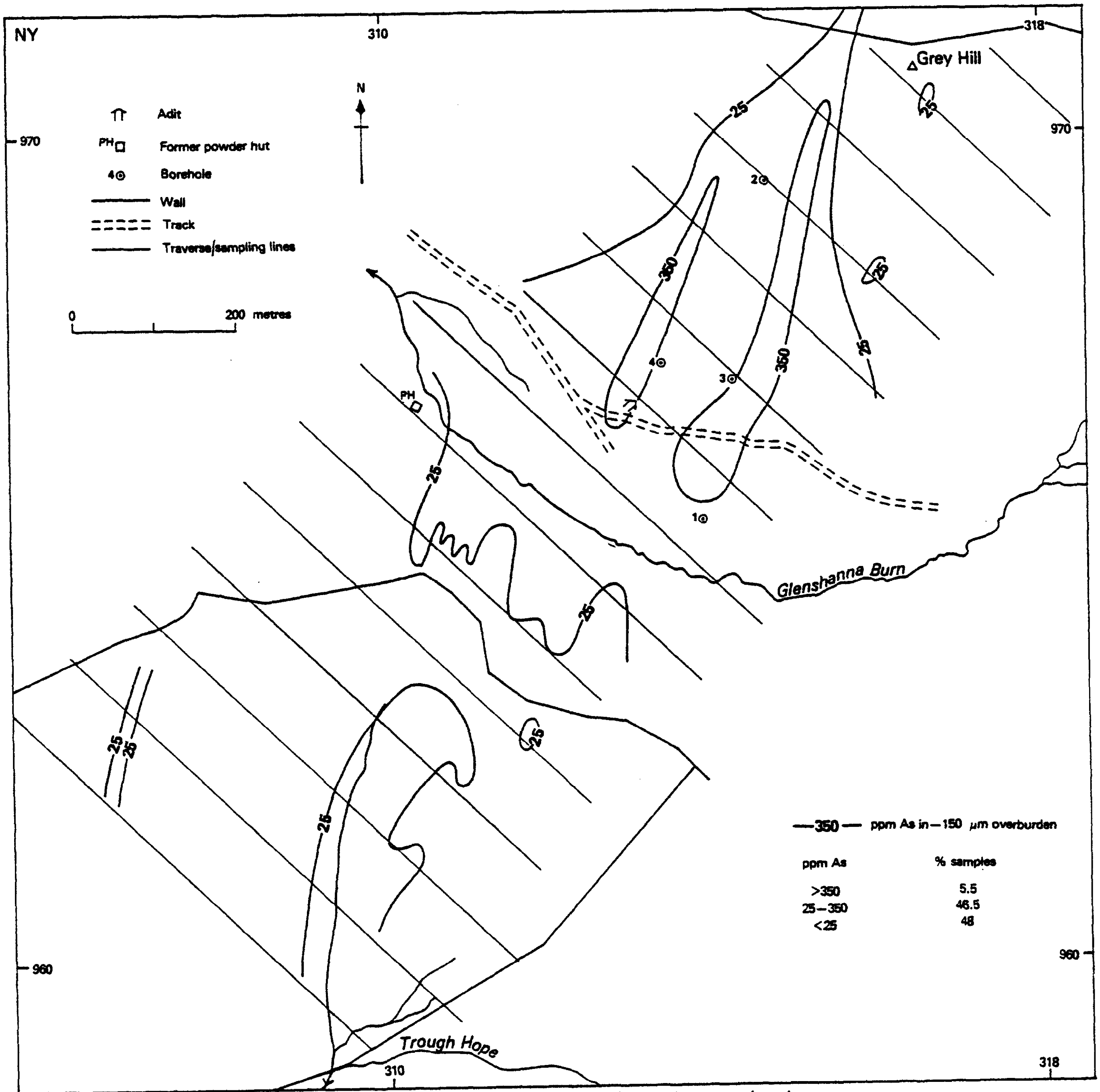

Appendix VI, Fig. 3 Distribution of arsenic in shallow overburden

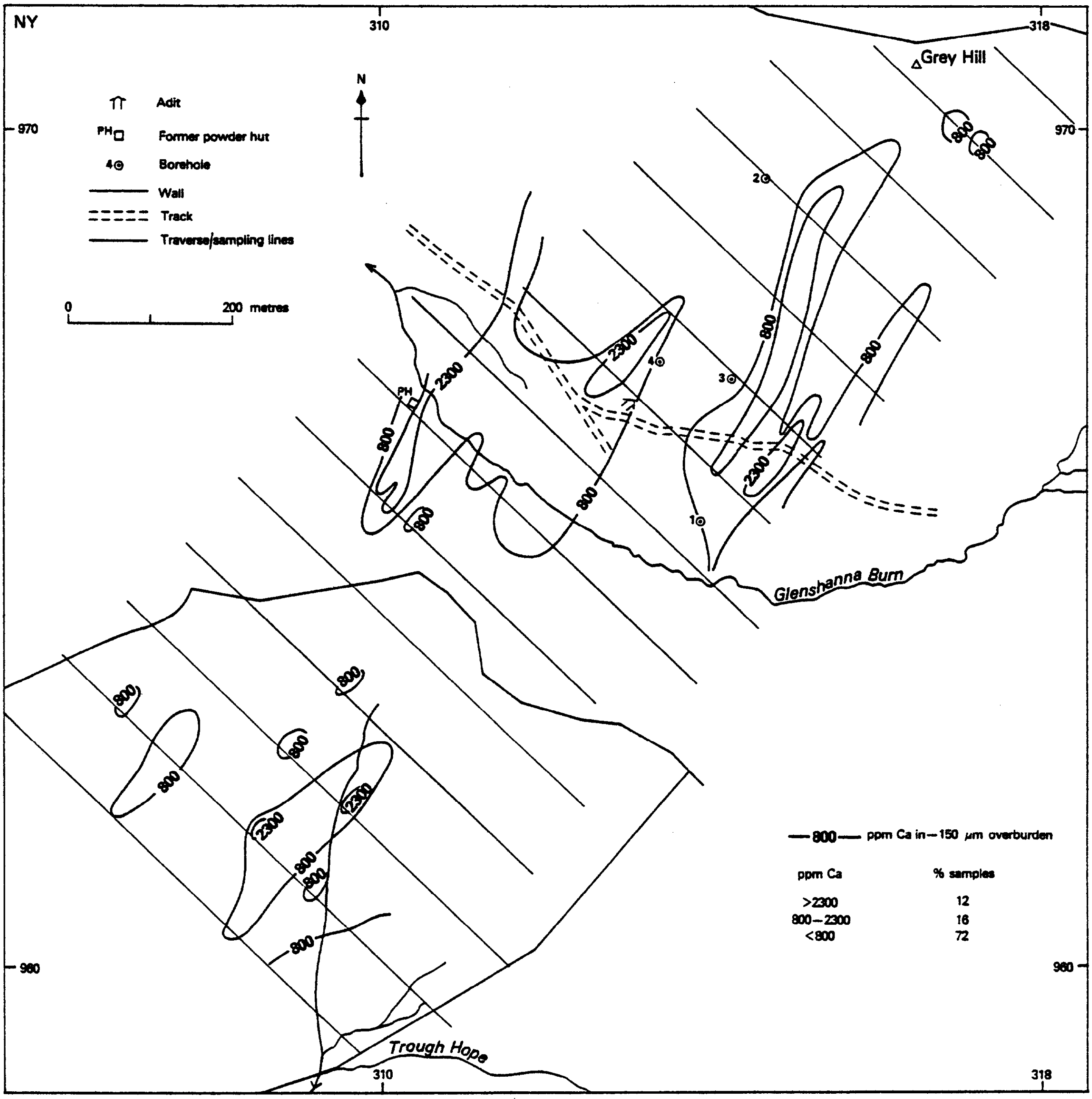

Appendix VI, Fig. 4 Distribution of calcium in shallow overburden

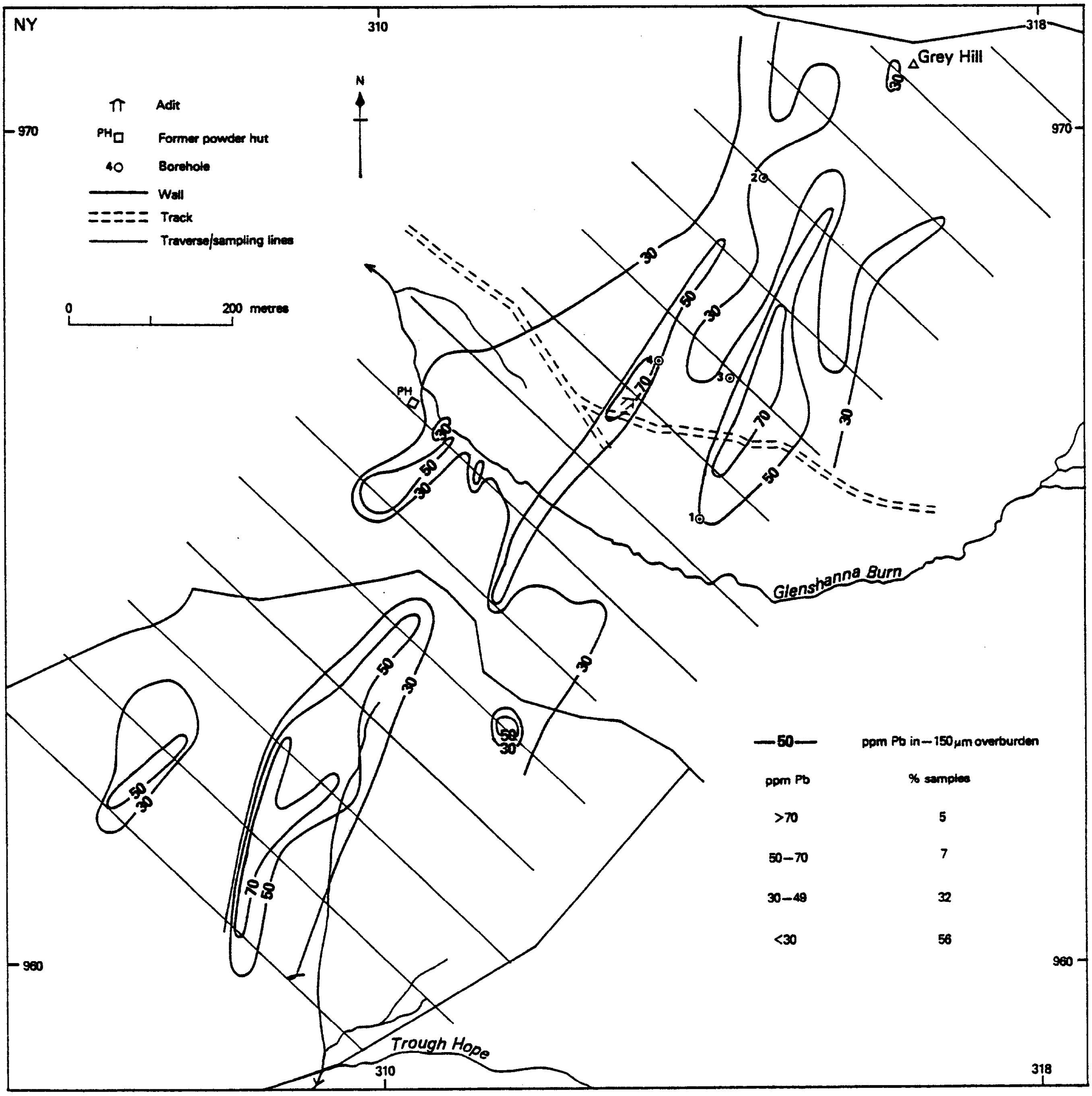

Appendix VI, Fig. 5 Distribution of lead in shallow overburden

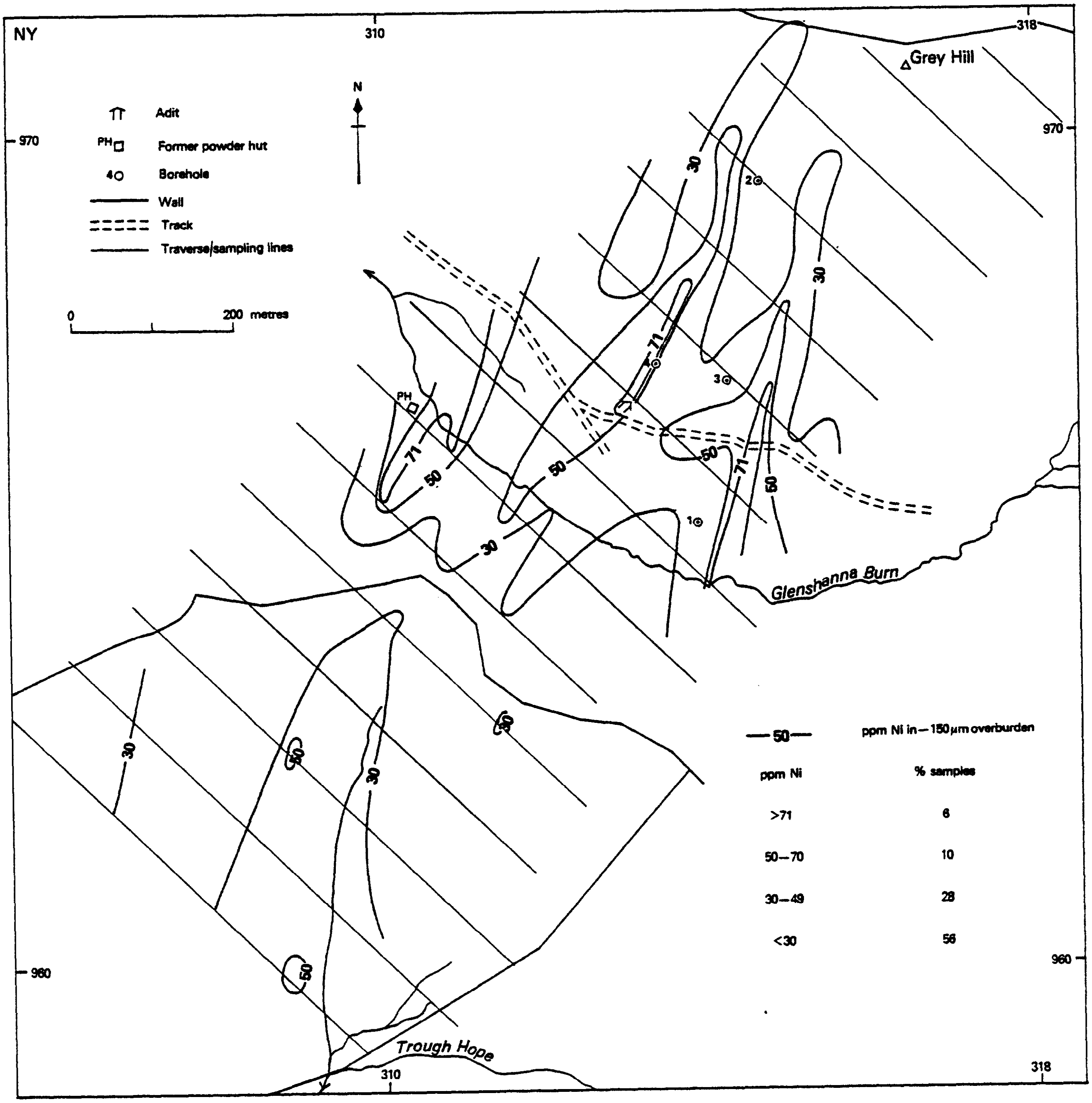

Appendix VI, Fig. 6 Distribution of nickel in shallow overburden

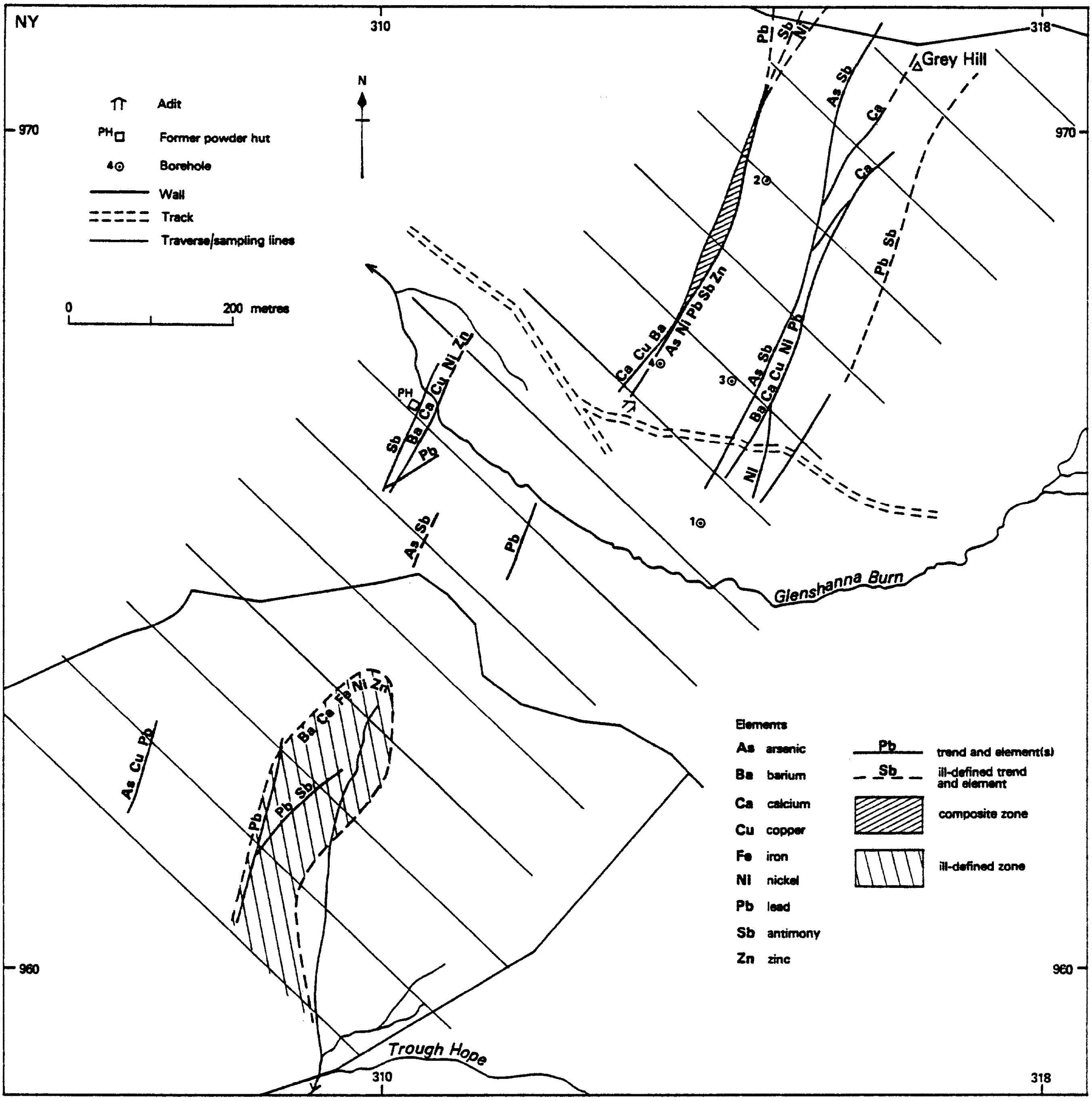

Appendix VI, Fig. 7 Element maxima trends in shallow overburden

APPENDIX VII

RAPID FIELD ESTIMATION OF ARSENIC

Introduction

The method is based on the well-known Gutzeit technique whereby arsenic released by an appropriate dissolution procedure is converted to arsine which then forms a coloured complex with $HgCl_2$.

A portion of prepared sample is mixed with solid $KHSO_4$, $SnCl_2$ and KI. On the addition of water H_2SO_4 is produced releasing some arsenic which is then reduced to As(III). When Zn dust is added nascent hydrogen is formed which reacts with As(III) to form arsine; the nascent hydrogen also serves to carry arsine from the reaction vessel, through a column of paper soaked in lead acetate to remove H_2S, and onto a piece of filter paper impregnated with $HgCl_2$. The coloured spot produced is compared visually with a set of standard spots and the arsenic content of the sample is calculated. The development and previous applications of the method have been described by Peachey and others (1982).

Although total arsenic is not determined the method identifies anomalous samples and assists in on-site decision making and the need for alkalies and strong acids is avoided. Moreover the method is rapid and can be operated by unskilled staff. Care should be taken when interpreting results since arsenic held in secondary phases is released more readily than arsenic held in primary phases.

Fourteen samples from a traverse were analysed using the field method (analyst: B. P. Vickers) and by X-ray fluorescence spectrometry (analyst: D. J. Bland). The results obtained by both methods are compared in Figure 1. The conclusions reached from earlier work are confirmed, i.e. there is a close coincidence between the distribution patterns shown in Figure 1 and although the field method detected only a fraction of the total arsenic the anomalous samples are clearly identified.

Method

The $HgCl_2$ papers, lead acetate papers and the standards were prepared in the main laboratory.

Apparatus: Balance or standardised scoops; Gutzeit apparatus (see Figure 2).

Chemicals: (AR Grade chemicals were used throughout)
Potassium bisulphate ($KHSO_4$)
Stannous chloride ($SnCl_2.2H_2O$)
Potassium iodide (KI)
Zinc powder
Mercuric chloride papers. These are available commercially but can be prepared by soaking filter papers in mercuric chloride solution (about 25 g $HgCl_2$ in 100 ml ethanol). The papers are air-dried, cut to size and stored in a box.

Lead acetate papers are prepared by soaking strips of filter paper (10 × 2 cm) in a saturated, aqueous solution of lead acetate. The papers are then air-dried.

Procedure:

1 Transfer 0.2 g sample and about 3.6 g $KHSO_4$ into the reaction bottle.
2 Add 10 ml of water.
3 Add 0.1 g $SnCl_2.2H_2O$.
4 Add 0.05 g KI.
5 Add 1.0 g Zn powder and *immediately* insert the bung holding the glass tube and cup containing the $HgCl_2$ paper.
6 Swirl and leave for 20 minutes or until the reaction subsides. Residues from the reaction vessels should be flushed away with large volumes of water.
7 Compare the colour of the spot on the $HgCl_2$ paper with a set of standards.
8 Calculate the arsenic content from:
As(ppm) = 5 × μg As corresponding to matched standard.

Standards: The need to prepare standards in the field can be avoided by making a colour chart, using water colours, from standards prepared beforehand in the laboratory (Stanton, 1966).

1 Stock standard solution: Dissolve 0.042 g of sodium arsenate ($Na_2HAsO_4.7H_2O$) in distilled water and add a few drops of concentrated HCl. Dilute to 100 ml with distilled water (1 ml ≡ 100 μg As).
2 5 μg/ml As solution: Dilute a 5 ml aliquot of the stock solution to 100 ml with distilled water.
3 Add to separate reaction vessels appropriate aliquots of the 5 μg/ml As solution to prepare the following set of standards: 1, 2, 3, 4, 5, 6, 7, 8, 9, 10, 20, 30 and 40 μg As.
4 Add 2 ml 0.5M HCl, 2 ml 2.5% KI, 10 ml 0.75% $SnCl_2$ in HCl and about 3 g Zn pellets. Immediately insert the bung holding the glass tube and cup containing the $HgCl_2$ paper and leave for 30 minutes or until the reaction subsides (Stanton, 1966).

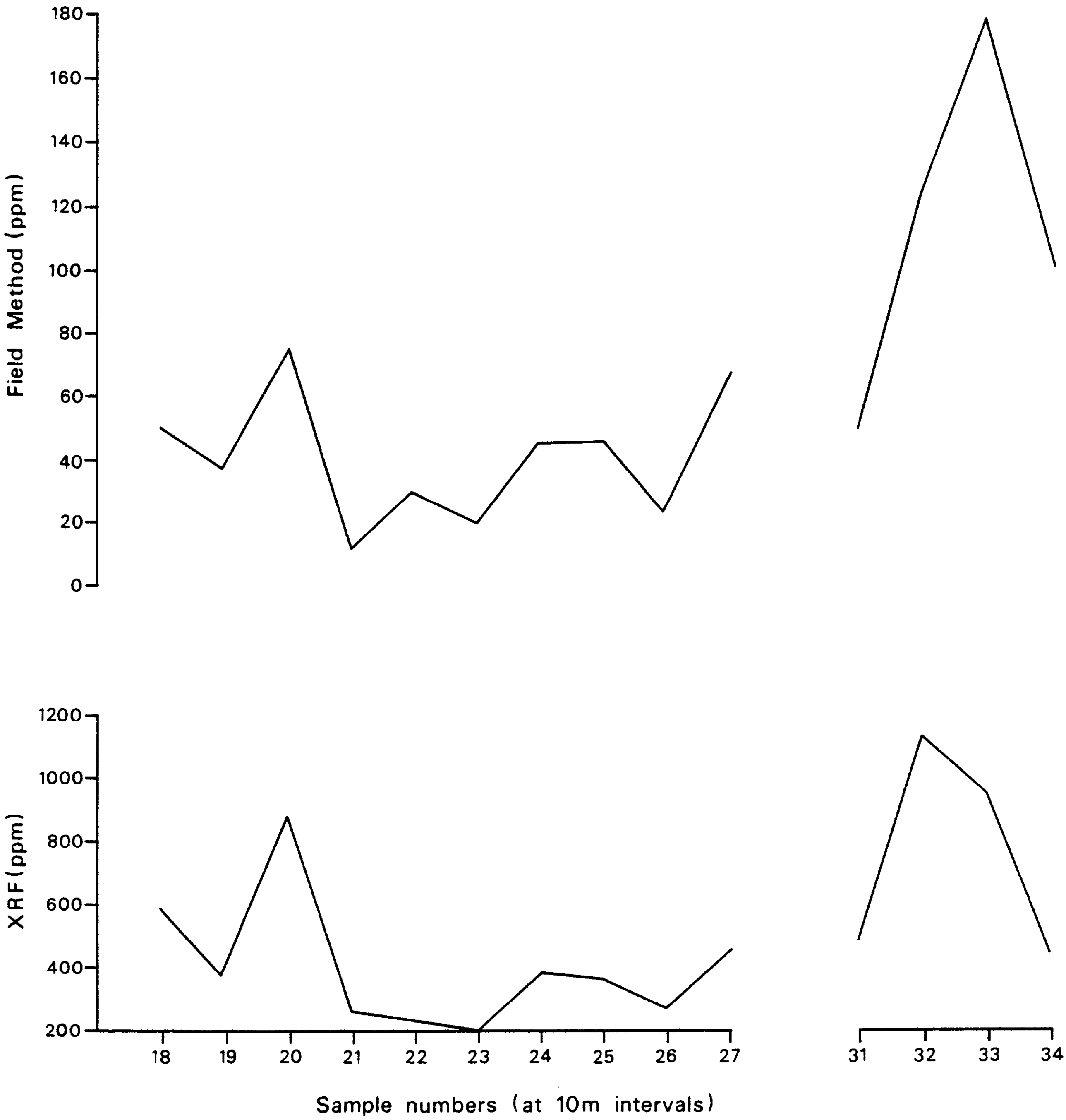

Appendix VII
Figure 1 : Arsenic results obtained by the field method and by X.R.F.

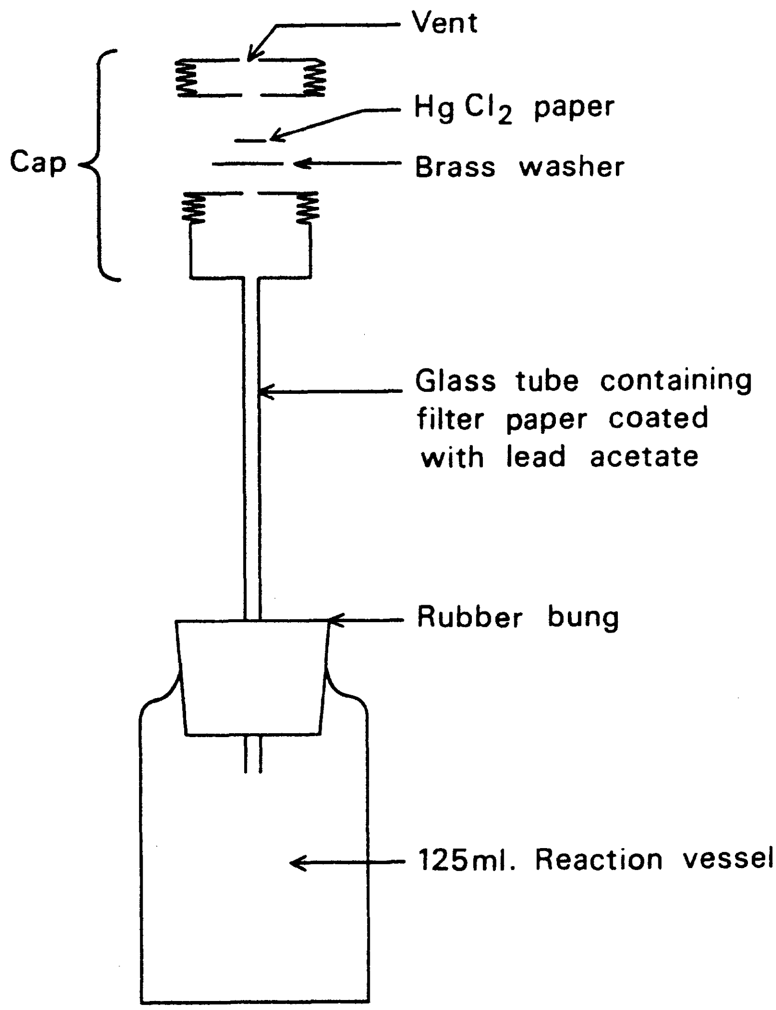

Appendix VII
Figure 2: "Gutzeit" apparatus (Scale-approximately half size)